Imperial College London

The stability of influenza haemagglutinin and its significance for pathogenicity, transmission and control

Anika Singanayagam

Imperial College London

Department of Medicine

Submitted for the degree of Doctor of Philosophy

Date: 18th October 2019

Supervised by Wendy Barclay and Maria Zambon

Declaration of Originality

I declare that the work presented in this thesis is my own unless otherwise stated.

The work presented was supported by a Wellcome Trust Clinical Research Training Fellowship [105736/Z/14/Z].

Copyright Declaration

Publication and presentation of work contained in this Thesis

Some of the data contained in this Thesis have been previously published and/or presented at scientific conferences, as listed below.

Publications

- **Singanayagam A**, Zhou J, Elderfield RA, Frise R, Ashcroft J, Galiano M, Miah S, Nicolaou L, Barclay W. Characterising viable virus from air exhaled by H1N1 influenza-infected ferrets reveals the importance of haemagglutinin stability for airborne infectivity. *Plos Pathogens* 2020;16(2): e1008362.
- **Singanayagam A**, Zambon M, Barclay W. Influenza virus with increased pH of HA activation has improved replication in cell culture but at the cost of infectivity in human airway epithelium. *J Virol* 2019; 93(17).
- Lindsey B*, Jagne J*, Armitage E*, **Singanayagam A,** Hadijatou SJ, Drammeh S, Senghore E, Mohammed N, Jeffries D, Hoschler K, Tregoning JS, Meijer A, Clarke E, Dong T, Barclay W, Kampmann B, de Silva TI. Effect of a Russian-backbone live-attenuated influenza vaccine with an updated pandemic H1N1 strain on shedding and immunogenicity among children in The Gambia: an open-label, observational, phase 4 study. *Lancet Resp Med* 2019; 7(8): 665-676. [*joint 1st authors]
- **Singanayagam A**, Zambon M, Lalvani A, Barclay W. Urgent challenges in implementing live attenuated influenza vaccine. *Lancet Inf Dis* 2018; 18(1):e25-32
- **Singanayagam A**, Zambon M, Lalvani A, Barclay W. Can defective interfering RNA's affect the live attenuated influenza vaccine. *Lancet Inf Dis* 2017; 17(12): 1235-1236

Presentations

- Factors determining the optimum pH stability for pathogenicity and transmissibility of human influenza viruses. *European Scientific Working Group on Influenza*, 2017
- Detection of infectious influenza virus in airborne droplets. *Transmission of respiratory viruses: from basic science to evidence based options for control*, 2017.
- Investigating the potential for influenza A virus resistance to an inhibitor of the host vacuolar ATP-ase. *Options for the Control of Influenza*, 2016.
- 2009 pandemic H1N1 influenza can rapidly develop escape mutations in the presence of a host-directed vacuolar ATPase inhibiting drug. *The International Society for Influenza and Other Respiratory Viruses*, 2014

Acknowledgements

I am immensely grateful to my supervisor, Wendy Barclay, for inspiring me with her enthusiastic and creative approach to science and for supporting me in joining her molecular virology laboratory from a clinical background. I would also like to thank my co-supervisor at Public Health England, Maria Zambon, whose straightforward and practical approach has been invaluable throughout; and in particular, for offering me the opportunity to spend time at PHE under her guidance. Both have been very valued role models.

Thank you to the many lab mates I have worked alongside in the Barclay Group who have shared ideas, protocols, taught me techniques and made me laugh. I am grateful to the Wellcome Trust for awarding me a Clinical Research Training Fellowship and for generous funding of this PhD.

Most importantly, without the constant support and encouragement of my family, particularly Satheesh and Amaya, this thesis would not have been possible.

Abstract

Influenza A viruses are highly diverse and predominantly exist in animal reservoirs. In the rare but significant event that an influenza virus acquires the capability to jump from animal to human host, a pandemic can result. The most recent example of this occurred in 2009 when the pandemic H1N1 (pH1N1) virus emerged from swine causing the first influenza pandemic of the 21st century. Over the subsequent decade, it has circulated as a human seasonal virus, causing further morbidity and mortality worldwide.

The ability of an influenza virus to infect and transmit between humans is multifactorial. In recent years, pH stability of the haemagglutinin (HA) surface protein has been realised as an important property associated with human adaptation and transmission. Understanding how pH stability impacts on virus/host interactions that support replication and transmission in humans is important for improving risk assessment of emerging viruses with pandemic potential.

In this study, recombinant influenza viruses with point mutations that alter the pH stability of pH1N1 HA were used to investigate the consequences of pH stability for pathogenicity and transmissibility. The data show that a stable HA is beneficial for virus infectivity in the mammalian upper respiratory tract, enabling virus to withstand the acidic environment. Conversely, entry into host cells via endosomal uncoating is facilitated by a HA that is less pH stable. A novel technique for isolating influenza virus directly from air exhaled by infected ferrets revealed that HA stability enhances virus survival in airborne droplets. However, using the same apparatus airborne virus was not isolated from human volunteers infected with pH1N1 virus.

Our findings indicate that different influenza viruses may show variation in how well they are controlled by antiviral strategies targeting pH-dependent steps in the virus replication cycle and how effective they are as part of nasally-administered live attenuated vaccines.

Table of contents

Abbreviations

ALI	Air-liquid interface
ANOVA	Analysis of variance
AUC	Area under the curve
B/Vic	B/Victoria lineage
BafA1	Bafilomycin A1
BSA V	Bovine serum albumin fraction V
Cal04	A/California/04/2009 (H1N1)
Cal09	A/17/California/2009/38 (H1N1)
$CCID_{50}$	50% Cell culture infectious dose
CDC	Centre for Disease Control and Prevention
CPE	Cytopathic effect
Ct	Cycle threshold
DMEM	Dulbecco's modified eagle medium
DNA	Deoxyribonucleic acid
EEA	European Economic Area
EID_{50}	50% Egg infectious dose
Eng09	A/England/195/2009 (H1N1)
EU	European Union
FCS	Foetal calf serum
FFA	Focus forming assay
FFU	Focus forming unit
GISRS	Global Influenza Surveillance and Response System
GMP	Good manufacturing practice
HA	Haemagglutinin
HPAI	Highly pathogenic avian influenza
IFITM	Interferon-induced transmembrane

IFN	Interferon
IIV	Inactivated influenza vaccine
IVTT	Influenza virus transmission tunnel
LAIV	Live attenuated influenza vaccine
LMIC	Low and middle income country
LRT	Lower respiratory tract
M	Matrix protein
MDCK	Madin-Darby canine kidney
MDCK-SIAT	MDCK cells expressing increased levels of α2,6-linked sialic acid
MDV	Master donor virus
MOI	Multiplicity of infection
NA	Neuraminidase
NEAA	Non-essential amino acids
NEP	Nuclear export protein
NGS	Next generation sequencing
NP	Nucleoprotein
NS	Non-structural protein
p.i.	Post inoculation
PA	Polymerase acidic protein
PB1	Basic polymerase 1
PB2	Basic polymerase 2
PBS	Phosphate buffered saline
PCR	Polymerase chain reaction
PFU	Plaque forming unit
pHNEC	Primary human nasal epithelial cell
PR8	A/Puerto Rico/8/34 (H1N1)

PS	Penicillin and streptomycin
RCT	Randomised controlled trial
RD	Respiratory droplet
Rg	Reverse genetics
RNA	Ribonucleic acid
RNP	Ribonuclear protein
RT-qPCR	Real time quantitative PCR
SA	Sialic acid
SPF	Specific pathogen free
$TCID_{50}$	50% Tissue culture infective dose
UK	United Kingdom
URT	Upper respiratory tract
USA	United States of America
vATPase	Vacuolar ATPase inhibitor
VE	Vaccine effectiveness
WHO	World Health Organisation
WT	Wild type

List of Figures

List of Tables

Chapter 1. Introduction

Influenza viruses, of which there are four types (A, B, C and D), are members of the *Orthomyxoviridae* family(1). Humans are the main host of influenza B and C viruses, influenza D viruses primarily infect cattle, whereas wild aquatic birds are the natural hosts for the majority of influenza A viruses(2). Of the four types of influenza virus, only influenza A viruses pose a risk of zoonotic infection and pandemic potential. Influenza A viruses are classified into subtypes based on their haemagglutinin (HA) and neuraminidase (NA) surface proteins, with 16 known HA and 9 NA subtypes detected in avian reservoirs. Two further "HA and NA-like" subtypes were recently isolated from influenza A-like viruses residing in bats(3) Among the diverse pool of influenza A viruses in animal reservoirs, only a limited number succeed in crossing the species barrier to infect humans and fewer still can establish sustained human-to-human transmissibility(4). To date, only H1, H2 and H3 HA subtypes and N1 and N2 NA subtypes are known to have established circulation in the human population. Other influenza A subtypes, such as H5N1, H7N9, H7N7 and H9N2, have infected humans in small numbers but with limited success in onward transmission.

1.1 Influenza A Virus Structure

The internationally accepted naming convention for influenza A virus strains is as follows: genus - host of origin – geographical origin - isolate number - year of isolation - HA and NA subtype; for example, A/duck/Alberta/35/1976 (H1N1). For viruses isolated from humans, the host of origin is excluded, such as A/England/195/2009 (H1N1)(2). Morphologically, the influenza virion can exist in spherical(5) or filamentous forms(6). Its genome is comprised of eight segments of

negative-sense single-stranded RNA. The eight gene segments each encode a major viral protein - PB1, PB2, PA, NP, HA, NA, M and NS1 - with multiple other proteins also expressed via alternative splicing or alternative reading frames. Examples of these include M2, NEP/NS2, M42, NS3, PB1-F2, PB1-N40, PA-N155, PA-182 and PA-X(7). The ribonucleoprotein (RNP) complex, which includes the viral RNA, heterotrimeric viral polymerase (PB1, PB2, PA) and several copies of the nucleoprotein (NP), is encapsulated by a lipid envelope which contains the HA and NA glycoproteins and well as the matrix M2 ion channel protein (Figure 1.1). Host proteins are also incorporated within the influenza virion(8).

A B

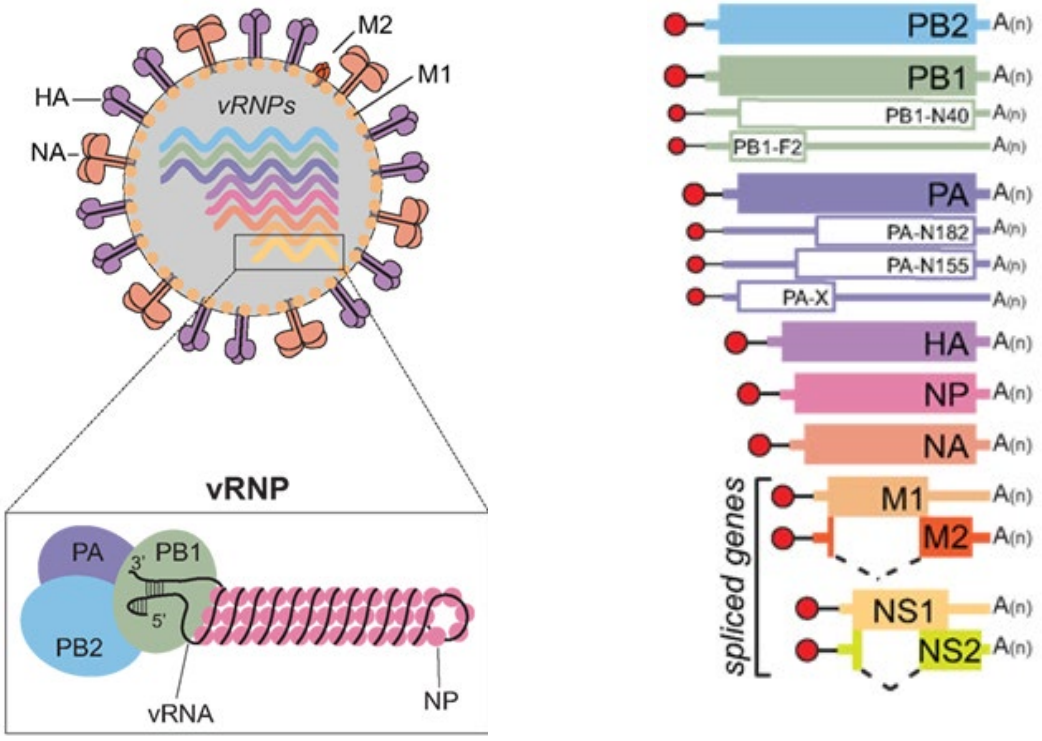

Figure 1.1 Structure of the influenza A virus. (A) Schematic diagram of the influenza A virion and viral ribonucleoprotein (vRNP). (B) Influenza viral proteins are represented by coloured boxes. Dashed lines depict alternative splicing of M and NS transcripts. The accessory proteins found in many strains are illustrated by empty boxes. Rarer proteins PB2-S1, M42 and NS3 are not shown. Image sourced from Dou *et al.* (2018) (7).

1.2 Influenza A Virus Life Cycle

Influenza A virus replication in humans and other mammals primarily takes place in epithelial cells of the respiratory tract. The viral life cycle is illustrated in Figure 1.2. In wild birds, the natural hosts of influenza viruses, the primary site of infection is epithelium of the intestinal tract. Virus attaches to its target cells via HA which binds to terminal sialic acids (SA) present in the oligosaccharides of glycoproteins and glycolipids at the cell surface(9). After binding, the virus is internalized into the acidic environment of endosomes. The virion is trafficked from early to late endosomes until a threshold of acidic pH triggers a conformational change in HA that results in fusion of the viral and endosomal membranes(10). Protons entering the virion core via the M2 ion channel protein lead to dissociation of M1 from the RNPs. Free viral RNPs are released into the cytoplasm and subsequently transported to the nucleus, a process involving an interaction between the nuclear localization signal on NP and cellular proteins such as importin α/β(11). The site of viral transcription and replication of influenza viruses is within the nucleus. The influenza polymerase first transcribes viral RNA into mRNA by “cap-snatching” host cellular mRNAs to use as 5’ primers(12). Viral mRNAs are exported into the cytoplasm for translation. To replicate its genome, the virus synthesizes complementary RNA (cRNA), which then functions as a template to copy further negative-sense viral RNA, occurring in a primer-independent manner. Newly synthesized viral RNP complexes are transported out of the nucleus by M1 and NEP(13). The envelope proteins HA, NA and M2 mature via the endoplasmic reticulum and trans Golgi network. Assembly and budding of progeny virions occurs at the plasma membrane where budding of new viral particles occurs at lipid raft microdomains(14). NA then cleaves sialic acids on the host cell to prevent aggregation of newly released viral particles. Upon virus release, the HA protein is cleaved by exogenous serine proteases present in the

human respiratory tract, which activates the fusogenic capacity of HA and enables the virus to infect the next host cell(15).

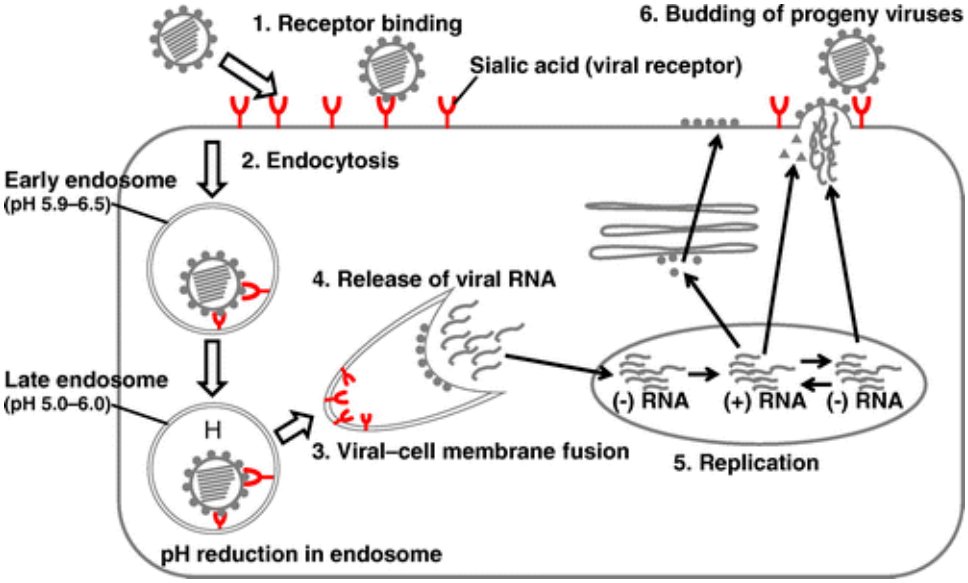

Figure 1.2 Schematic diagram of the influenza virus life cycle. Image sourced from Dadoji *et al*. (16) (Mary Ann Liebert, Inc., New Rochelle, NY).

1.3 A Focus on Haemagglutinin

HA is a homotrimeric glycoprotein that covers ~80% of the viral surface(5) and constitutes the major viral antigen. It has two critical functions in the viral life cycle – receptor binding and membrane fusion. The membrane fusion capacity of HA is the primary focus of this Thesis.

1.3.1 HA phylogeny and numbering

HA subtypes have been phylogenetically subdivided into two groups. Group 1 consists of subtypes H1, H2, H5, H6, H8, H9, H11, H12, H13, H16 and Group 2

contains subtypes H3, H4, H7, H10, H14 and H15(17) (Figure 1.3). The length of influenza HA varies between subtypes and strains, which can render a level of complexity when comparing amino acid changes between HA subtypes. Insertions, substitutions and deletions within HA can occur in a strain/subtype-specific manner as well as differences in the length of the N-terminal signal peptide cleavage site(18). Subtype-specific HA numbering can be used but means that comparisons across subtypes are not straightforward. The historically favoured “H3 numbering scheme” based on A/Aichi/2/68 (H3N2) is frequently cited, particularly in the context of receptor binding mutations. To reduce confusion in the field, Burke and Smith(18) described a reference numbering system based on the mature HA sequence by analysing known HA structures to identify amino acids that are structurally and functionally equivalent across all HA subtypes. This reference numbering scheme is used in this Thesis unless otherwise stated.

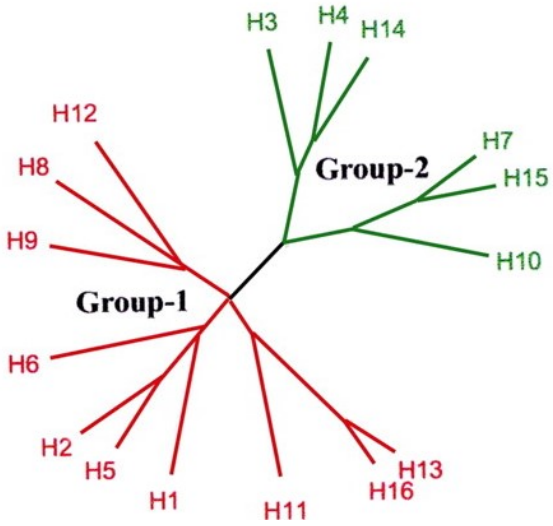

Figure 1.3 Influenza HA phylogeny and numbering. (A) Phylogenetic grouping of the 16 HA subtypes. Image sourced from Gamblin *et al*. (17).

1.3.2 Structure and functions of haemagglutinin

The influenza HA glycoprotein has a molecular weight of 220K and is organised as a trimer of three identical monomers. Each monomer contains two subunits, HA1 and HA2. HA2 chains form major components of the proximal stem region, which forms the centre of the molecule. The HA1 chains also contribute to the stem structure but primarily form the three distal globular head domains (Figure 1.4A)(19,20).

1.3.2.1 Antigenicity, receptor binding and cleavage

HA is the main target for the host neutralising antibody response. Serum haemagglutination inhibition (HI) titres are a major correlate for protection against influenza. Five antigenic sites have been defined in the HA head and are referred to as Sa, Sb, Ca1, Ca2 and Cb(21). The location of these is shown in Figure 1.4B. The receptor-binding site (RBS) is a shallow pocket of conserved residues located on the distal head of the HA molecule between Sb, Ca2 and Sa. The edges of the RBS are formed by the 130-loop, 190-helix and 220-loop and the base contains four highly conserved residues (Y98, W153, H183 and Y195) (H3 numbering) (Figure 1.4C)(22). The HA protein is synthesised as a polypeptide precursor (HA0) which becomes glycosylated and is assembled into homotrimers that travel via the Golgi apparatus to the plasma membrane. HA0 must be post-translationally cleaved by host proteases into two subunits, HA1 and HA2, to activate its fusogenic potential and infectivity(23).

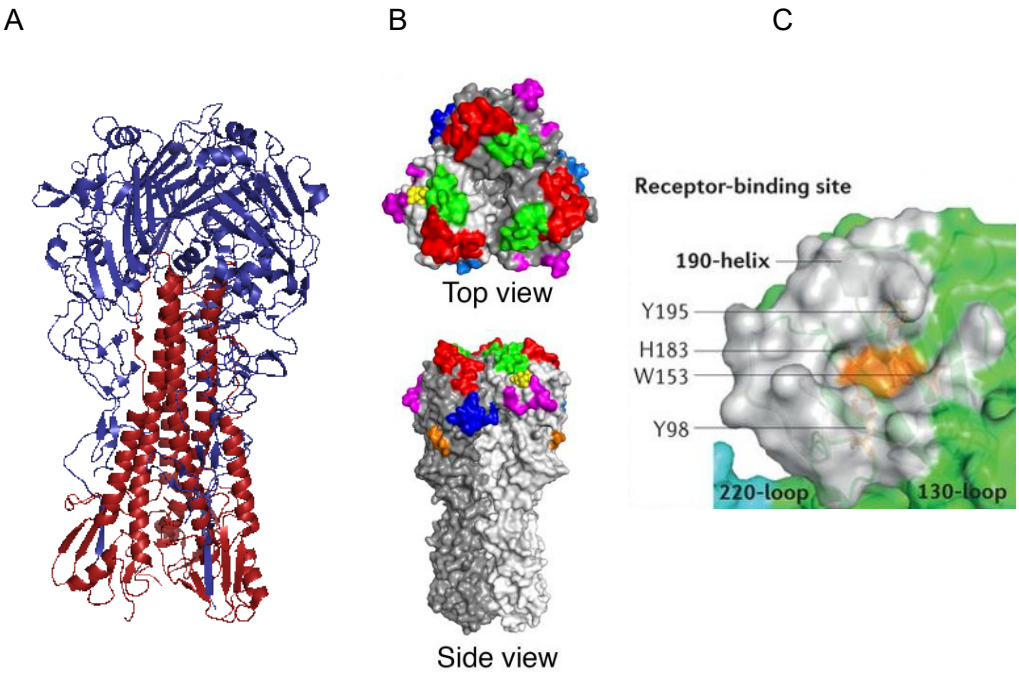

Figure 1.4 The influenza haemagglutinin surface protein. (A) Structure of the HA trimer with HA1 coloured blue and HA2 coloured red (modelled using Pymol molecular visualisation tool (PDB: 4jtv). (b) Antigenic sites shown on the HA trimer are coloured as follows: Sa in red, Sb in green, Ca1 in blue, Ca2 in magenta, and Cb in orange. Image sourced from Liu *et al*. (24). (C) shows a sialic acid molecule (coloured yellow) present in the HA receptor binding pocket and is sourced from Shi *et al*. (22).

1.3.2.2 Membrane fusion

Upon HA cleavage, the hydrophobic N-terminus of HA2 (known as the fusion peptide) relocates to the interior of the trimer, priming it for pH-induced membrane fusion. HA is held in a high-energy (metastable) state that can be triggered to undergo an irreversible conformational change when exposed to an environmental cue(10). In an experimental setting, low pH, heat and urea exposure have been described to be capable of triggering HA unfolding(25) but all of the potential triggers for HA in its native state are perhaps not fully recognised.

As discussed in Section 1.2, incoming influenza virions are trafficked from early (~pH 5.4-6.2) to late (~pH 5.0-5.5) endosomes. Once triggered by low pH, conformational change in HA enables the hydrophobic fusion peptide to insert into the opposing endosomal membrane. A cluster of HAs form a “fusogenic unit”, suggested to include three to four HA units(26,27). Insertion of the fusion peptide into the endosomal membrane connects the two lipid bilayers through a postulated extended intermediate. Lipid mixing of outermost opposing membranes (known as “hemifusion”) is followed by formation of a “fusion pore” through which RNPs can escape to the cytoplasm (Figure 1.5A)(26).

It is generally believed that influenza virus fusion and release occurs in late endosomes where intraluminal pH is acidic enough to trigger HA fusion, although direct evidence is lacking. Endosomal acidification is mediated by host vacuolar ATPase proton pumps that deliver protons to the endosomal lumen(28). If the viral genome is released too early in the endocytic pathway, prolonged exposure to the cytosolic environment may make it less likely that RNPs can navigate to the nucleus without becoming inactivated. On the other hand, if the virus is too acid stable, fusion may not be triggered before the virus is trafficked to degradative lysosomes (Figure 1.5B).

It has been suggested that the exact compartment that HA triggering occurs may vary depending on the acid stability of the particular strain and endosomal pH range within a given cell type. HA pH stability can be altered by mutations located throughout the HA molecule, with 50-100 mutations implicated to either stabilise or destabilise HA (29). These stability-altering mutations are frequently located in regions of HA that undergo extensive rearrangement during the fusion process, including the stem region close to the fusion peptide or the interface between the three subunits of the HA trimer(30–32). M and NA proteins have also been shown to

influence pH stability(33,34). For these reasons, predicting the effect of HA mutations on pH stability via sequence analysis and/or modelling is usually not reliable and phenotypic assays are necessary to assess HA pH stability(30). Some of the phenotypic assays that have been used to characterise pH stability and their limitations are discussed below.

A

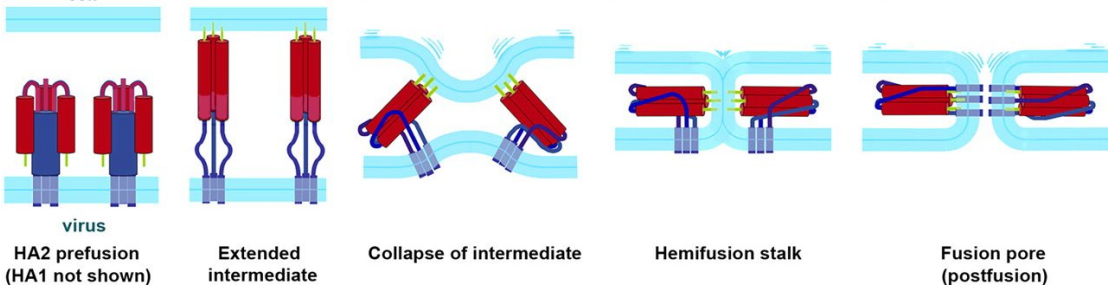

B

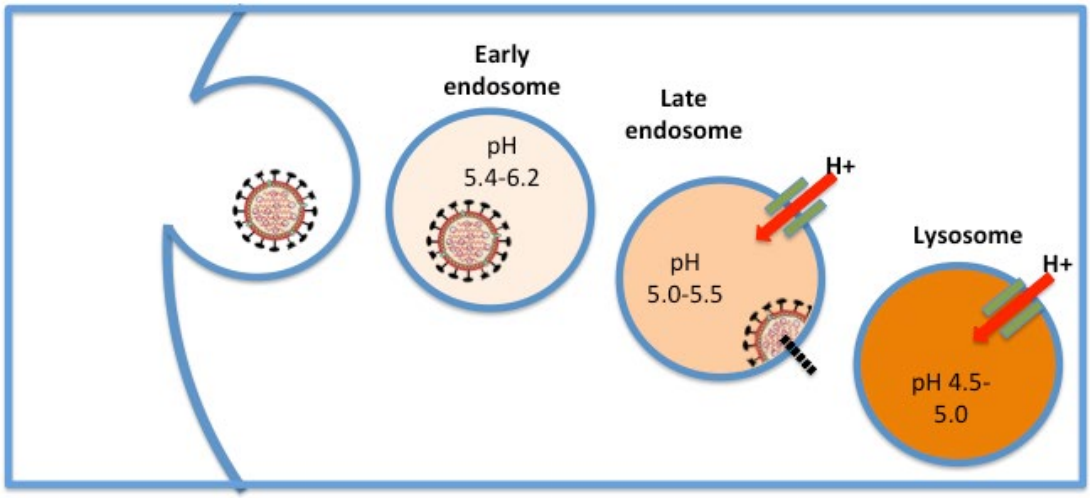

Figure 1.5. Membrane fusion of influenza haemagglutinin. (A) Proposed mechanism for virus fusion, sourced from Floyd *et al.*(26), (B) Schematic diagram of influenza entry in the endosomal pathway.

Phenotypic assays to measure HA membrane fusion

When assessing viral fusogenic capacity it is important to consider several aspects of the process including the pH at which fusion first occurs, the extent and rate that fusion proceeds and the ability of HA to remain fusogenic under low pH conditions. Several terms are interchangeably used in the literature to refer to membrane fusion potential of HA including “pH of fusion”, “pH of HA activation”, “pH sensitivity” and “pH or acid stability”. A variety of phenotypic assays have been used to characterise HA fusogenic capacity.

Cell-to-cell fusion assays. Cells are with transfected with HA or infected with the virus of interest and exposed to low pH conditions to induce cell-to-cell fusion that can be observed visually as “syncytia” or read out via dye transfer or reporter gene expression(30). This type of assay is useful in identifying the pH at which membrane fusion is first initiated but does not offer any information on the kinetics of fusion beyond that. Whether the fusion response of HA when it is expressed at the cell surface accurately reflects its behaviour as it exists on the surface of a virus particle fusing with an endosome is unclear. The distribution and quantity of cell-expressed HA and the curvature of the membrane on which it is expressed is likely to be different from in its native state. This is particularly relevant where transfected HA is used which does not include the intact viral membrane or secondary proteins that may impact of fusogenicity.

Acid inactivation assays. A sample of influenza virus can be tested for its ability to withstand inactivation following exposure to varying low pH buffers. The quantity of infectious virus remaining can be read out by standard infectivity assays such as plaque assay, $TCID_{50}$ or haemagglutination assay(35). Thus, the “pH of HA activation” may be described by a particular point such as when 50% or 90% of viruses have become non-infectious. HA inactivation and loss of viral infectivity can also be triggered by heat or urea and HA fusogenic potential can be assessed using these factors as surrogates. The limitation of these types of assay is that the response of HA to acidic stimuli is being assessed in the absence of a target membrane. However, the assay can be useful for understanding the ability of the HA to remain fusogenic under acidic conditions.

Single particle tracking. New assays that employ total internal reflection fluorescence microscopy (TIRF) of dye-labelled virions can enable detailed analysis of the sequence of molecular steps involved in the fusion process. For example, the kinetics of fusion (when is it fastest and most abundant), rates of hemifusion and pore formation and can pinpoint when fusion activity stops(26,36–39).

1.4 Influenza epidemics and pandemics

1.4.1 The burden of influenza in humans

Four influenza viruses currently circulate amongst humans: A/H1N1, A/H3N2, B/Yamagata lineage and B/Victoria lineage. In temperate regions, influenza causes seasonal epidemics during winter months whilst in tropical climates the virus can circulate throughout the year and cause unpredictable outbreaks. Human seasonal epidemics occur with an average reproductive number of 1.28 and attack rate of 10-20%(40). The burden of annual seasonal influenza is relatively underappreciated, particularly in low-and-middle income countries (LMIC), where surveillance structures are less robust(41). Over the past 100 years, the overall burden from seasonal influenza is likely to surpass that which has occurred due to pandemics(42). Reliable and timely estimates of the burden of annual influenza disease and resultant economic impact are critical to aid decision-making on public health policy such as vaccination programs.

Within the EU/EEA, influenza ranked top of the list of 31 infectious diseases, contributing 30% of the annual disease burden in a study from 2018(43). Globally, the WHO estimates that seasonal influenza may result in 290 000-650 000 deaths each year due to respiratory disease alone(44). Moreover, a significant proportion of the morbidity and mortality from influenza is not due to the primary infection itself but a consequence of complications and secondary infections that may arise after viral replication has ceased. Rates of hospitalisation and death attributable to influenza are highest in certain “at risk” groups: the elderly (>65 years), very young (<5 years) and patients with underlying comorbidities(40).

1.4.2 Antigenic drift and antigenic shift

Influenza viruses are highly diverse and constantly evolving. They have high mutation rates (estimated at $>10^{-3}$ substitutions per site per year) resulting from an error prone RNA polymerase that lacks proofreading capability(45). Point mutations in the antigenic regions of the HA and NA surface proteins that allow evasion of host immune responses can arise, which is known as antigenic drift. Further diversity is generated because of the segmented nature of the influenza genome. Coinfection of a single host cell with two different influenza A viruses can result in genetic reassortment and generation of progeny viruses containing a novel composition of gene segments from both parental viruses. This phenomenon, known as antigenic shift, can result in the emergence of completely novel viruses to which prior immunity is lacking within the human population and the potential for a pandemic to result. As well as wild birds and humans, influenza A viruses infect a wide range of animal hosts. Pigs are susceptible to infection with both avian-origin and human-origin influenza viruses and thus are thought to be a potential “mixing vessel” where genetic reassortment could result in viruses with pandemic potential.

1.4.3 Influenza pandemics of the 20th Century

An influenza pandemic requires that an animal or animal-human influenza A virus crosses the species barrier and establishes efficient human-to-human transmission. The new virus is antigenically different from previously circulating strains and the human population therefore lacks pre-existing immunity, which can result in rapid spread and increased severity of illness. In the 20th century, 3 influenza pandemics occurred, as detailed in Table 1.1.

Pandemic (date and common name)	Considered Area of Emergence	Influenza A Virus Type	Estimated Case Fatality Rate	Estimated excess mortality worldwide	Age groups most affected (simulated attack rates)
1918-1919 Spanish Influenza	Unclear	H1N1	2-3%	20-50 million	Young adults
1957-1958 Asian Flu	Southern China	H2N2	<0.2%	1-4 million	Children most affected
1968-1969 Hong Kong Flu	Southern China	H3N2	<0.2%	1-4 million	Across all age groups

Table 1.1. Pandemics of the 20th Century. Source: European Centre for Disease Prevention and Control.(46)

The 1918 influenza pandemic was the most devastating of these, resulting in an estimated 20-50 million deaths worldwide and estimated to have infected 30-50% of the global population. Young adults were the worst affected, a group that usually has low mortality rate from influenza(47). Secondary bacterial pneumonia was a critical contributor to death from 1918 influenza, prior to the discovery of antibiotics(48). In an attempt to reconstruct the 1918 H1N1 virus and understand its high virulence, sequencing of lung autopsy material was undertaken in 1997(49). Subsequent experiments(50–53) to characterise its virulence using recombinant virus constructs containing some or all of the genes from the 1918 virus identified several important traits. The 1918 virus is able to replicate *in vitro* in the absence of the protease trypsin and attains high titres upon infection of human airway cell cultures. Protease cleavage and activation of haemagglutinin is restricted to the respiratory tract for most influenza viruses but the 1918 virus can be cleaved by ubiquitous cellular

proteases and therefore replicate systemically(54). In animal models, recombinant 1918 virus was more pathogenic than seasonal influenza viruses(55). The virus spread rapidly throughout the respiratory tract and induced an aberrant innate immune response (known as a “cytokine storm”) resulting in pulmonary infiltration of inflammatory cells and acute haemorrhage. The viral genetic composition and its high replicative ability in human cells together with induction of a “cytokine storm” are believed to be important contributors to the severe disease and mortality from the 1918 virus. The origins of the 1918 virus remains controversial, with some believing its viral ancestor to be solely of avian origin and others challenging this hypothesis(56–58).

In 1957 a H2N2 virus emerged and displaced the H1N1 virus that had been circulating since 1918. This virus was a reassortant containing avian-origin HA, NA and PB1 genes and the remaining five genetic segments from the circulating human H1N1 virus. The virus circulated in the human population until 1968 when it was displaced by another reassortant virus. This H3N2 virus, which continues to circulate today, possessed a novel avian-origin HA and PB1 and the remaining six genes from the circulating H2N2(59).

A further event of note occurred in 1977 when a H1N1 virus was introduced into the human population and began to co-circulate with H3N2. This virus caused mild disease, mainly in those aged <20 years(60). It was found to have near identical sequence to H1N1 viruses circulating in the 1950s(61), suggesting the possibility of accidental laboratory release, although the source of this virus is unconfirmed.

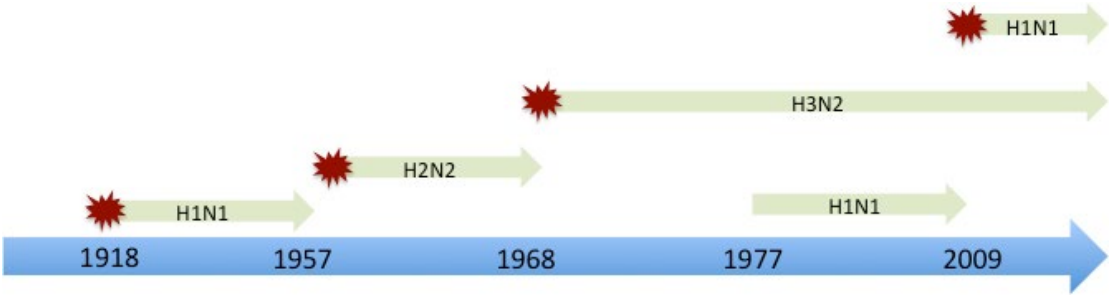

Figure 1.6 Timeline of human influenza circulation. Adapted from Krammer *et al.* (62).

1.4.4 The 2009 H1N1 influenza pandemic

The first pandemic of the 21st century occurred in 2009 when a swine-origin H1N1 virus emerged in Mexico and established sustained circulation in the human population. This virus resulted from reassortment between a triple-reassortant North American swine virus (containing a combination of avian, human and swine-origin gene segments) and a Eurasian avian-like swine virus(63) (Figure 1.6). The resultant virus was readily transmissible between humans, rapidly spread across the globe and displaced the previously circulating seasonal H1N1 virus from 1977.

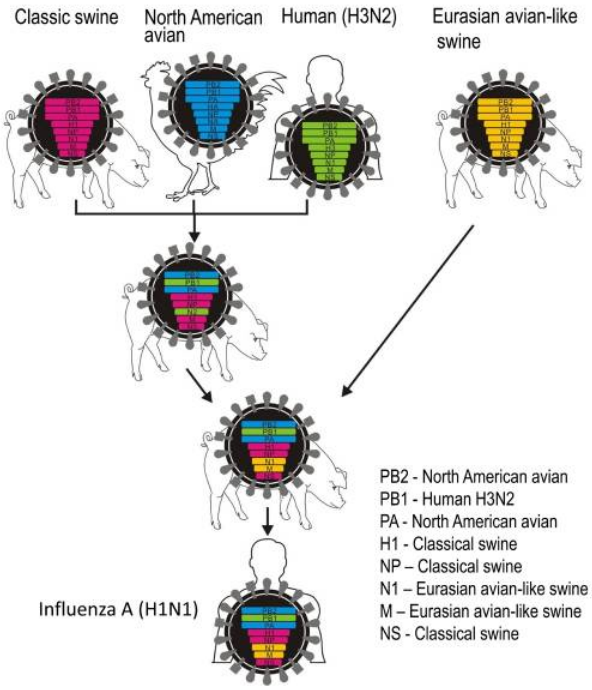

Figure 1.7 Origins of the 2009 pandemic H1N1 virus. Image sourced from Neumann *et al.* (64).

The first confirmed case of 2009 pandemic H1N1 (pH1N1) was from a 6-month-old child in Mexico who became unwell in late February 2009. By the end of April, two months after the first confirmed case, the virus had been detected in seven countries across several continents (Canada, Israel, Mexico, New Zealand, Spain, UK and USA). The virus continued to spread swiftly across the globe and on June 11th 2009, the WHO declared the start of an influenza pandemic, by issuing a phase 6 pandemic alert(65). The first two UK cases were confirmed on 27th April in travellers returning from Mexico. The first wave of illness in the UK peaked in July and subsided by mid-August after school closures for the holiday period. Second wave and third waves of activity were detected in autumn/winter of 2009-2010 and then 2010-2011 respectively(66). The WHO declared the end of the pH1N1 pandemic on August 10th 2010.

In total, the WHO reported ~18,500 laboratory-confirmed deaths from pH1N1, but the global mortality burden is likely to be higher. Modelling studies(67,68) have estimated ~100,000-400,000 respiratory deaths with an additional 83,000 cardiovascular deaths associated with 2009 pH1N1. 51% of respiratory and cardiovascular deaths occurred in Southeast Asia and Africa. The majority (estimated at 62%-85%) affected were aged <65 years, compared to only 19% in this age group in seasonal years(67). Although overall mortality from the 2009 pandemic was not significantly greater than in seasonal years, the number of years of life lost (estimated at 9,707,000 during the first 12 months of the pandemic) is reportedly 3.4 times higher than from seasonal epidemics, reflecting the disproportionate toll on young people(68). The relatively low attack rate in the elderly suggests some pre-existing immunity.

The emergence of a H1N1 pandemic virus in 2009 was completely unpredicted by the influenza research community where focus had been on the potential threat from H5N1 viruses circulating in birds in Asia and causing spill over human infections. The 2009 influenza pandemic highlighted the need for a broad and flexible pandemic

preparedness policy and has provided an unprecedented opportunity to study the emergence and adaptation of a novel zoonotic virus to human beings.

1.4.5 Influenza at the animal-human interface

In addition to the four pandemic viruses of the past 100 years, a number of avian or swine viruses have crossed the species barrier to infect humans but have failed to cause sustained onward transmission. The majority of these cases have been a result of direct human contact with infected poultry, pigs, or contaminated environments(69). These events have caused considerable public health concern and economic losses. Large-scale animal culling, closures of live poultry markets, animal vaccinations and surveillance initiatives have been initiated in response to these zoonotic infections(70). Of particular note, outbreaks of the highly pathogenic H5N1 avian influenza virus resulted in 455 human fatalities and 861 infected cases between 2003-2017, a case fatality rate of 53% (data as of 20 June 2019)(71). In 2013, human infections with avian H7N9 were detected in China and this virus went on to cause 1,568 laboratory-confirmed human infections in annual waves. The fifth wave in 2016/17 led to the emergence of a highly pathogenic strain that subsequently caused 33 human infections (data as of 20 June 2019)(71). The major concern has been that one of these viruses could evolve to efficiently infect and sustain human-to-human transmission and initiate a severe pandemic. However, since the introduction of poultry vaccination in China in 2017, cases of H7N9 have declined. Moreover, only one human case of H5N1 has been detected since February 2017. However, new concerns have been raised about avian infections with highly pathogenic H5N6 and H5N8 subtypes, although these viruses are yet to cause much human disease.

Given the potentially severe medial, social and economic consequences of an influenza pandemic, there is emphasis on the need for robust preparedness policies and to take action on “lessons learnt” during the 2009 pandemic. In addition to surveillance of human influenza infections, surveillance in domestic and wild animals and in humans who are exposed at the animal–human interface is critical to pandemic preparedness. To this end, the WHO Global Influenza Surveillance and Response System (GISRS), a coordinated global network of public health laboratories, has been set up to review surveillance data to monitor influenza epidemiology, alert for novel influenza viruses, assess pandemic risk and select candidate vaccine viruses for vaccine development.

1.5 Viral determinants of cross-species transmission

Cross-species transmission events (known as “host jumps”) often result in rapid viral evolution for adaptation to the new host. In order to risk assess the possibility that an emerging influenza virus could provoke a human pandemic, it is critical to understand the minimal adaptive changes that are required for the virus to efficiently replicate and transmit in humans. Animal models (mice, guinea pigs and ferrets) play a key role in delineating mammalian adaptation requirements for avian viruses and understanding their pathogenicity in mammalian hosts. Ferrets are used to assess the ability of influenza viruses to transmit through the air and this information feeds directly into pandemic risk assessment algorithms that have been derived by WHO (72) and CDC(73).

A body of research has identified a variety of adaptations that can enhance viral replication, pathogenicity and/or transmission in mammals, with HA being a critical

determinant. Influenza viruses that are adapted to humans have mutations in key residues in the RBS of HA that are thought to increase binding to α2,6-linked SA, whereas avian influenza viruses usually have affinity to α2,3-linked SA(74). α2,6-linked SA is prevalent in the human URT(75) where as duck intestines, the site of replication for avian influenza viruses, predominantly express α2,3(76). Both α2,3- and α2,6- linked SA have been detected in the human LRT(77). It is thought that the lack of α2,3-linked SA in the URT is an important factor that restricts avian viruses from efficiently infecting and transmitting amongst humans. It has been observed that that the topology of α2,3- and α2,6- linked SAs differ, with α2,3-linked SA being more “cone-shape” and α2,6-linked SA being “umbrella shaped”(78). Specific mutations in HA have been characterized that alter receptor binding specificity toward α2,6 binding, notably E190D/G225D for H1 viruses and Q226L/G228S for H2/H3 viruses (H3 HA numbering)(79–81). Importantly, it has been shown that mutations that increase α2,6 SA binding can support transmission through the air(82,83) although fundamental questions still remain on why and how α2,6 binding correlates with mammalian adaptation. Mutations in the PB2 protein, notably E627K and D701N (or residues 590/591 in 2009 pH1N1) have also been shown to be critical for efficient replication in mammalian cells(84) and transmission through the air(85,86). The E627K mutation may adapt influenza viruses to use the host factor acidic nuclear phosphoprotein 32kDa (ANP32) that is present in a shortened form in humans compared to birds(87). Other viral adaptations described to be required for human-to-human transmission include filamentous morphology(88), a longer NA stalk length(89), HA-NA balance(90), and antagonism of interferon production by NS1(91).

1.5.1 Gain-of-function experiments on highly pathogenic avian H5N1 influenza

In 2012, two controversial studies were published which used a “gain-of-function” approach aiming to understand the minimal requirements for a highly pathogenic avian H5N1 virus to transmit through the air between ferrets, a model for human transmissibility. Herfst *et al*.(92) introduced HA receptor binding mutations Q226L/G228S and the PB2 mutation E627K into A/Indonesia/5/2006 (H5N1). The receptor binding mutations resulted in an increase in the HA pH of activation. After ten passages in the ferret URT, an airborne transmissible virus was generated which had acquired two further mutations in HA - H110Y (which increases the pH stability of HA) and T160A (which results in the loss of a potential N-linked glycosylation site in the HA head). The second study by Imai *et al*.(93) took a slightly different approach introducing the HA receptor binding mutations Q226L and N224K into a different strain of H5N1, A/Vietnam/1203/2004. These residues were selected via random mutagenesis of the HA head which identified mutations that resulted in increased α2,6-linked SA binding. The receptor binding mutations also increased the pH of HA activation. They reassorted this H5 HA with the remaining seven genes from a pH1N1 virus and passaged the resultant virus in ferrets, leading to generation of an airborne transmissible virus. This ferret-passaged airborne transmissible virus had acquired 2 further mutations: T318I (which increased the pH stability and thermostability of HA) and N158D (which results in loss of the same glycosylation site as in the study by Herfst *et al*.). These two studies yielded remarkably similar results and highlighted two previously under appreciated viral determinants of airborne transmissibility – HA stability and HA glycosylation. In this Thesis, the consequences of HA stability for viral infectivity, pathogenicity and transmissibility of influenza A viruses are explored.

1.6 Transmission of influenza between humans

To understand the barriers a zoonotic influenza virus must overcome to successfully infect humans and then transmit efficiently from human-to-human, it is critical also to understand the mechanisms of influenza transmission in humans. Influenza viruses can be transmitted between humans by direct contact, indirectly via contaminated fomites, or through the air in respiratory droplets and aerosols(94). The relative importance of each mode of transmission and the effect of environmental conditions on routes of transmission remain undefined. In a severe pandemic situation, understanding routes of human transmission is important for developing evidence-based public health policy and implementation of infection control interventions such as social distancing, hand hygiene or facemasks as well as advising on indoor environmental settings that may limit influenza transmission. In healthcare practice, advice on the use of surgical facemasks versus respirators and their ability to protect workers from influenza remains heterogeneous because of lack of understanding of the routes, modes and particle sizes mediating influenza transmission(94).

1.6.1 Contact transmission

Infectious particles can be transferred to the mucous membranes of the URT directly via self-inoculation after touching an infected person or surface. Particles released into the air by infected hosts may fall to ground and remain infectious to an onward host as contaminated fomites for a period of time. Influenza virus has been shown to remain viable on the hands(95,96) and environmental surfaces(97) for periods consistent with the potential for onward transmission. Yet, the extent and significance of virus deposition in the environment remains unclear. Studies have shown that

virus can remain viable on non-porous surfaces for longer periods of time than porous surfaces(97). However, the duration of surface virus retention is dependent upon the viral titre, the material and the microenvironment. Where others have sampled frequently touched surfaces in natural settings such as public transport(98), airports(99), hospitals(100) or day-care centres(101), detection of influenza virus has been inconsistent. Overall, whilst there is a lack of direct evidence to support a role for contact transmission in influenza spread it is generally believed to occur. Further experimental work is needed.

1.6.2 Droplet and aerosol transmission

Activities including breathing, talking, coughing and sneezing can release respiratory particles of different sizes into the air(102–106), the composition of which may change during acute infection. Shear forces generated by airflow acting on airway lining fluid can produce droplets. It has also been hypothesised that droplets are produced from reopening of collapsed small airways during normal breathing. These droplets can range in diameter from 0.001-1000μm depending on the site of origin within the respiratory tract and the mechanism of generation. Exhaled droplets can contain water, mucus, surfactant and pathogens. Additionally, volatile gases dissolve into droplets and can influence pH(107,108).

Practically, The Infectious Diseases Society of America define “respirable” particles as those <10μm that can deposit in both lower and upper airways and “inspirable” particles as those 10-100μm that predominantly deposit on upper airways(109). The terminology used to define respiratory particles by size has been heterogeneous throughout the literature. In the Thesis, the term “aerosol” is used to indicate particles <10μm including droplet nuclei resulting from dessication of larger droplets, that may travel both short and longer distances. The term “droplets” is used to indicate both

large particles (>20μm) that are likely to follow a more ballistic trajectory as well as intermediate particles (10-20μm) that are described to share properties of both small and large particles(110). Particle behaviour in the air, such as the time to sedimentation and distance of travel, can be inferred by size to some extent but is also affected by factors such as airflow streams and ambient conditions such as humidity and temperature(110). Therefore, assertions made on the behaviour of droplets purely based on size should be treated with caution. Indeed, one study showed that droplets up to 50μm can be carried to 6 metres away from an infected person in a high velocity expulsion such as a cough or sneeze(111).

Short-range “droplet transmission” describes spraying of infected large respiratory droplets directly onto the mucous membranes of a recipient host via coughing or sneezing. This would require close contact and/or inspiration by the susceptible host to occur directly after particle release by the infected case. Some have suggested that the dynamics of this make it an unlikely mode of transmission between humans but there is insufficient evidence to support or refute this(94). Short-range transmission could also occur via aerosols or droplet nuclei including at distances traditionally thought to be consistent with a “large droplet” transmission event.

Long-range “indirect transmission”, sometimes referred to as “airborne transmission” or “aerosol transmission”, can arise through inhalation of infected droplets, droplet nuclei or aerosols, which may deposit in upper and lower airways. Traditionally, influenza was thought to be a short-range transmissible pathogen. The contribution of long-range aerosol transmission in influenza spread remains a subject of debate(110,112,113).

1.6.3 The ferret model of influenza transmission

Ferrets (*Mustela putorius furo*) are the primary animal model used to investigate influenza transmissibility. Other animal models for influenza include mice, guinea pigs, cotton rats, hamsters and non-human primates. Small animal models are advantageous because they can allow for experimentation using more pathogenic influenza viruses, which could not be used to challenge humans and allow for sampling from a variety of body compartments.

Ferrets display clinical signs such as fever, nasal discharge and sneezing that are similar to that seen in human disease. Importantly, they can be infected with avian, swine and human influenza viruses without a need for prior adaptation of the virus and severe infection with extra-pulmonary spread is seen following infection with the HPAIs(114,115). Influenza viruses bind to sialic acids in the ferret respiratory tract that are distributed similarly to in humans(116) and ferret transmission patterns have been demonstrated to reflect transmission patterns observed in humans(117). In contrast, influenza viruses may require adaptation for robust infection of mice. Mice do not transmit influenza as readily as ferrets nor do they manifest typical human-like symptoms. However, mice confer an advantage of being relatively inexpensive allowing for larger scale experiments, with available immunological reagents and potential for genetic manipulation.

Typically, the ability of an influenza virus to transmit by direct and indirect routes is investigated by introducing a naïve ferret to the same cage as an infected donor ferret. This set up allows for all forms of transmission including direct contact, fomite, droplet and aerosol. To test for the ability of an influenza virus to transmit by an indirect route (droplets and aerosols emitted from the infected donor), which is more

challenging for the virus, naïve ferrets are housed in adjacent cages to the infected donor. Cages are separated by perforated panels and spaced with a small gap that allows for shared air but excludes any direct contact. Daily clinical assessment and quantification of viral titre via a nasal wash or nasal swab can be performed(115).

The ferret model has been critical in identifying virus gene segments and amino acid mutations that contribute to both pathogenicity and transmissibility and for assessing the potential for human-to-human transmission. In general, influenza viruses that cause sporadic zoonotic infections in humans are limited in their transmissibility to ferrets in adjacent cages whereas human seasonal viruses that have the capacity for sustained human-to-human transmission are readily transmitted in this experimental set up. Extrapolation of the results of ferret transmission studies to human infection should be performed carefully and with insight into the limitations, some of which are discussed below.

1.6.3.1 Inoculation dose and route

Traditionally, donor ferrets are inoculated by intranasal administration of high titres of virus (usually 10^4-10^6 PFU) in liquid suspension. This is not particularly reflective of the infectious dose in a naturally infected human. Moreover, the kinetics of ferret infection have been demonstrated to differ depending on inoculum dose, volume and route of administration, which limits comparisons between studies that use slightly different techniques(114). More recently, researchers have trialed inhalational exposure systems or chains of transmission that may offer a more representative mode of inoculation(103,118).

1.6.3.2 Virus quantification

For the most part, the daily or alternate day kinetics of infection in influenza-infected ferrets is assayed by quantifying virus from a “nasal wash” involving instillation of liquid into the ferret’s nostrils and collection of the expectorate, though an alternative is to obtain a nasal swab. However, these methods might artificially collect virus that would never be naturally released, or dilute inhibitory factors that otherwise negatively impact the survival of virus in respiratory droplets. There is a lack of understanding about the amount of infectious virus that is released into the air relative to that quantified by nasal washing/swabbing techniques.

1.6.3.3 Lack of reagents

A lack of ferret specific immunological reagents and incomplete ferret genome sequencing has limited investigation of immune responses in the ferret model. This limits the breadth of information that can be obtained from ferret experiments. In the influenza field, mouse models are employed for investigation of immune responses to infection.

1.6.3.4 Timing and distance of exposure

The engineering of ferret cages such as distance between adjacent cages (reported to vary between 3mm and 10cm) and perforation size between cages (reported to vary from 0.05 to 0.5cm^2)(115) may also affect results of transmission experiments.

In general, naïve sentinel ferrets are maintained in a close proximity to infected donors continuously for the course of an experiment (usually 5-14 days). This experimental set up therefore does not recapitulate human contact events, which are typically of much shorter duration and greater distance. Consequently, there is a paucity of information about the kinetics and spatial dynamics of influenza contagiousness in ferrets or humans. Environmental conditions such as temperatures, humidity and airflow can also have significant impact on transmissibility and should ideally be monitored and standardised.

1.6.3.5 Routes of transmission

The traditional set up of ferret transmission experiments into adjacent cages does not discriminate between transmission by respiratory droplets and aerosols, which can both occur over short range. One study by Andrewes and Glover (1941)(119) attempted to exclude droplet transmission by spacing ferrets 1.5m apart, separating them by S or U shaped ducts, or placing sentinel ferrets in cages above the infected donor. Similar work has also been carried out using a guinea pig transmission model(120) and both studies suggested that aerosols are a potential route of transmission. Zhou *et al*.(102) used an impactor positioned between cages to exclude droplets of different sizes and found that virus could transmit through the air in particles >1.5μm and that the presence of larger particles correlated with improved transmissibility.

1.7 Control measures for seasonal and pandemic influenza

1.7.1 Vaccines

Vaccines are the primary strategy to reduce the burden of seasonal influenza disease and to protect the population in the event of a pandemic. However, current manufacturing timelines take months to prepare a vaccine and in the early stages of a pandemic antiviral drugs are likely to play a critical role. In the 2009 H1N1 pandemic, a vaccine did not become available until 6 months after the start of the pandemic and a further 2 months were required for sufficient stocks to be prepared and distributed. Recommendations for seasonal vaccine strains also have to be made 6-8 months before production during which time the virus can undergo antigenic drift. Surge vaccine production in a pandemic situation may also be limited by availability of the embryonated chickens' eggs that are used to grow vaccine viruses. To overcome this, emerging egg-free techniques such as cell-culture grown vaccine viruses or recombinant DNA technologies are under development.

1.7.1.1 Inactivated influenza vaccines

The predominant type of influenza vaccine that has been available since the 1940s is the inactivated influenza vaccine (IIV). Overall, influenza vaccines have had only modest and unreliable effectiveness reported. A key problem, particularly for H3N2 viruses, has been the emergence of HA mutations during egg propagation that alter virus antigenicity(121). Vaccine effectiveness is particularly poor in the elderly population who suffer from a large proportion of seasonal disease. Immunity from vaccination is short-lived and requires annual updating. New technologies such as

addition of vaccine adjuvants or high dose vaccines are being developed with an aim to improve vaccine immunogenicity.

1.7.1.2 Live attenuated influenza vaccines

More recently, live attenuated influenza vaccines (LAIV) have been introduced in some countries. The six internal genes of LAIV are derived from a cold-adapted viral strain that is generated by passaging at low temperature (25°C). The LAIV is administered intranasally rather than by injection and vaccine viruses are restricted to replication in the upper respiratory tract and cannot replicate in the warmer temperatures of the lower respiratory tract, Consequently, vaccination results in a mild and self-limiting infection yet can stimulate a robust immune response. Whilst the IIV only stimulates a neutralising antibody response, it is thought that the LAIV can induce cellular, humoral and mucosal responses(122–124). LAIV has been used widely in Russia for over 50 years based on the backbone of cold-adapted master donor viruses (MDV) A/Leningrad/134/57 or B/USSR/60/69. In 2003, an LAIV product based on A/Ann Arbor/6/60 or B/Ann Arbor/1/66 MDV became licensed in the USA and is available for people aged 2–49 years. The same product has been available in Canada since 2010 for people aged 2–59 years, and in the European Union since 2011 in people aged 2–17 years. The LAIV was introduced into childhood vaccination programs in the UK in 2013 and in Finland in 2015.

1.7.2 Antiviral drugs

Two classes of antiviral drug are currently licensed to treat influenza and used worldwide – the adamantanes and the NA inhibitors. Antiviral drugs are predominantly targeted at patients with severe illness during an annual season and

are also used for post exposure prophylaxis. Stockpiling of antivirals forms part of pandemic preparedness strategies. Currently circulating H3N2 and pH1N1 influenza viruses are universally resistant to the adamantane drugs (amantadine and rimantadine), mediated by an S31N mutation in the M gene that has arisen and fixed. Adamantanes are ineffective against influenza B viruses(125). The NA inhibitors (NAIs) are therefore the sole remaining licensed class of drugs in current use. NAIs include oseltamivir (an oral drug), zanamavir (inhaled), peramivir (intravenous, licensed in the USA and EU) and laninamivir (inhaled, licensed in Japan). The emergence of oseltamivir resistance is of significant concern, particularly for H1N1 viruses. In 2007/8, oseltamivir resistance, mediated by the H275Y mutation in NA, emerged in seasonal H1N1 viruses and rapidly spread, becoming dominant by the 2008/9 season(126). Analysis has shown that on a background of other permissive mutations, H275Y does not confer a fitness cost to this H1N1 virus(127). Resistance to NA inhibitors has been observed to occur through multiple mechanisms yielding varied effects on viral fitness and can arise during drug treatment.

1.7.2.1 Novel antiviral drugs

There is a clear and pressing need for new anti-influenza drugs with a novel site of action. A number of new drugs have recently been licensed in other countries or are in the latter stages of the drug development pipeline. These include the polymerase inhibitor favipiravir (licensed in Japan), the inhibitor of cap-dependent endonuclease activity baloxavir marboxil (licensed in the USA and Japan) and the membrane fusion inhibitor umifenovir (arbidol, licensed in Russia and China). Resistance has been demonstrated to each of these drugs in pre-clinical or clinical settings(128–130) and so ideally, future treatment of influenza would involve a combination of drugs that can limit the emergence of drug resistance. When evaluating new drugs, it is crucial to

understand the potential for drug resistance and its effects on viral fitness, pathogenicity and transmissibility.

Thesis Aims

The overall aim of this thesis is to evaluate the consequences of changes in HA pH stability on the capacity of influenza A viruses to infect, circulate and cause disease in humans. Using recombinant viruses with altered pH of HA activation, the significance of pH stability for viral replication in human airway cells and for viral pathogenicity and transmissibility in mammalian models (mice and ferrets), are explored. Using a novel technique for collection of viable influenza viruses from the air, we investigate the hypothesis that increased HA stability can facilitate airborne transmission by enhancing virus survival as it travels between hosts within airborne droplets. Finally, the knowledge acquired is applied to investigate underlying reasons for the real-world problem of poor effectiveness seen in live attenuated influenza vaccines in recent years, which is hypothesised could be partially attributed to pH instability of the pH1N1 vaccine component.

Chapter 2. The significance of haemagglutinin stability for influenza A virus replication and pathogenicity

2.1 Introduction

HA pH stability is proposed to be a key host range barrier and determinant of influenza virus pathogenicity (29,30). It has been observed that influenza viruses that circulate seasonally amongst humans have more pH stable HAs (lower fusion pH) than those isolated from poultry or swine. Galloway and colleagues (131) tested representative viral strains from each of 16 HA subtypes using two different fusion assays and observed that human isolates tended to fuse at 0.1-0.5 pH units lower than avian isolates of the same subtype. Using a panel of human and avian isolates, Shelton *et al.* (132) observed a similar trend using a different fusion assay. Two studies (133,134) have reported an increased pH of fusion for viruses isolated from pigs relative to those that have subsequently circulated in humans. Taken together, these findings support the idea that evolving increased HA stability (low pH of fusion) is an important factor for a virus to jump from birds/pigs to humans. However, the biological explanation for this is not well understood.

2.1.1 HA stability and viral replication/pathogenicity in the avian host

H5N1 and H7N9 viruses that infect poultry and cause sporadic zoonotic infections have HA's that fuse at higher pH (5.6-6.0) (30,135). Du Bois and colleagues (136), using a H5N1 virus, showed that increasing HA activation pH between 5.2 and 6.0 correlated with increased replication and pathogenicity in chickens. Reed *et al.* (137)

engineered point mutations into a H5N1 virus with pH of fusion of 5.9 to investigate the impact of HA stability on pathogenicity in ducks. N114K (pH of fusion 6.4), Y7H (pH of fusion 6.3) and K58I (pH of fusion 5.4) HA mutants resulted in lower pathogenicity in ducks than the wild type virus. A H8Q mutation with pH of fusion of 5.6 had similar pathogenicity to the wild type virus, suggesting there is an optimum pH of fusion for pathogenicity in birds that exists between 5.5 and 6.2.

2.1.2 HA stability and viral replication/pathogenicity in the mammalian host

Seasonal human influenza isolates are more acid stable (pH of fusion ~5.0-5.4). The limited isolates that have been tested from the 1918, 1957 and 1968 pandemics also had a more stable HA (131,133). Table 2.1 summarises studies that have recorded a pH of fusion for human pandemic and seasonal influenza A virus clinical isolates. Interestingly, the 2009 pandemic H1N1 had an intermediate pH of fusion (~5.5) when it first emerged from swine. Russier and colleagues (134) showed that antecedent swine viruses had a higher pH of fusion and later circulating pH1N1 isolates were more stable (pH of fusion 5.2-5.4), suggesting that stabilising the HA supports human circulation. Similarly, Cotter *et al.* (138) found that a more recent pH1N1 isolate that had acquired an E47K HA2 mutation was more acid stable than a prototypic strain. To investigate the impact of HA stability on evolutionary dynamics, Klein *et al.* (139) analysed the genetic sequence of 9,797 pH1N1 and 16,716 H3N2 viruses isolated between 2009 and 2016 in order to derive a computational estimate of thermal stability. They found, in both pH1N1 and H3N2, that later viral variants were descended from virus lineages predicted to encode more stable HA proteins.

Virus strain	Subtype	Pandemic/Seasonal	pH of fusion	Source
A/California/4/2009 A/California/7/2009	pH1N1	2009 Pandemic	5.5 5.6 5.4 5.5 5.2	Galloway *et al.*(131) Russier *et al.*(134) Cotter *et al.*(138) Pulit-Penaloza *et al.*(140) O'Donnell *et al.*(34)
A/Hamburg/5/2009	pH1N1	2009 Pandemic	5.4	Baumann *et al.*(133)
A/TN/1-560/2009	pH1N1	2009 Pandemic	5.5	Russier *et al.*(134)
A/Texas/15/2009	pH1N1	2009 Pandemic	5.4-5.5	Pulit-Penaloza *et al.*(140)
A/Brisbane/10/2010	pH1N1	Seasonal	5.0	Cotter *et al.*(138)
A/Georgia/F32551/2012	pH1N1	Seasonal	5.3	Galloway *et al.*(131)
Multiple strains from 2010-2012 tested	pH1N1	Seasonal	5.2-5.4	Russier *et al.*(134)
A/Brisbane/59/2007	sH1N1	Seasonal	5.3-5.4	Pulit-Penaloza *et al.*(140)
A/Pennsylvania/08/2008	sH1N1	Seasonal	5.7	Galloway *et al.*(131)
A/California/10/1978	sH1N1	Seasonal	5.1	O'Donnell *et al.*(34)
A/Brevig Mission/1/1918	H1N1	1918 Pandemic	5.1	Baumann *et al.*(133)
A/Japan/305/1957	H2N2	1957 Pandemic	5.2	Galloway *et al.*(131)
A/Singapore/1/1957	H2N2	1957 Pandemic	5.2	Baumann *et al.*(133)
A/Hong Kong/1/1968	H3N2	1968 Pandemic	5.2	Baumann *et al.*(133)
A/Aichi/2/1968	H3N2	1968 Pandemic	5.2	Galloway *et al.*(131)
A/Victoria/3/1975	H3N2	Seasonal	5.0	Galloway *et al.*(131)
A/Washington/897/1980	H3N2	Seasonal	5.0	O'Donnell *et al.*(34)
A/Panama/1999	H3N2	Seasonal	5.1	O'Donnell *et al.*(34)

Table 2.1 pH of fusion reported for human influenza isolates. Studies that have reported a value for the pH of fusion of a natural human influenza virus isolate. The year of isolation is indicated at the end of the strain name. Early strains from pandemic years are indicated in the third column as pandemic where as strains isolated from later years are indicated as seasonal.

In addition to the quantifying the stability of natural virus isolates as described above, a few studies have investigated the impact of HA stability on viral replication and pathogenicity in mammalian models. Using the same avian H5N1 virus panel as in the study on ducks by Reed *et al.* described above (137), Zaraket *et al.* (141) found, in mice, that the K58I mutation that decreased pH of fusion from 5.9 to 5.4 resulted in

greater replication and virulence. This is in contrast to the results in ducks showing that the same K58I mutant was attenuating. In a further study by Zaraket *et al.* (142), K58I introduced into an H5N1 isolate that reduced pH of fusion from 6.0 to 5.5 resulted in improved growth in the ferret URT. Similarly, Shelton *et al.* (132) introduced the stabilising H8Q mutation into a virus with H5 HA and observed improved nasal shedding from ferrets.

Whilst the majority of the work on HA stability and pathogenicity has focussed on H5N1, a few more recent reports have studied human influenza isolates. Cotter *et al.* (138) found that pH1N1 virus engineered to have pH of fusion of 5.0 had improved infectivity in the ferret URT than virus with pH of fusion of 5.4. Russier *et al.* (134) compared a wild-type pH1N1 virus (pH of fusion 5.5) with a destabilised Y7H mutant (pH of fusion 6.0) and found the Y7H mutant to be attenuated in mice and to replicate less well in the ferret nasal tract. Overall, the impact of pH stability on pathogenicity appears to be host specific. Yet there is a lack of experimental work that has systematically investigated the impact of stability lowering mutations on pathogenicity of a human influenza virus in a mammalian model and how/why this might differ from the avian host i.e. how this relates to cross-species transmission (discussed in Chapter 1.5).

To summarise the work performed in these studies, there is experimental evidence that a more acid labile HA (high fusion pH) is advantageous for replication and pathogenicity of influenza viruses in birds. However, if the virus becomes too unstable (pH of fusion>6.2) this can have attenuating consequences. On the other hand, in humans, influenza viruses are evolving a more stable HA. There is limited understanding on whether a higher pH of fusion would result in a similar increase in pathogenicity in humans as has been demonstrated in birds. However, it is clear from the limited experimental evidence that exists in mammalian models, primarily using

avian H5N1 isolates with high starting pH of fusion, that the impact of HA stability for pathogenicity in mammals appears to be different to that demonstrated in birds. What is the optimum HA fusion pH for replication and pathogenicity in humans? And if a difference in the consequences of HA stability exists between humans and birds, what is the biological reason for this disparity? Is the evolution of a more stable HA in humans being driven by a trade off in favour of survival during the long-range airborne transmission events required for human circulation, which is opposing its impact on viral replication/pathogenicity?

2.2 Results

2.2.1 Identification and characterisation of residues in 2009 pandemic H1N1 haemagglutinin that alter stability

We sought to derive a panel of influenza viruses that differ only in HA stability in order to investigate the impact of this property on virus phenotypes, focussing particularly on consequences in mammalian models. A literature search for HA mutations previously described to alter HA stability was performed. Using reverse genetics, we generated recombinant viruses from a typical first wave 2009 pandemic H1N1 virus (A/England/195/2009, “Eng09”) with these point mutations introduced into the HA gene. Viruses were identical in all seven other genes. Table 2.2 lists the HA mutant viruses that were rescued and Figure 2.1 models their location on a HA monomer.

Mutation	Source	Rescued successfully?
HA1-Y7H	(134,137,141,143)	Y
HA1-H8Q	(132,137,141)	N
HA1-A9T	Passaging studies*	Y
HA1-E21K	(138)	Y
HA1-E103Y	(92)	N
HA1 E103H	(92)	Y
HA2-E47K	(138)	N
HA2-T49S	(133)	Y
HA2-K58I	(141,144,145)	N
HA2-H72N	(133)	Y
HA2-H72D	(133)	Y
HA2-K75R	(133)	Y
HA2-D112G	(144)	Y
HA2-S113F	(133)	Y
HA2-N114K	(137,141)	Y

Table 2.2 Point mutations that alter HA stability. Point mutations reported to alter the stability of HA were derived from the literature. *The A9T mutation was identified in studies passaging Eng09 in the presence of the vATP-ase inhibitor bafilomycin A1 carried out prior to this PhD (A Singanayagam, data not shown). Mutations were engineered into the Eng09 HA by reverse genetics. Viruses that were rescued successfully in MDCK cells are indicated.

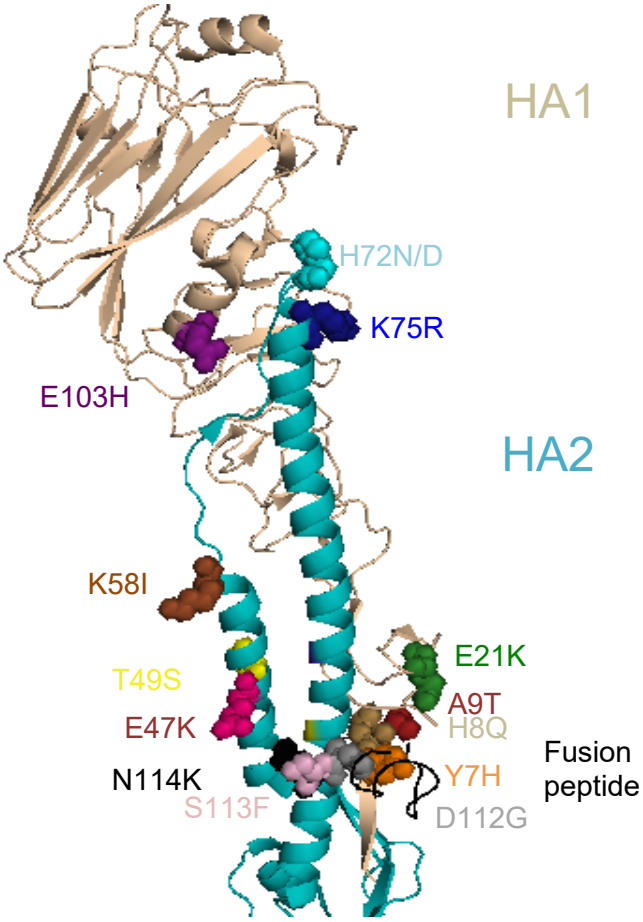

Figure 2.1 HA mutations modelled onto a HA monomer. Location of HA stability altering point mutations are modelled on H1 haemagglutinin using Pymol molecular visualisation tool (PDB: 4jtv). HA1 is coloured light brown, HA2 is teal and the fusion peptide is black. The majority of mutations are located in the HA stem or at the interface of the HA subunits.

As a preliminary screening test, we carried out a pH inactivation assay to compare the stability of each mutant under low pH conditions (Figure 2.2) and a syncytia assay to determine the pH of fusion (Figure 2.3). Consistent with previous studies, the wild type (WT) HA had a pH of fusion of 5.5 and point mutations introduced in HA resulted in changes to virion stability.

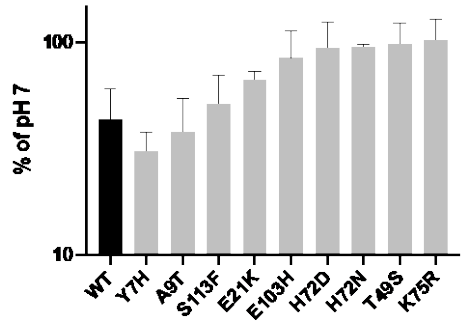

Figure 2.2 pH of inactivation of HA mutant viruses. 10^7 PFU of each virus was mixed with MES buffer pH-adjusted to 5.8 or 7.0. The remaining infectivity at 5.8 is shown relative to the infectivity at pH 7. Results are expressed as mean +/- SD of triplicate samples.

A - +

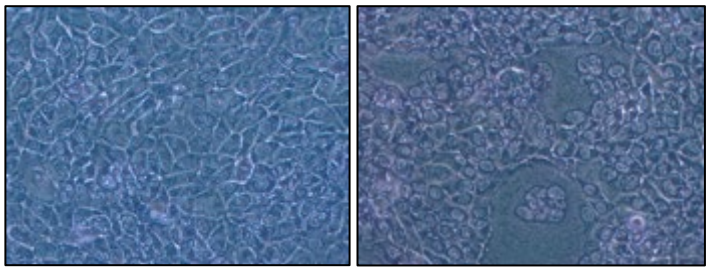

B

Mutant	pH of fusion	Change relative to WT
Y7H	5.9	+0.4
N114K	5.8	+0.3
A9T	5.8	+0.3
D112G	5.7	+0.2
S113F	5.7	+0.2
WT	**5.5**	**+0.0**
E103H	5.4	-0.1
H72D	5.4	-0.1
T49S	5.4	-0.1
K75R	5.4	-0.1
E21K	5.3	-0.2
H72N	5.3	-0.2

Figure 2.3 Syncytia assay on HA mutant viruses. (A) Example of a negative and positive syncytia assay. (B) The pH of fusion of HA mutant viruses was tested by syncytia assay in MDCK cells. The change in pH of fusion relative to wild type (WT) virus is shown.

We selected three stabilising and three destabilising mutations for more detailed study. To study the effects of these mutations, we performed a pH inactivation assay for each HA mutant in comparison to the wild type virus at multiple pHs (Figure 2.4).

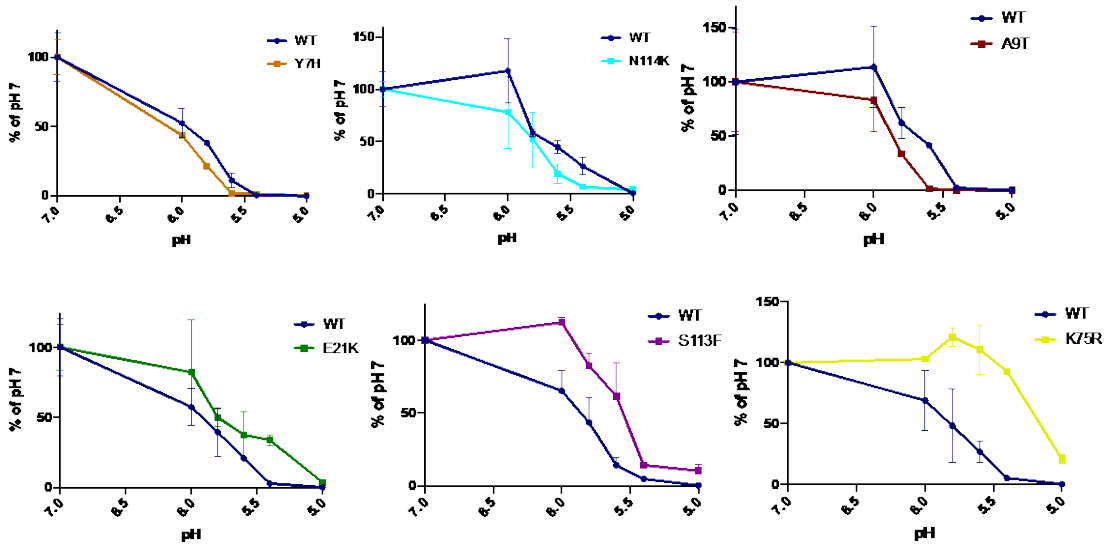

Figure 2.4 pH of inactivation of selected HA mutant viruses. pH of inactivation was tested at multiple pHs relative to wild type (WT). Results are expressed as mean +/- SD of triplicate samples.

Finally, we selected three HA mutants (Y7H, A9T and E21K) covering a range of HA stability for further studies (Table 2.3). Viral stocks were prepared in MDCK cells and passaged minimally after rescue to reduce the possibility of additional mutations arising. Of particular concern to this regard was that previous studies have shown that cell culture passage can result in mutations that alter pH of fusion(146–148). Stocks were whole genome sequenced and confirmed to have similar genome copy-to-PFU ratio prior to use (Table 2.3). As a final phenotypic characterisation of HA stability, the thermostability of the three mutants and wild type virus was tested at 54°C (Figure 2.5). Together, these data confirm a hierarchy of viral stability of our panel of viruses, determined by HA, from least to most stable of Y7H<A9T<WT<E21K.

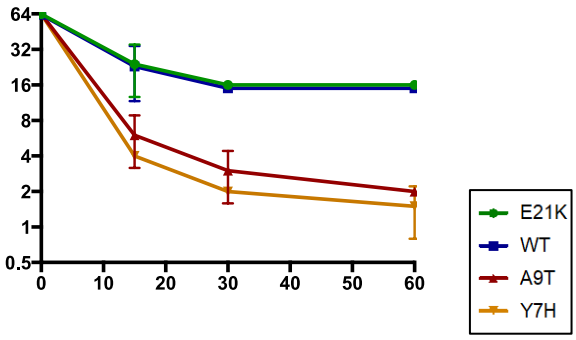

Figure 2.5. Thermostability assay on final HA mutant panel. 64 haemagglutinating units (HAU) of each virus were incubated at 54°C for the indicated time, in triplicate. Remaining HAU titre of is reported at each time point. Results are expressed as mean +/- SD of triplicate samples.

Virus	Genome copy-to-PFU ratio	pH of fusion (syncytia formation)	90% pH of inactivation	Thermostabilty (fold change at 30 minutes)
E21K	2.0	5.3	5.15	4
WT	1.5	5.5	5.45	4
A9T	1.8	5.8	5.55	21
Y7H	3.5	5.9	5.75	32

Table 2.3 Summary of results. Results of the assays used to characterise the stability of the four HA mutant viruses selected for further study.

We modeled the consequences of our selected mutations on the HA structure. All three mutations were located in the HA stem (in HA1), close to the fusion peptide. We identified (from our own modeling studies and previous work in the literature) that mutations Y7H and A9T interact directly with residues in the fusion peptide. The hydroxyl group of tyrosine at position 7 in HA1 forms hydrogen bonds with residues 10 and 12 in the fusion peptide, which destabilises HA when mutated to histidine (134,143) (Figure 2.6A). The hydrophobic alanine residue at position 9 in HA1 interacts with W14 in the fusion peptide. Mutation to hydrophilic threonine results in destabilisation of HA (Figure 2.6B). Residue 21 in HA1 forms a stabilising

intermonomer salt bridge with HA2 residue E47 when mutated from E to K (138) (Figure 2.6C).

Figure 2.6 Modelling structural interactions of final HA mutant panel. The location and interactions of mutations (A) Y7H (orange), (B) A9T (red) and (C) E21K (green) are modelled using Pymol molecular visualisation tool. Residues are shown as sticks. Dotted lines to other residues represent interactions identified. HA1 is coloured light brown, HA2 is teal and the fusion peptide is black.

Our aim was to use this panel of viruses to delineate the consequences of HA stability on replication and pathogenicity of a human influenza virus using mammalian models.

2.2.2 Replicative ability of HA mutant pH1N1 viruses in continuous cell cultures

To understand the impact of HA stability on influenza growth kinetics, we infected MDCK or A549 (human alveolar epithelial) cells with the HA mutants. Under multicycle conditions, Y7H and A9T mutants appeared to replicate faster, but the differences were not significant (Figure 2.7A); however, under high MOI conditions, replicative fitness differences became more apparent. Viruses A9T and Y7H, with HA mutations that increased the activation pH, grew to ~1 log higher titres than the more acid stable viruses E21K and WT in MDCK (Figure 2.7B) and A549 (Figure 2.7C) cells.

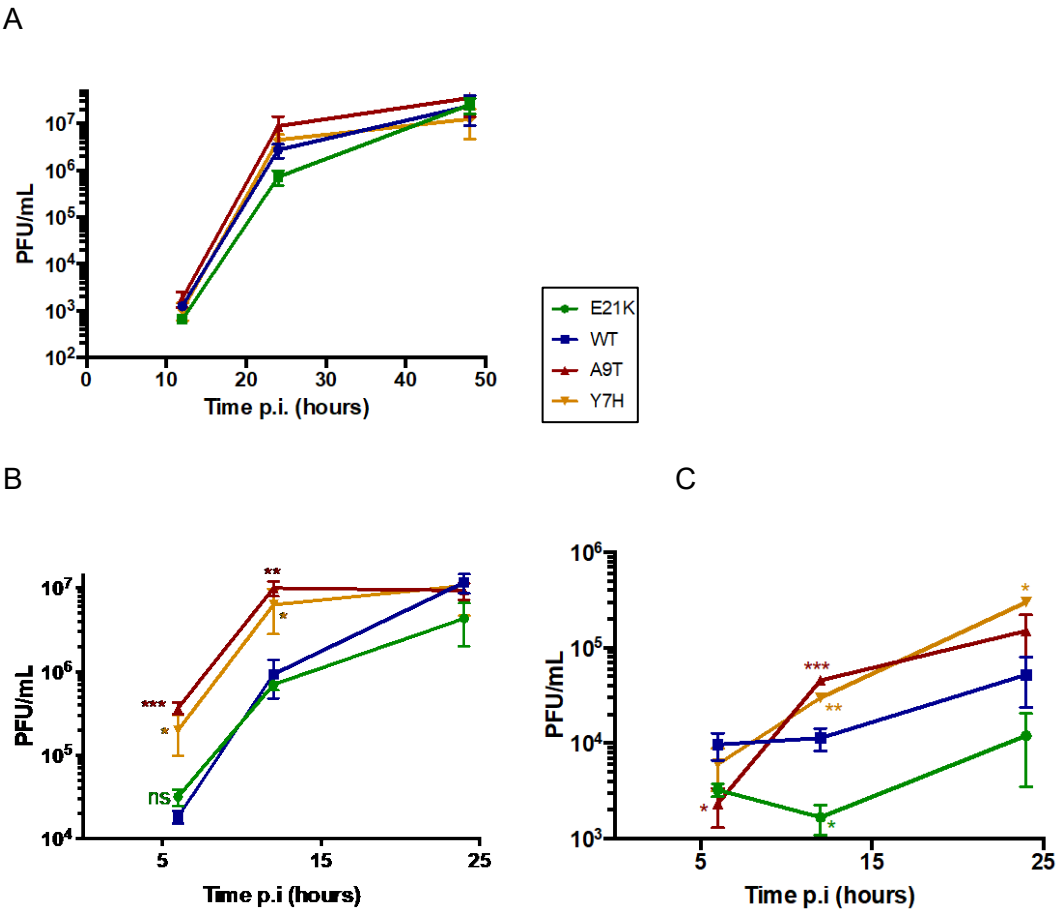

Figure 2.7 Replicative ability of HA mutant viruses in continuous cell lines. MDCK cells (A and B) or A549 cells (C) were infected at low multiplicity (MOI of 0.0001 PFU/cell) (A) or high multiplicity (MOI 3 PFU/cell) (B and C). Supernatant was harvested at time points indicated and virus titre determined by plaque assay. Results are expressed as mean +/- SD of triplicate samples. One-way ANOVA with Tukey post test was used to compare wild type (WT) to the other viruses. *p<0.05, **p<0.01, ***p<0.001, ns=not significant.

In a virus driven replicon ("UpLUC") assay in which a luciferase encoding viral-like RNA was amplified and expressed by each virus infected at equal MOI, Y7H and A9T resulted in a significantly higher signal (Figures 2.8A and 2.8B). This assay measures the efficiency of delivery of the viral genome to the nucleus and the result suggests the replicative advantage shown by Y7H and A9T was occurring at an early stage in the viral replication cycle.

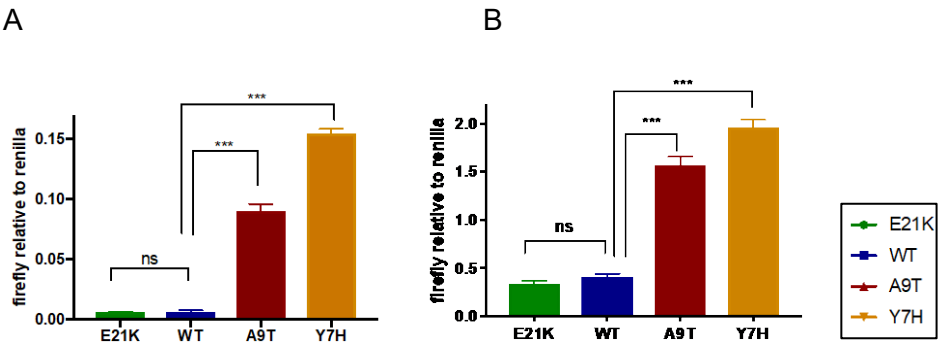

Figure 2.8 Replicative ability of HA mutant panel in the UpLUC assay. 293T (A) or A549 (B) cells were transfected with a 3-5-8 viral-like firefly luciferase reporter and then infected with each HA mutant virus at MOI of 1 PFU/cell. Luciferase activity was measured at 24 hours post infection. Results are expressed as mean +/- SD of triplicate samples. One-way ANOVA with Tukey post test was used to compare wild type (WT) to the other viruses. *p<0.05, **p<0.01, ***p<0.001, ns=not significant.

We could pinpoint this replicative advantage to virus uncoating in endosomes. Mutants Y7H and A9T, with high HA activation pH, stimulated increased production of firefly luciferase in the UpLUC assay only when viruses entered via fusion in endosomes and not when viruses were induced to fuse at the cell surface (Figure 2.9). This suggests that having a higher pH of HA activation enables influenza viruses to more efficiently uncoat in endosomes and release their genomes to the nucleus.

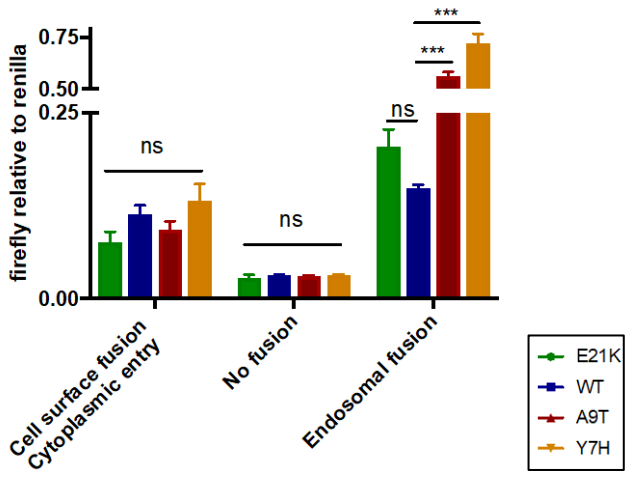

Figure 2.9 Acid bypass to compare the replicative ability of HA mutant viruses fusing at the cell surface or in endosomes. 293T cells were transfected with a 3-5-8 viral-like firefly luciferase reporter and then infected with each HA mutant virus at MOI of 1 PFU/cell under three different conditions. Viruses are exposed to low pH whilst bound to the cell surface and endosomal entry blocked using NH_4Cl was performed. This results in virus fusing at the cell surface and entering via the cytoplasm. Positive (endosomal entry = exposure to neutral pH and no endosomal block) and negative (no fusion = exposure to neutral pH and endosomal block with NH_4Cl) controls were included. Luciferase activity was measured at 24 hours post infection. Results are expressed as mean +/- SD of triplicate samples. One-way ANOVA with Tukey post test was used to compare wild type (WT) to the other viruses. *p<0.05, **p<0.01, ***p<0.001, ns=not significant.

2.2.2.1 Delineating the mechanism for improved replicative ability conferred by HA instability

We sought to understand the mechanism for this observation. Following host cell entry, influenza is trafficked from early (~pH 5.4-6.2) to late (~pH 5.0-5.5) endosomes until a threshold of acidic pH triggers the HA protein to undergo the irreversible conformational change that precedes fusion. Two major hypotheses have been put forward in the literature to explain the replicative advantage associated with a higher pH of fusion but experimental evidence has been lacking.

(Hypothesis 1) Ability to fuse earlier in the endosomal pathway may provide viruses with a higher pH of fusion with a mechanism to escape the effects of the restriction factors, IFITM 2/3, which have been described to be located in late endosomes and act to inhibit viral fusion

(Hypothesis 2) Viruses that have evolved more acid stable HAs may not be triggered to fuse until they reach the low pH of lysosomes, where they become trafficked for degradation

Genetic screens first characterised the IFITM protein family members IFITM1, 2, and 3 as antiviral restriction factors (149). In particular, IFITM3 has been described as a potent influenza A virus restriction factor(149–151). IFITM 2 and 3 have been shown to localise to late endosomes and lysosomes(152,153) and are thought to inhibit viral fusion(154), where as IFITM1 is expressed predominantly at the cell surface and in early endosomes(152). To test our hypothesis that viruses with capability to fuse at higher pH could escape the antiviral effect of IFITM3, we overexpressed IFITM3 in 293T cells and infected with the HA mutants at equal MOI. Increasing amounts of overexpressed IFITM3 were seen to inhibit viral replication. However, we did not observe any difference in sensitivity to IFITM3 between viruses with different pH of fusion in this assay (Figure 2.10A and 2.10B).

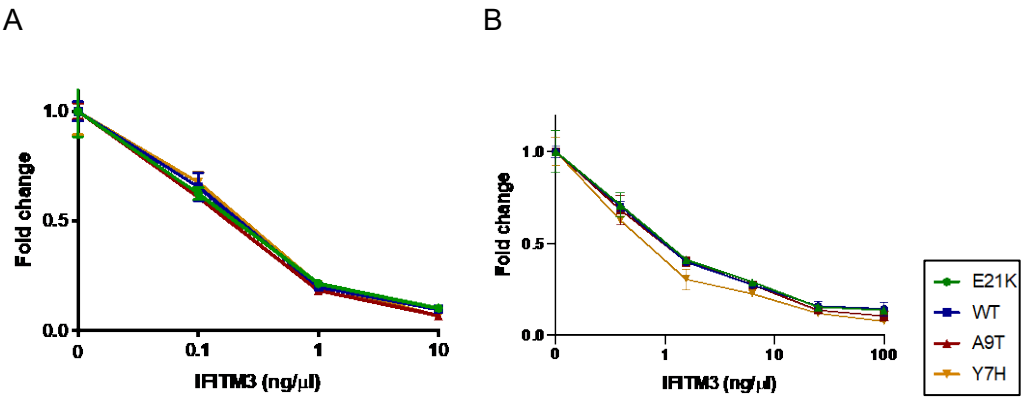

Figure 2.10. Investigating the effect of IFITM3 on the HA mutant virus panel. (A and B) 293T cells were transfected with the 3-5-8 viral like luciferase reporter and indicated quantities of PCAGGS-IFITM3 and then infected with each HA mutant virus at MOI of 1 PFU/cell. PCAGGS-empty was used as a negative control. Luciferase activity was measured at 24 hours post infection. Results are expressed relative to the PCAGGS-empty negative control and mean +/- SD of triplicate samples are shown. A and B show the same experiment performed independently on two separate days.

To further confirm our findings, we tested the sensitivity of our panel of HA mutants to type 1 interferon (IFN). IFN acts to upregulate hundreds of host interferon-stimulated genes that can have antiviral effects. IFITMs have been shown to be major contributors to the anti-influenza effect of IFN, contributing 50-80% of the *in vitro* effects of IFN against influenza(149,152,153). A549 cells were pre-treated with type 1 IFN and then infected with the HA mutant panel at equal MOI. Again, we could not detect any difference in IFN sensitivity between our mutant viruses (Figure 2.11).

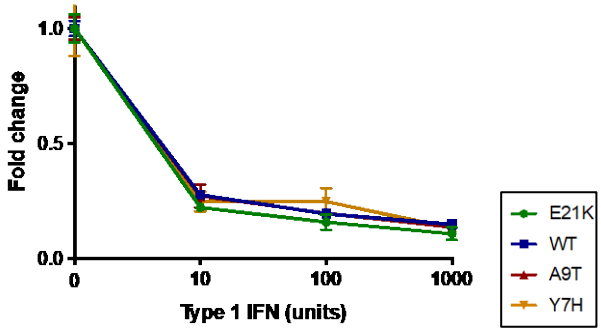

Figure 2.11 Investigating the effect of type 1 IFN on the HA mutant virus panel. A549 cells were transfected with the 3-5-8 viral like luciferase reporter and pre treated for 20 hours with type 1 IFN at the indicated dose then infected with each HA mutant virus at MOI of 1 PFU/cell. Luciferase activity was measured at 24 hours post infection. Results are expressed relative to the untreated negative control and mean +/- SD of triplicate samples are shown.

Finally, we tested the sensitivity of the virus panel to amphotericin B, a drug that has been demonstrated to prevent IFITM3 mediated restriction of influenza A (155). We hypothesised that replication of the more acid stable WT/E21K viruses could be rescued if the reason for their reduced replicative ability was due to greater restriction by constitutively expressed cellular IFITM3 than A9T/Y7H. The UpLUC assay was carried out in A549 cells in the presence of varying doses of amphotericin B. We found that increasing doses of amphotericin B increased the replication of our influenza virus panel, in line with previous reports. However, there was no clear difference in the relative effect of amphotericin between the fusion mutant viruses (Figure 2.12). A similar result was found using 293T cells (data not shown).

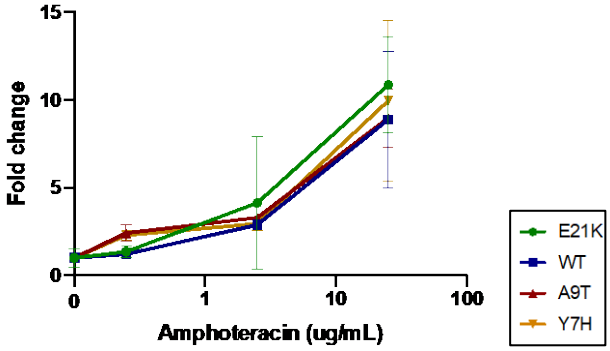

Figure 2.12 Investigating the effect of amphotericin B on the HA mutant virus panel. A549 cells were transfected with the 3-5-8 viral like luciferase reporter then infected with each HA mutant virus at MOI of 1 PFU/cell. After 1 hour, cells were washed and incubated in 10% DMEM with the indicated concentration of amphotericin B. Luciferase activity was measured at 24 hours post infection. Results are expressed relative to the untreated negative control and mean +/- SD of triplicate samples are shown.

Despite using three different approaches, we were unable to detect any differential impact of IFITM3 on our viruses with varying pH of fusion. Subsequent to our experiments, two important studies were published that also addressed this question using different approaches. Our results concur with work performed by Sun *et al.* (156) who detected no difference in virus infectivity between recombinant 6:2 PR8 viruses with either human (H1N1 or H3N2, low pH of fusion) or avian (H7N9 or H5N1, high pH of fusion) HA and NA in A549 cells stably expressing IFITM3. On the other hand, Gerlach *et al.* (157) used a similar approach but in MDCK cells stably expressing IFITM2 or 3 and did detect increased restriction of 6:2 PR8 viruses with acid stable human/avian HA/NA (H1N1) compared to those with unstable avian HA/NA (H7N9/H5N1). Moreover, they showed this effect using stability altering HA point mutations engineered into a 6:2 PR8/H3N2 virus. Gerlach *et al.* also identified a differential effect of type 1 IFN on their panel of viruses that correlated with pH of fusion using multiple continuous and primary human airway epithelial cell types. The reason for the discrepant results observed in the studies by Sun *et al*., Gerlach *et al*

and in our study, are not completely clear though are perhaps related to differences in the cells, virus strains and experimental assay used.

The advantage conferred by a higher pH of HA activation may be because viruses with more pH stable HA fail to uncoat and are trafficked to lysosomes where they are degraded. When 293T cells were infected with our panel of mutants at equal PFU per cell and incubated for longer, the WT and E21K signal did not achieve the same levels as for A9T/Y7H (Figure 2.13). This might suggest that a proportion of virions entering the cell were lost to lysosomal degradation. Further work to directly visualise virions in endosomes and lysosomes could help to confirm or refute this hypothesis.

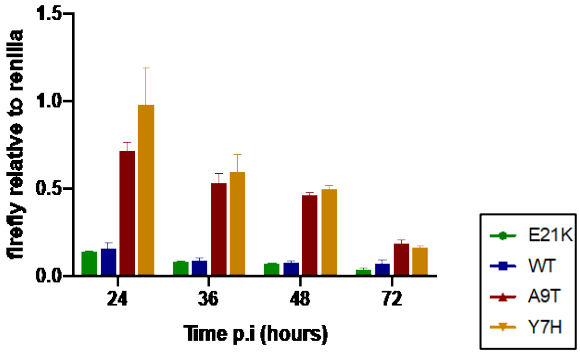

Figure 2.13 Replicative ability of HA mutant panel over time in the UpLUC assay. 293T cells were transfected with a 3-5-8 viral-like firefly luciferase reporter and then infected with each HA mutant virus at MOI of 1 PFU/cell. Luciferase activity was measured at time points indicated post infection. Results are expressed as mean +/- SD of triplicate samples.

2.2.3 Replicative ability of HA mutant pH1N1 viruses in primary human nasal epithelial cells cultured at air-liquid interface

Having identified that an increased pH of fusion conferred a growth advantage to viruses in continuous cell cultures, we sought to investigate this in a more human relevant experimental model. Primary human nasal epithelial cells (pHNEC), cultured at air-liquid interface (ALI), are a fully differentiated primary cell model that mimic the morphological and physiological features of the human airway including beating cilia, mucous production and active ion transport. pHNECs are therefore a more relevant experimental model for influenza in the human upper respiratory tract (URT) than traditional continuous cell culture systems.

We infected pHNECs at low multiplicity to perform a multi-cycle growth analysis. Strikingly, we observed a very different fitness hierarchy compared to that seen with the continuous cell cultures. The viruses with higher pH of fusion, Y7H and A9T were attenuated, where as the more acid stable influenza viral mutants, E21K and WT, replicated to higher titres (Figure 2.14A). The area under the curve for WT was significantly greater than for A9T ($p=0.0295$) and Y7H ($p=0.0286$).

As discussed in Chapter 1, in the absence of a target membrane, HA conformational change results in irreversible virus inactivation and therefore is directly related to virus stability and survivability outside the host cell. Therefore, we hypothesised that increased acid stability could be advantaging virus by enabling improved survival in the extracellular environment, which is reported to be mildly acidic in the mammalian URT. We tested the pH of apical washes from 27 wells of pHNEC cultures derived from two different human donors and measured a median pH of 6.5 (range 5.8-7.0)

(Fig 2.14B), which correlates with measurements reported from the URT of healthy human subjects (30).

To confirm the importance of extracellular pH on viral growth properties in the ALI pHNEC cultures, we infected pHNECs at low multiplicity in the presence of a liquid media overlay buffered to pH 7.4, aiming to maintain the extracellular apical space at a neutral pH, akin to experiments on continuous cell lines. Under these conditions, we found that the advantage of increased HA stability for multi-cycle replication in pHNECs was abrogated (Figure 2.14C).

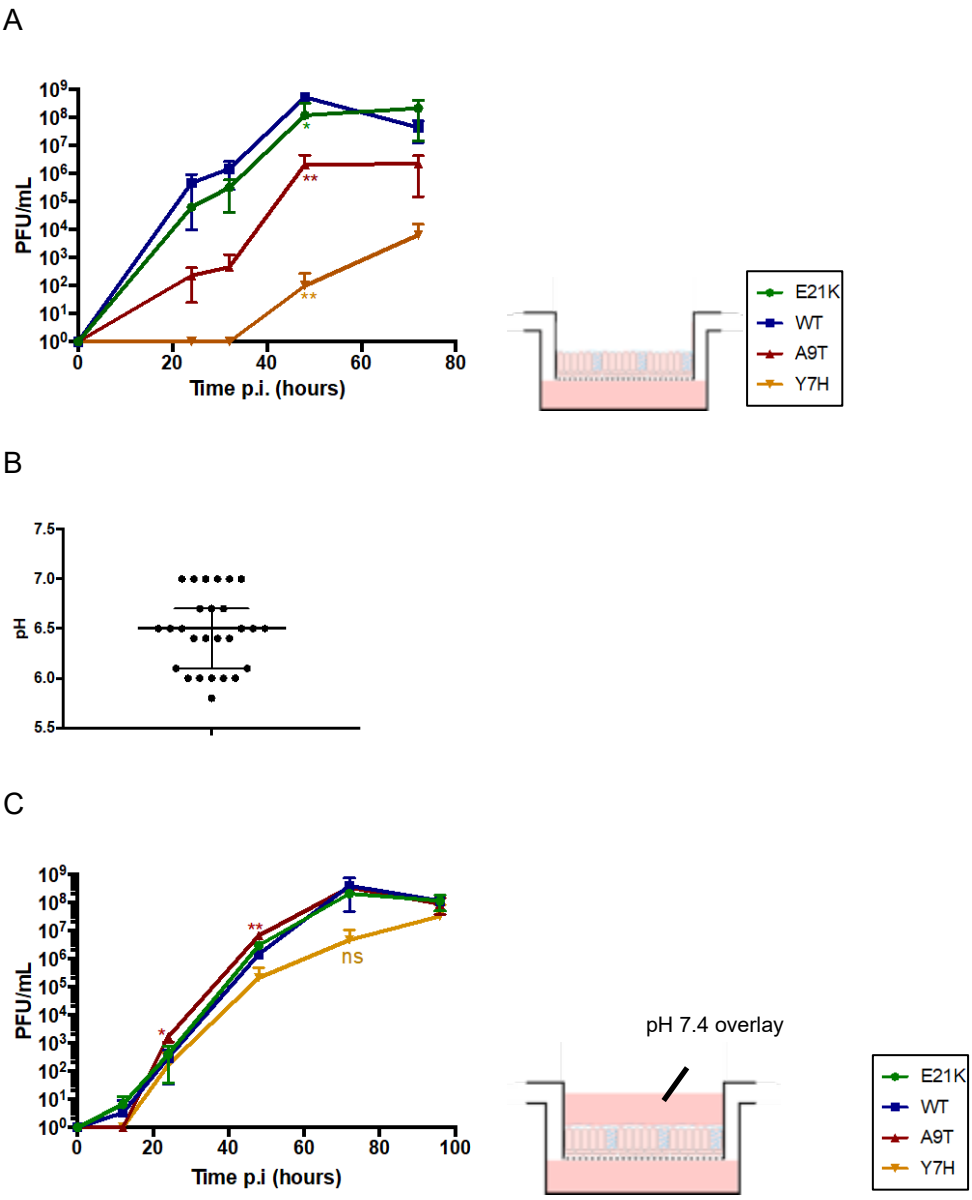

Figure 2.14 Replicative ability of HA mutant viruses in primary human nasal epithelial cells cultured at air-liquid interface. pHNECs (A and C) were infected at low multiplicity (MOI of 0.001 PFU/cell). At indicated time points post infection, the apical surface was washed with 200uL DMEM and virus titre determined by plaque assay. A liquid overlay buffered to pH 7.4 was maintained on the apical surface in C. Results are expressed as mean +/- SD of triplicate samples. One-way ANOVA with Tukey post test was used to compare wild type (WT) to the other viruses. *p<0.05, **p<0.01, ***p<0.001, ns=not significant. (B) The pH of apical washes from 27 pHNEC cultures was tested using an unbuffered 0.9% saline wash adjusted to pH 7.4. Median and interquartile range is shown.

2.2.4 Pathogenicity of HA mutant pH1N1 viruses in a mouse model

Mice are commonly used to study influenza pathogenesis and can be experimentally infected with influenza virus. Clinical disease and quantitative virology can be assessed in order to evaluate viral pathogenicity(158). To investigate how the fitness hierarchies we observed *in vitro* would translate in an *in vivo* setting, we experimentally infected groups of 15 BALB/c mice with each HA mutant virus ($2x10^5$ PFU). WT virus replicated to the highest titres in mouse lung. On day 2, lung viral titres were significantly increased for WT virus compared to E21K (p=0.0069), A9T (p=0.008) and Y7H (p=0.0035) (Figure 2.15B): a similar hierarchy to that observed in pHNECs (WT>E21K>A9T>Y7H). Furthermore, infection with WT virus (pH of fusion 5.5) caused greater weight loss, peaking on day 3 (Figure 2.15A), than the viruses with fusion pH of 5.3 (E21K, p=0.0004)), 5.8 (A9T, p=0.0016) or 5.9 (Y7H, p<0.0001). The area under the weight loss curve for the WT virus was significantly different from E21K (p=0.047) and Y7H (p<0.0001) but failed to reach significance for A9T (p=0.46).

By day 5, the lung viral titres of WT, E21K and A9T had reduced, but the titre of Y7H was significantly elevated in comparison (Figure 2.15B). However, this was not reflected in the weight loss. The reason for this is unclear, although one intriguing hypothesis is that the virus by day 5 could have mutated to become more pH stable. Deep sequencing of this sample would help to understand this. There could also be a difference in the production of cytokines between the viruses and it would be of interest to measure cytokine profiles from infected mouse lungs on day 2 and 5.

A

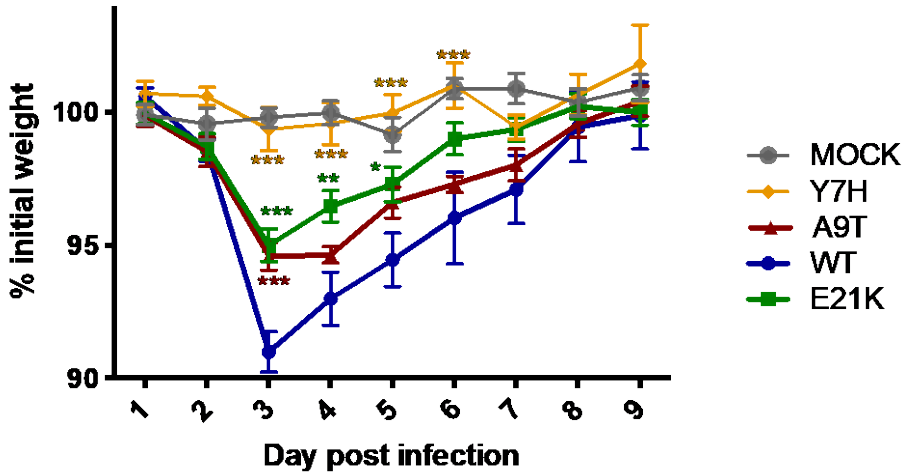

B

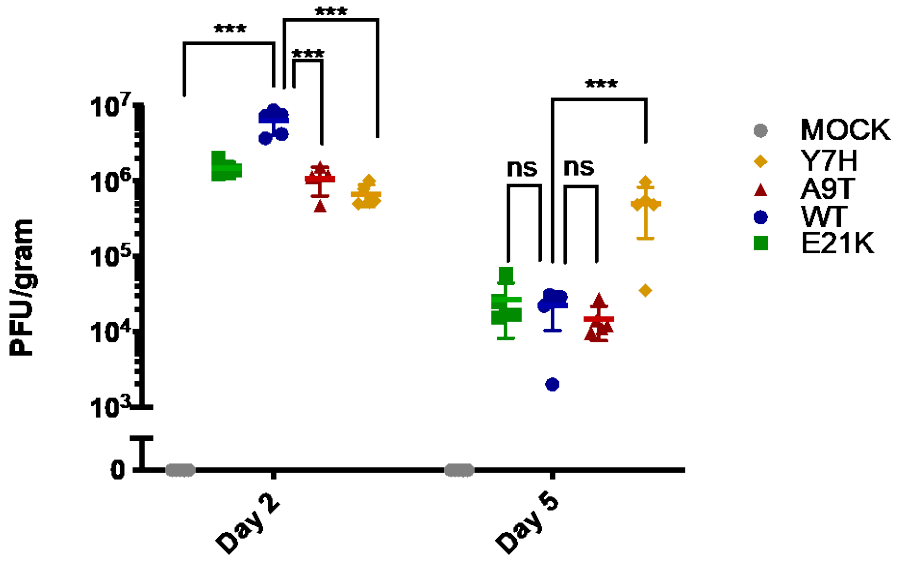

Figure 2.15 Pathogenicity of HA mutant viruses in mice. Groups of 15 BALB/c mice were inoculated with $2x10^5$ PFU of virus in 40µL or vehicle (PBS). (A) Mean +/- SEM percentage weight change over the course of infection is shown. (B) Mean +/- SD lung viral titres on day 2 and day 5 post infection (n=5) were titrated by plaque assay on MDCK cells. One-way ANOVA with Tukey post test was used to compare wild type (WT) to the other viruses. *p<0.05, **p<0.01, ***p<0.001.

2.2.5 Sensitivity to antiviral drugs that act on the HA fusion machinery correlates with HA activation pH

Recent years have seen a significant increase in the development of novel antiviral therapeutics that directly target the fusogenic ability of HA (159). Examples include directly-acting proteins (160,161), peptides (162,163), small molecules (164–167) and broadly neutralising antibodies (168) that target relatively conserved regions of the HA stem. A further class of host-targeting drugs, the vacuolar ATPase inhibitors, act on the proton pumps that regulate the pH of host cell endosomes and can inhibit virus by preventing the endosomal acidification required for triggering of the fusion process (169–173). Given that the site of action of these drugs is intricately linked to the HA fusion process, we hypothesised that virus might avoid inhibition by mutating to alter its pH of fusion. Additionally, escape mutations within the HA stalk might impact on HA activation pH and affect virus phenotype as described earlier in this Chapter.

We tested the sensitivity of our panel of HA mutants to (i) arbidol hydrochloride (a small molecule drug that inhibits HA fusion (130,174) and is licensed for use against influenza in Russia and China), (ii) bafilomycin (a vacuolar ATPase inhibitor that increases endosomal pH (169)) and (iii) FI6 (a broadly neutralising monoclonal antibody that targets the HA stem(175)). We found that the viruses with higher HA activation pH (Y7H, A9T) were somewhat less sensitive to these drugs (Fig 2.16). These data suggest that antiviral therapeutics that act on the HA stem/fusion machinery could exert selective pressure on virus leading to changes in HA pH stability. Whilst this is perhaps unlikely to manifest as clinically relevant resistance, it may indicate that, within a single host, selective drug pressure during treatment could lead to emergence of variants with reduced HA pH stability. The potential

consequences of this link to findings described in both Chapters 2 (viral pathogenicity) and Chapter 3 (viral transmissibility). In the context of pH1N1, selective drug pressure that acts to increase pH of fusion >5.6 would perhaps attenuate virus in the human airway, limiting the clinical consequence of any drug escape mutants. However, it is important to note that drug resistance to stem-targeting drugs could arise via mutations at the drug-binding site and that a change in HA pH stability (either an increase or decrease) could be an unintended consequence of such mutations (176,177).

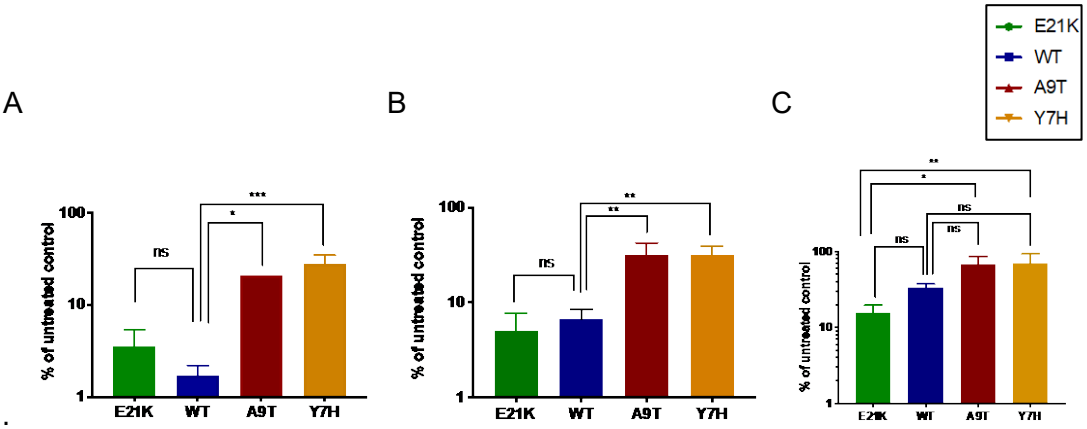

Figure 2.16 Sensitivity to drugs targeting the fusogenic ability of HA. The sensitivity of HA mutants to (a) 20μM arbidol hydrochloride (a small molecule fusion inhibitor), (b) 1nM bafilomycin (a vacoular ATPase inhibitor) and (c) 0.01μg/mL FI6 (a broadly neutralising monoclonal antibody) was tested by assaying remaining infectivity after infection of MDCK cells. One-way ANOVA with Tukey post-test was used to compare wild type (WT) virus to the other viruses. *p<0.05, **p<0.01, ***p<0.001, ns=not significant.

2.3 Discussion

Testing of natural influenza A virus isolates has identified that human viruses are more acid stable than avian viruses. Yet, a biological understanding for this observation has not been elucidated. In studies on H5N1 avian influenza virus in birds, an increasing pH of fusion resulted in increased pathogenicity, with an optimum pH of fusion for pathogenicity between 5.5-6.2. Whether this also applied to virus behaviour in a mammalian host is not fully understood.

2.3.1 Optimum viral pH stability is determined by a balance between extracellular and intracellular pressures

In this Chapter, we demonstrate that an acid labile HA (high pH of fusion) confers a replicative advantage to virus within host cells by enabling more efficient uncoating in endosomes. In support of this, several previous studies have shown that serial passage in cell culture selects virus with increased pH of fusion(146–148), suggesting that instability offers a selective advantage to virus in this setting. We found that this phenomenon became more apparent using an assay representing the early stages of the viral replication cycle and when cells were infected at high multiplicity allowing for a single cycle of replication. Others have described the same phenomenon using certain cell types that have higher endosomal pH such as Vero cells(138,178) or A549 cells(142). However, oftentimes, influenza growth kinetics are assessed in MDCK cells infected at low multiplicity, which does not readily reveal these differences. It is important to be aware of situations where this or other traditional assays for influenza titration and growth kinetics might misrepresent - a real-world example of this with the live attenuated influenza vaccine, is discussed in Chapter 4.

In direct contrast, in pHNECs cultured at air-liquid interface, we found that the viruses with a higher pH of fusion were attenuated. This attenuation was abrogated when the extracellular environment was pH neutralised. Whether elements other than pH contribute to extracellular HA triggering requires further study. Nonetheless, viruses with more fragile HA proteins appear to be more likely to be triggered to undergo premature HA activation in the extracellular environment of pHNECs, rendering them non-infectious at the point of entry into the cell. The dose of incoming virus that is required to reach a target cell and initiate infection will therefore be higher for viruses

with an unstable HA. Thus, optimum acid stability for the replication of human influenza viruses appears to be determined by a balance between adequate stability to withstand extracellular environmental conditions, and adequate pH sensitivity to enable efficient viral uncoating within endosomes once target cells have been successfully reached.

2.3.2 Host specific differences in extracellular and intracellular environments

We propose that the evolution of a virus' acid stability will depend on a variety of selective pressures including sites of replication, target cells, host species, ecology and routes of transmission. Opposing pressures from both extracellular and intracellular environments encountered could limit HA pH of fusion to an optimal range that may shift depending on viral and host factors or ecology.

2.3.2.1 Local extracellular conditions

Host specific differences in the local extracellular environment of target tissues and mucosal surfaces may therefore account for some of the differences between the optimum acid stability of humans versus birds. In ducks, influenza viruses replicate in cells of the lower intestinal tract, which has a more neutral pH of 6.0-8.0, as well as in the respiratory tract(179). Unfortunately, the pH at mucosal surfaces of poultry has not been documented. In humans, the site of replication is the upper respiratory tract. The human nasal cavity is recorded to be mildly acidic with an average pH of 6.3 (5.3-7.0) in adults and 5.9 (5.5-6.7) in children. In children, average pH in the nasopharynx was recorded to be even lower at 5.7 (5.6-6.3) (30). In mice, a more neutral nasal pH has been described (Figure 2.17).

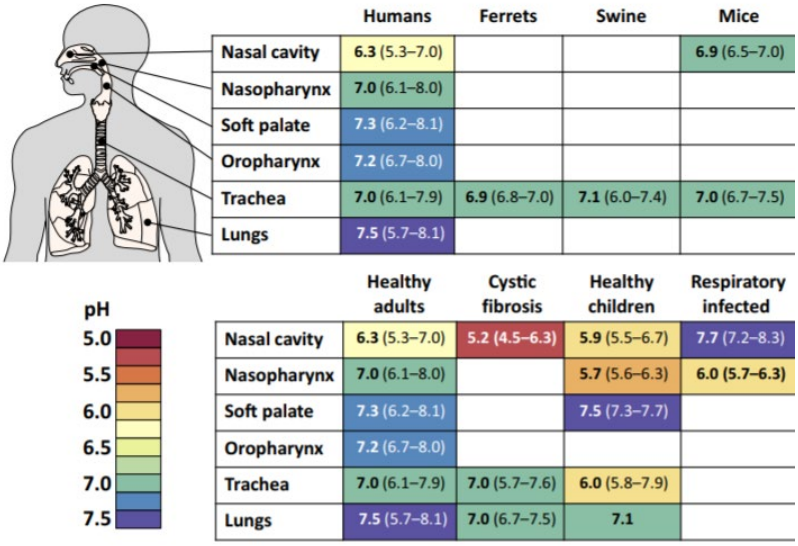

	Humans	Ferrets	Swine	Mice
Nasal cavity	6.3 (5.3–7.0)			6.9 (6.5–7.0)
Nasopharynx	7.0 (6.1–8.0)			
Soft palate	7.3 (6.2–8.1)			
Oropharynx	7.2 (6.7–8.0)			
Trachea	7.0 (6.1–7.9)	6.9 (6.8–7.0)	7.1 (6.0–7.4)	7.0 (6.7–7.5)
Lungs	7.5 (5.7–8.1)			

	Healthy adults	Cystic fibrosis	Healthy children	Respiratory infected
Nasal cavity	6.3 (5.3–7.0)	5.2 (4.5–6.3)	5.9 (5.5–6.7)	7.7 (7.2–8.3)
Nasopharynx	7.0 (6.1–8.0)		5.7 (5.6–6.3)	6.0 (5.7–6.3)
Soft palate	7.3 (6.2–8.1)		7.5 (7.3–7.7)	
Oropharynx	7.2 (6.7–8.0)			
Trachea	7.0 (6.1–7.9)	7.0 (5.7–7.6)	6.0 (5.8–7.9)	
Lungs	7.5 (5.7–8.1)	7.0 (6.7–7.5)	7.1	

Figure 2.17. pH of the respiratory tract in humans, ferrets, swine and mice. Compilation of reported respiratory pH values. Image sourced from Russell *et al*.(30)

We show that influenza virus with a pH of fusion of 5.5 replicated to higher titres in mouse lungs and caused increased weight loss in mice, compared to isogenic viruses with either less or more stable HAs. Our observations are consistent with others in the literature and taken together, suggest an optimum pH for fusion of HA in mice of 5.4-5.6. For example, Zaraket and colleagues(141) found that an H5N1 mutant virus with a fusion pH of 5.4 displayed greater pathogenicity in mice than those with higher fusion pH (5.6 - 6.3). Smeenk *et al*.(180) reported increased virulence in a mouse-passaged H1N1 strain was mediated in part by HA mutations that lowered pH stability from 5.8 to 5.6. Conversely, Keleta *et al*.(181), working with a mouse-passaged H3N2 strain that had a more stable HA, showed increased murine virulence conferred by mutations that increased HA fusion pH from 5.2 to 5.6. Russier *et al*.(134) also showed that a pH1N1 Y7H mutant with fusion pH of 6.0 was attenuated in a mouse model. Finally, serial passage of a pH1N1 virus with a starting pH of fusion of 5.6 did not alter its pH of fusion in a study by Ilyushina and colleagues(182). Nonetheless, it should be noted that mice are an imperfect model for human influenza infection – mice predominantly express α2,3-linked SA receptors

in their respiratory tract and may have a different extracellular pH in the respiratory tract than humans. It should also be considered that our HA point mutations may have pleiotropic effects, such as on cytokine induction. Indeed by day 5, the lung viral titres of WT, E21K and A9T had reduced, but the titre of Y7H was significantly elevated in comparison. However, this was not reflected in the weight loss observed. The reason for this is unclear although one intriguing hypothesis is that the virus by day 5 could have mutated to become more pH stable. Deep sequencing of this sample would help to understand this. There could also be a difference in the production of cytokines between the viruses and further work to assess lung histology, cytokine responses and the mouse lethal dose (MLD) of the mutant viruses could have added further weight to these findings.

2.3.2.2 Intracellular conditions

Intracellular differences such as the endosomal pH environment that a virus is exposed to may also vary in different cell types and hosts. Variations in the kinetics of acidification and pH levels in endosomes have been shown for immortalised cell lines(142,178) and primary cell cultures(183), suggesting that acid stability might restrict virus' ability to replicate in certain cell types. In theory, if endosomes do not reach an adequately acidic pH to trigger a more stabilised HA, the virion will pass to lysosomes and become degraded. In this case, the dose of incoming virus that is required to successfully reach the nucleus and initiate replication will be higher for virus with a stable HA. Marvin *et al.* (184) demonstrated that Raw264.7 murine macrophages had less acidic endosomal compartments than MDCK cells. In murine macrophages, but not MDCK cells or primary human blood derived macrophages, a higher pH of fusion was required for the VN/1203 HPAI H5N1 and H1N1/WSN influenza viruses to uncoat and deliver their genomes to the nucleus. The more acid stable pH1N1/Cal09 virus, however, did not enter the nucleus and replicate but

rather, was shown to accumulate in LAMP1 staining lysosomes, suggesting perhaps that Cal09 HA was not exposed to an endosomal pH low enough to trigger fusion prior to lysosomal exposure. Whether or not these findings translate to cell types relevant for primary influenza infection in humans requires further study. Perhaps HPAI H5N1 viruses have evolved an unstable HA as a means of subverting this barrier to productively replicate in macrophages? Indeed, Marvin *et al*.(184) showed that productive viral replication decreased macrophage phagocytic function and cell surface FcR levels, linking acid stability to the host response and potentially to disease outcome. Macrophage phagocytosis is important for the uptake and clearance of apoptotic epithelial cells in the lung(185,186) as well as phagocytosis of bacteria that might result in secondary infection(187). It would be interesting to investigate whether this is a phenomenon specific to the HPAI viruses or whether differences in macrophage phagocytic function could be observed *in vivo* using mice challenged with our pH1N1 viruses of varying stability.

The activity and distribution of cellular restriction factors such as IFITMs may also impact on the ability of virus to replicate in certain cell types and it is certainly possible that this varies between birds and humans. Sun *et al*.(156) showed high endogenous levels of IFITM3 in human endothelial (HULEC) cells that were not present in human epithelial cells (A549, Calu3 or primary human bronchial epithelial cells). Endothelial cell endogenous IFITM3 restricted replication of human but not avian viruses and siRNA knockdown of IFITM3 in HULEC cells partially rescued human influenza virus infectivity. However, this pattern of infectivity could not be wholly correlated with virus' pH of fusion in this study. For example, an avian H9N2 virus with low pH of fusion had high infectivity in HULEC cells. Work by Gerlach *et al*.(157), on the other hand, did show directly that HA stability could affect sensitivity to IFITM and IFN – viruses with unstable HA were shown to escape the effects of IFN and IFITM2/3. However, these findings were not supported by the work carried

out in our study. Interestingly, in a study by Wee *et al*.(188), mouse embryonic fibroblast cells obtained from mice lacking all Ifitm genes (*IfitmDel* mice) were found to have less acidic endosomal compartments than WT cells. IFITM3 co-immunoprecipitated with the vacuolar ATPase (subunit Atp6c0b), the proton pump that acidifies endosomes. This suggests a direct interaction that may link IFITM3 levels to endosomal pH. Future work to test our panel of HA mutants in IFITM3 knock out cell lines or mice might be more fruitful in delineating any link between pH stability and IFITMs.

2.3.2.3 Between host conditions

Finally, the routes of transmission and the external environment to which a virus is exposed to as it moves between hosts is likely to be critical to the evolution of a virus' acid stability and may constitute a further trade-off against within-host-cell fitness. The HPAI H5N1 and H7N9 viruses have evolved less stable HA proteins compared to human influenza viruses. Domestic poultry, which frequently harbour these emerging viruses, tend to be housed in close proximity where direct contact, higher inoculum transmission events are likely to be the predominant mode of viral transmission. The advantage of a stable HA in withstanding environmental stressors will be of less importance than for the long-range airborne transmission of human influenza viruses. Environmental persistence is likely to outweigh the benefits of efficient endosomal release and within-host fitness in the setting of respiratory droplet transmission, which might explain why human influenza viruses have evolved more stable HAs. In the next Chapter, the role of HA stability for virus survival in airborne droplets will be explored.

Chapter 3. The significance of HA stability for transmission of influenza A virus

3.1 Introduction

A critical role for HA protein stability in transmission of influenza virus was first uncovered in two controversial ferret transmission studies on H5N1 virus in 2012 that yielded remarkably similar results (92,93). In these studies, highly pathogenic avian H5N1 viruses were artificially generated to have increased ability to transmit through the air between ferrets. Using different approaches, both studies found that mutations altering certain viral properties were required for transmission of H5N1 through the air. These included: 1) HA receptor binding 2) polymerase activity 3) HA glycosylation and 4) HA stability. This was the first description of a role for HA stability in supporting influenza airborne transmissibility. An earlier study (189) described a HA stem mutation amongst changes required for ferret transmissibility of an avian H9N2 virus and whilst it is likely that this mutation was associated with increased HA stability, investigation of a stability phenotype was not considered at the time.

In the previous Chapter, we showed how increased virion stability can confer a survival advantage for viruses depositing on the upper respiratory tract, as they are less susceptible to inactivation in the acidic extracellular environment. It has been shown that viruses with less stable HA can transmit more readily by direct contact in comparison to through the air(134), suggesting that transmission through the air poses a particularly stringent bottleneck. Indeed, studies have demonstrated that

transmission through the air is associated with a genetic bottleneck of only 1-2 genomes, where as more genomes are transferred during contact transmission (118,190–192). The higher inoculum transferred by direct contact perhaps allows for successful host cell infection despite considerable losses in the extracellular environment of the URT. We hypothesised that as well as increasing survival in the mildly acidic URT, increased HA pH stability (low pH of fusion) might play an additional role in facilitating airborne transmission by enhancing virus survival as it travels between hosts within airborne droplets.

To understand this, it was necessary to derive a means of reliably isolating and quantifying virus directly from airborne droplets. For the most part, the focus of influenza transmission models, particularly ferrets, has been on the ability of virus to replicate in the respiratory tract of a donor animal and its ability to initiate infection in a recipient. A critical unknown in the field is how much infectious virus a ferret or human exhales and what happens to infectivity as virus exists in airborne droplets. To date, there have been only limited studies that have successfully sampled virus directly from airborne droplets. These have primarily used bioaerosol samplers or impactors to assay for viral nucleic acid(102–104,193–196). However, presence of viral nucleic acid does not necessarily correlate with viable virus that is capable of initiating infection in a recipient host. The sampling devices used preclude reliable quantification of infectiousness because of inherent limitations such as shear forces that can damage virions(197).

With this in mind, previous unpublished work from the Barclay laboratory (R. Elderfield, J. Ashcroft and W. Barclay) led to the design and manufacture of a bespoke device capable of detecting and quantifying infectious influenza virus from airborne droplets, using a direct viral plaque collection technique. In this chapter, we describe the implementation of this device to understand the ability of influenza-

infected ferrets and humans to release infectious virus into the air and use the device to understand the implications of HA stability for virus infectivity in airborne droplets.

3.2 Results – Part 1

3.2.1 Set up and validation of a novel method for collecting and quantifying infectious influenza virus from airborne droplets

The influenza virus transmission tunnel (IVTT) consists of a 100cm (length) x 18cm (width) x 9cm (height) half-cylindrical clear acrylic exposure tunnel that can hold three plates of susceptible cells at different distances from the source (Figure 3.1). Virus is introduced into one end of the tunnel either using a nebulisation unit or via breath from an infected animal and directional airflow maintained by a bias flow pump. Virus-laden droplets falling onto open culture plates are detected as viral plaques, enabling quantification and further analysis. The use of direct viral plaque collection is a more sensitive method of detection for viable virus than existing impaction techniques and the unique aspect of this apparatus is the ability to characterise individual depositing viruses isolated from the air.

A

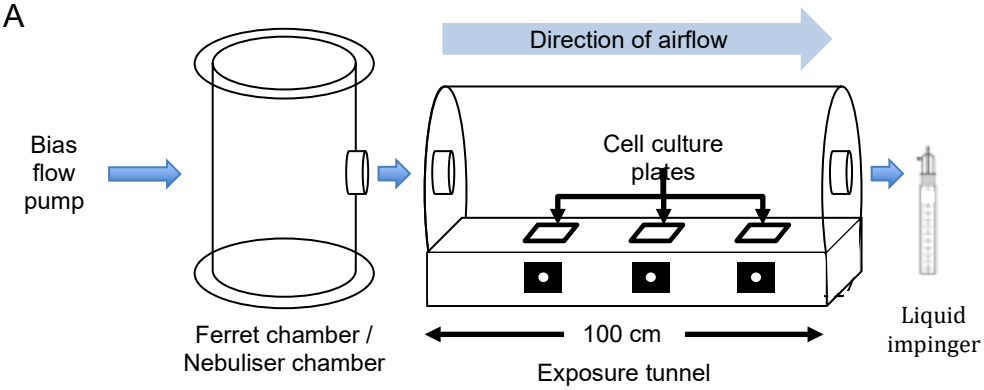

B

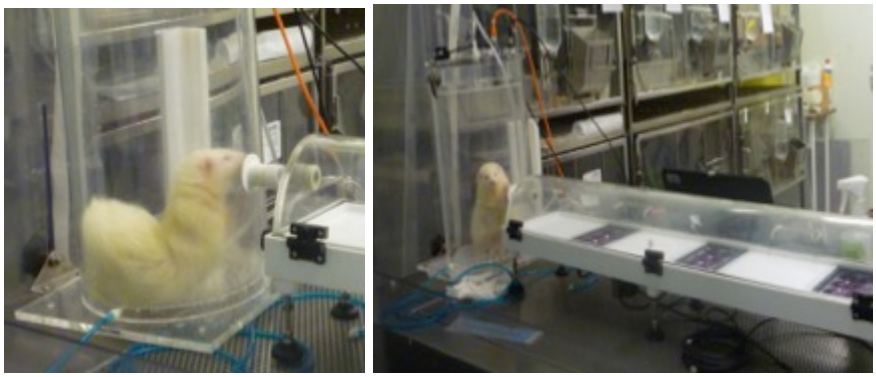

C

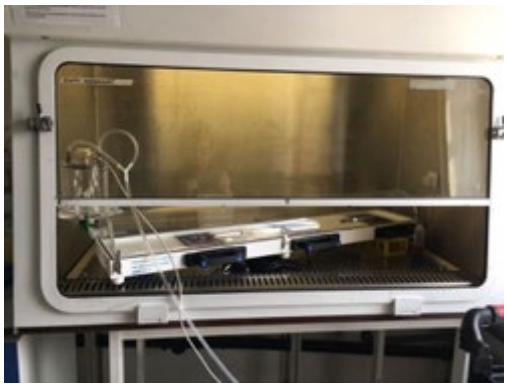

Figure 3.1 The influenza virus transmission tunnel (IVTT). (A) Schematic diagram of the IVTT apparatus. Airflow is generated using a bias flow pump, which connects to a 37.5cm (height) x 25cm (diameter) ferret chamber for *in vivo* experiments, or a 10cm (height) x 9cm (diameter) nebuliser chamber for *in vitro* experiments with nebulised virus. The IVTT is a half cylindrical clear acrylic 100cm (length) x 18cm (width) x 9cm (height) exposure tunnel containing cell culture plates situated 30cm, 60cm and 90cm from the tunnel opening. Air can be sampled from the end of the IVTT into a SKC Biosampler. Photographs of the IVTT in use for (B) isolating virus from an influenza virus-infected ferret and (C) assessing nebulized influenza virus inside a category 2 safety cabinet.

Initial set up and validation of the equipment was carried out by Barclay laboratory researcher Dr Ruth Elderfield, where parameters for collection such as air flow, input virus preparation and plaque isolation protocol, were established. These parameters were employed and further honed through the studies described in this Thesis. The final parameters used for testing are described in further detail in the Chapter 6 (Materials and Methods). Briefly, three 6-well plates of confluent MDCK cells overlaid with 0.5mL of supplemented DMEM are introduced into the IVTT and exposed to airborne virus introduced either via nebulisation or via breath from an infected animal or person. Cells are exposed for a period of 10 minutes then overlaid with a semi-solid agarose media and incubated at 37°C 5% CO_2 to allow for plaque formation. As initial validation of the apparatus performed by Dr Ruth Elderfield, increasing titres of Eng/09 virus nebulised into the IVTT resulted in increasing number of plaques collected on the culture plates situated at 30cm, 60cm and 90cm. The majority of infectious viral plaques were collected on the first exposed plate of cells (situated at 30cm) with a decline in plaque count seen by plate 2 (60cm) and plate 3 (90cm) (Figure 3.2).

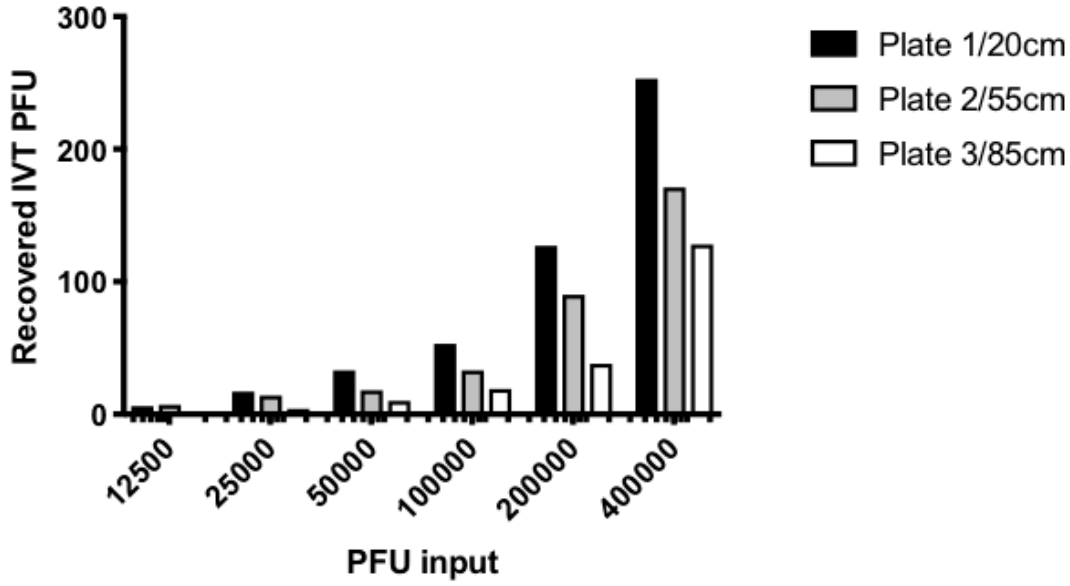

Figure 3.2 Validation of the IVTT. Increasing titres of pH1N1 virus (Eng/09) diluted in 50 µL PBS were nebulised into the IVTT for 10 minutes. Numbers of viral plaques detected on the three IVTT cell culture plates (situated 30cm, 60cm and 90cm from source) were visually counted.

Within the IVTT, we expected that droplets collected were likely to be of a certain minimum size in order to settle the short distance (~5cm) onto cell culture plates within 10 minutes. To derive an estimate of particle sizes depositing onto culture plates, computational modelling was performed in collaboration with Dr Laura Nicolaou, Department of Mechanical Engineering, Imperial College London and Johns Hopkins University. By adopting a model for the airflow, motion and evaporation of particles in the IVTT, Dr Nicolaou estimated that particle sizes ≥7.8µm can be collected on cell culture plates. To understand how airborne particles distribute within the tunnel we nebulised pH1N1 Eng09 virus mixed with a DNA plasmid tracer into the IVTT. Following 10-minutes cell culture plate exposure, we sampled any non-sedimenting aerosols from the air within the IVTT into an SKC Biosampler for an additional 10 minutes. The SKC Biosampler has been used previously for collection of viable airborne influenza viruses and is cited to be one of the more efficient available methods(198). The device has been used previously as a

standard with which to compare other techniques(199–201). Others have described that the SKC Biosampler can collect particle sizes between 0.3µm to 8µm(202,203). No infectious virus was collected from the air sample, whereas tracer DNA and viral RNA were detected (Figure 3.3). This experiment was designed by Dr Anika Singanayagam and kindly performed by postdoctoral scientist Dr Jie Zhou, Barclay Laboratory. Introducing fresh culture plates into the IVTT for a further 30 minutes after the initial 10-minute sampling window, to allow for any particles that might take longer to settle, also failed to isolate additional virus plaques.

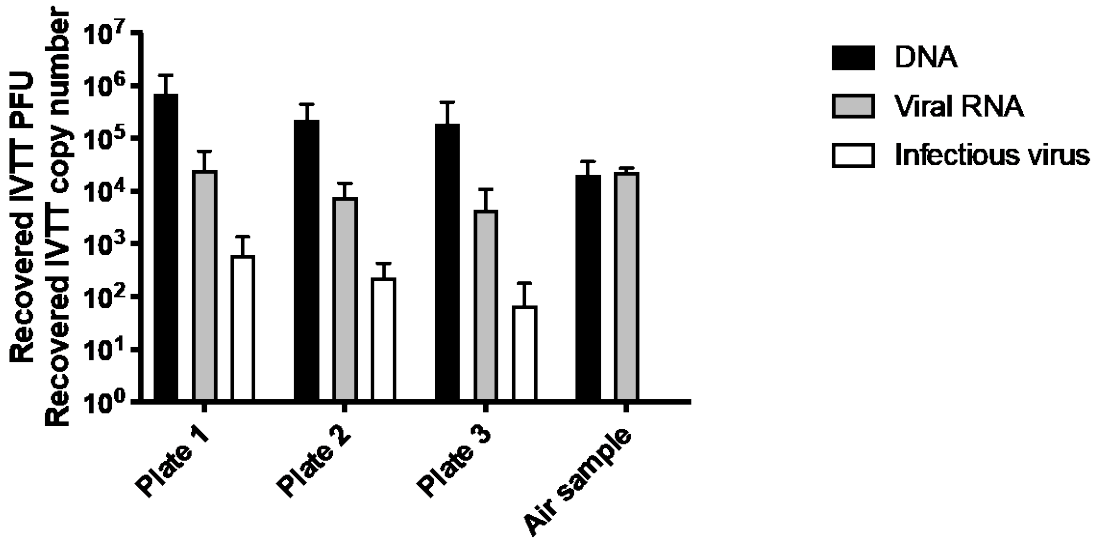

Figure 3.3 Distribution of infectious virus, viral RNA and tracer DNA nebulized into the IVTT. $2x10^7$ PFU of Eng/09 virus and $1x10^9$ copies of plasmid DNA diluted in 100 µL PBS were nebulised into the IVTT simultaneously and cell culture plates exposed for 10 minutes, in triplicate. Infectious virus was collected as plaque forming units (PFU) on MDCK cell culture plates (white bars). Plasmid DNA and viral RNA were collected into 1120µL PBS supplemented with 0.375% BSA-V place in the central space of the 6 well plates and quantified by real-time quantitative PCR (black and grey bars). After the 10 minute collection window, air was sampled into 15mL PBS with a SKC Biosampler connected to the end of the IVTT for a further 10 minutes and subjected immediately to plaque assay for infectious virus and real-time quantitative PCR for DNA and viral RNA. Error bars show standard deviation of three independent experiments.

These results suggest that the IVTT is capable of sampling viable virus from airborne droplets (droplets have been defined as particles >10μm in this Thesis, see Chapter 1.6) but, as found in previous studies, the efficiency of collection of viable virus from aerosols (defined as particles <10μm, see Chapter 1.6) and droplets/droplet nuclei with gravitational settling times of >10 minutes using an air sampling device, is less certain. The reason for the lack of infectious virus collection using the SKC Biosampler is likely due to virion damage during the sampling process but alternatively may represent that influenza virus viability is not well maintained in small aerosols. Emerging data suggests that droplets, rather than aerosols, may play a central role in transmissibility between ferrets, signifying that the IVT offers a useful model for investigating between host aspects of ferret-to-ferret transmission. Zhou *et al*.(102) demonstrated that presence of larger droplet sizes (>4.7μm) increased airborne transmission risk between ferrets. Airborne transmission did not occur when only aerosols <1.5μm were present, suggesting that fine aerosols do not contain significant amounts of contagious virus, despite representing 76.8% of particles released by experimentally-infected ferrets. Gustin *et al*.(103) also detected a five times higher amount of viable virus in particles >4.7μm despite the most frequent size of exhaled particle being <1μm.

3.2.2 Sampling of infectious virus exhaled by influenza-infected ferrets

3.2.2.1 Detection of exhaled infectious virus from ferrets is efficient using the IVTT

In vitro experiments using nebulised virus are limited in that airborne particles will not necessarily display the same size distribution nor have the same composition of salts/proteins/lipids as from respiratory secretions and thus virus may display a

different lifespan to that occurring in an *in vivo* setting. We therefore moved to attempt collection of infectious virus from infected ferrets.

Six ferrets were intranasally inoculated with 10^4 PFU of pH1N1 virus (Eng/09). This was performed in a series of 3 independent experiments with two ferrets, each performed on different days. The experiment on donors #1 and #2 was performed by Dr Anika Singanayagam, donors #3 and #4 by Dr Ruth Elderfield and donors #5 and #6 by Dr Ruth Elderfield and Dr Anika Singanayagam. All six infected animals shed robust titres of virus in the nasal wash from day 1 p.i. until day 5/6. The clinical illness induced by this virus, dose and route of inoculation was mild, with limited weight loss, coughs and sneezes observed in infected ferrets. This clinical picture is consistent with previous studies performed in the Barclay laboratory(204). Each ferret was sampled in the IVTT on days 1-4 p.i.. Donors #3, #4, #5 and #6 were additionally sampled up to day 7 p.i.. Infectious virus was detected in the IVTT on day 2 p.i. emitted into the air from all ferrets and to a lesser extent on day 3/4 [Figure 3.4A-F]. No virus was collected after day 5 p.i.. No ferrets were observed to cough or sneeze during the 10-minute breath collection on day 2 when the majority of virus was detected in the IVT. As seen for nebulised virus, the number of plaques detected declined with increasing distance along the IVTT. Nonetheless, infectious virus emitted from 5 out of 6 ferrets could be detected on plate 3, 90cm from the ferret chamber (Figure 3.4G).

Because the IVTT only samples the proportion of exhaled droplets that fall by gravity onto the surface area covered by the three cell culture plates, we performed further calculations to extrapolate the total number of virus particles that would be collected over the entire surface of the tunnel. This was performed in collaboration with Dr Laura Nicolaou and conversion calculations derived by Dr Nicolaou are detailed in Chapter 6 Materials & Methods. These calculations estimated the amount of infectious virus emitted by pH1N1-infected ferrets within 10 minutes to be at least 72

PFU (donor #2) and as much as 1388 PFU (donor #1) at the peak of detection on day 2 p.i. (i.e. a maximum rate of 138 PFU/minute was detected). This figure is 1-2 orders of magnitude higher than the peak rate 4 PFU/minute estimated in previous studies by the CDC(103,205) in which an impactor was used to collect infectious virus from infected ferrets. In the studies by the CDC, the largest quantity of virus directly collected from a single ferret over 30 minutes using apparatus that aims to collect every exhaled particle was 11 PFU. Using the IVTT, we were able to directly collect 327 PFU from one ferret in one third of the sampling time and with a technique that acknowledges that only a proportion of exhaled particles are being sampled.

3.2.2.2 Correlation of exhaled infectious virus with nasal wash titres and the timing of contagiousness

There was a clear peak in airborne infectious virus detected in the IVTT on day 2 for all ferrets, with lower amounts of infectious virus detected on days 3 / 4 and none after day 5. Interestingly, whilst this correlated with peak nasal wash titre in some ferrets (donors #2, #3, #5, #6), in others the timing was discordant. For donors #1 and #4, peak virus shedding in the nasal wash was on day 3 and 4 respectively. On these days, a low number of plaques were detected in the IVTT, but an order of magnitude less than was detected on day 2. On other days where a substantial amount of virus was present in the nasal wash, there was no viable airborne virus detected (Figure 3.4). This suggests that measurement of nasal virus, which is the typically used assay in influenza transmission studies, may not reliably predict the infectivity of virus that is released into the air from infected animals. It is possible that a nasal wash or nasal swab might artificially collect virus that would never be

naturally released, or dilute inhibitory factors that otherwise negatively impact the survival of virus released into airborne droplets or aerosols.

In a study previously published by the Barclay laboratory (Roberts *et al*.(204)), ferrets infected with pH1N1 Eng/09 successfully transmitted to sentinel ferrets in adjacent cages that were exposed to the infected donors for a limited time period, between 24 and 54 hours p.i. (i.e. on days 1-2). During this time, respiratory symptoms such as sneezes and coughs were rare. Interestingly, our data using the IVTT shows that airborne infectious virus peaks during this time window. On the other hand, sentinel ferrets exposed by Roberts *et al*. between 120 and 150 hours p.i. (i.e. on days 5-6), when respiratory signs such as coughs and sneezes were prominent, did not become infected. Again, our data from the IVTT is consistent with this, as infectious virus was not detected in the IVTT during this time. To test whether the ferrets exposed in the same manner could become infected on days 3-4, when a low level of infectious virus was detected in the IVTT, we exposed 2 sentinel ferrets housed in adjacent cages between 72 and 120 hours p.i. (days 3-4). These two sentinel ferrets also failed to become infected, suggesting that the low titre of infectious virus present in the air was not adequate to initiate infection in this experimental set up. In a study by Zhou *et al.*(102) using a somewhat different experimental set up, pH1N1-infected ferrets were similarly found to be most contagious early after infection (100% of sentinels became infected on day 1 p.i.). Infectivity declined as infection progressed, although 25% of ferrets exposed on day 5 p.i. still became infected.

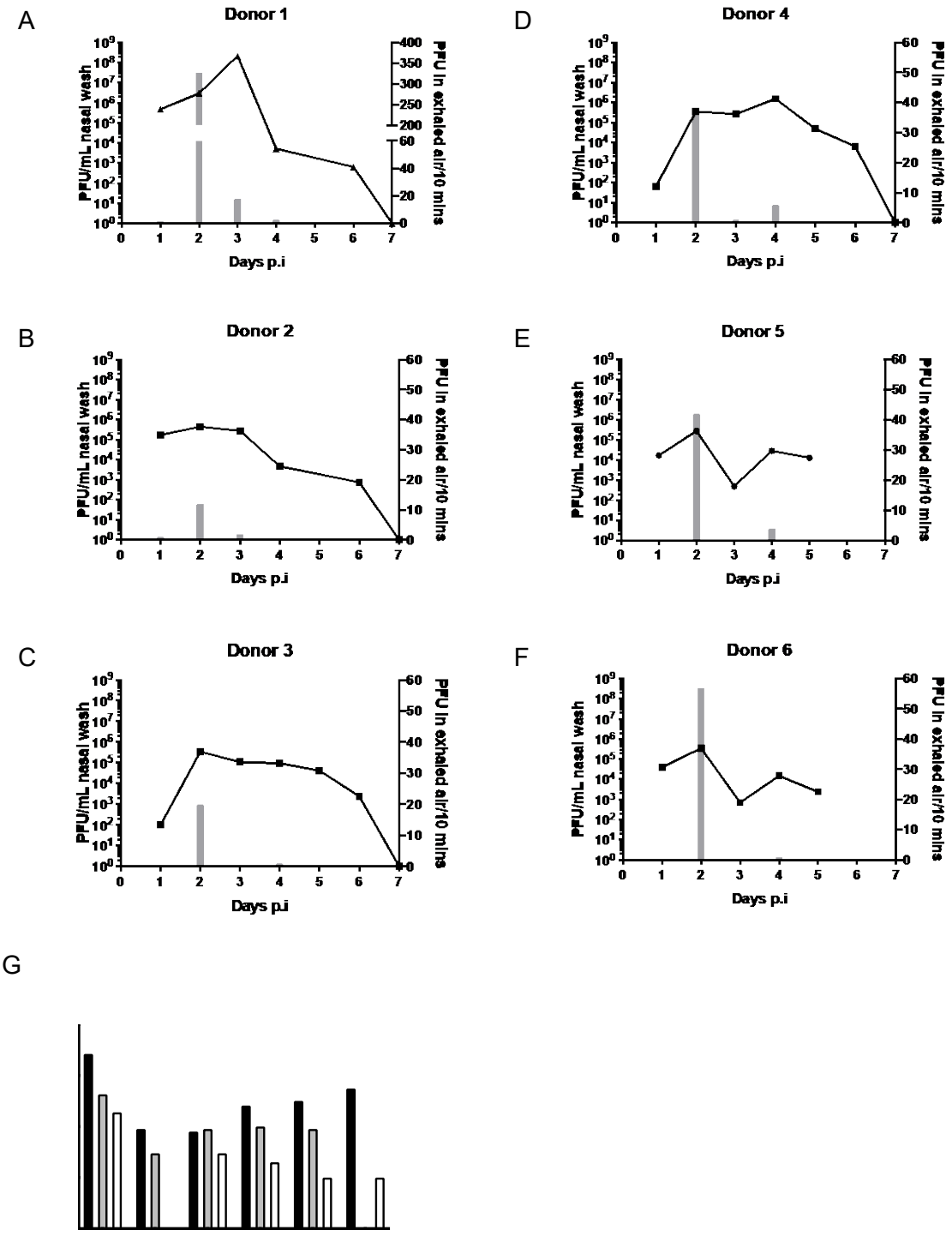

Figure 3.4 Ferrets emit a peak of infectious virus on day two post inoculation. Ferrets were intranasally inoculated with 10^4 PFU of Eng/09 virus diluted in 0.2mL PBS. On days 1 to 4, air was sampled for 10 minutes using the IVTT and then each ferret was nasal washed while conscious. Virus titre (PFU/mL) detected by plaque assay from nasal wash samples is shown as lines in (A) to (F) on the left y-axis. Total numbers of viral plaques (PFU) detected in the IVTT is shown as grey bars in (A) to (F) on the right y-axis. (G) The distribution of viral plaques collected in the IVTT on plates 1 (30cm, black bars), 2 (60cm, grey bars) and 3 (90cm, white bars) on day 2 is shown.

3.2.3 HA pH stability is advantageous for virus survival in airborne droplets

3.2.3.1 Ferrets infected with a stable pH1N1 HA mutant release more infectious virus into the air

Having successfully ascertained that viable virus can be efficiently collected by the IVTT from droplets exhaled by pH1N1-infected ferrets, we sought to implement this methodology to investigate how viability in airborne droplets might vary depending on a virus' HA stability using the pH1N1 mutant viruses described in Chapter 2.

We inoculated four ferrets each with either Y7H (more pH labile) or E21K (more pH stable) viruses and sampled exhaled breath on days 1 to 4 p.i.. Two ferrets (donors #1 and #2) in each group were infected with 10^4 PFU and two ferrets (donors #3 and #4) were infected with 10^6 PFU. Based on data shown in Chapter 2.2.3 that identified replicative differences between Y7H and E21K in primary airway cells, we predicted that Y7H might replicate in the ferret nose at lower titres than E21K. In order to achieve comparable titres of virus shed into the air, we elected to inoculate Y7H at the higher dose to attempt to achieve more comparable nasal wash titres between E21K and Y7H and also to enhance our chances of detecting airborne virus derived from minority variants.

The amount of viral replication in the ferret nose was not significantly different between E21K- and Y7H-infected ferrets when assessed by AUC analysis other than Y7H donor #3 that had an increased AUC and a higher peak nasal wash titre (Figure

3.5A and 3.5B]. The onset and peak of shedding was delayed by one day in ferrets infected with 10^4 PFU of Y7H compared to those infected at the higher dose or those infected at either dose with E21K. This delay probably represents reduced infectivity of Y7H in the ferret nasal tract. Overall, more plaques were detected from air exhaled by the four ferrets infected with the more stable E21K virus (total n=184 plaques) than by the four ferrets infected with Y7H virus (total n=23 plaques) [Figure 3.5C and 3.5D]. E21K virus plaques were detected on plate 2 at 55cm (n=57 plaques) and plate 3 at 85cm (n=7 plaques) where as Y7H had limited ability to retain infectiousness over distance.

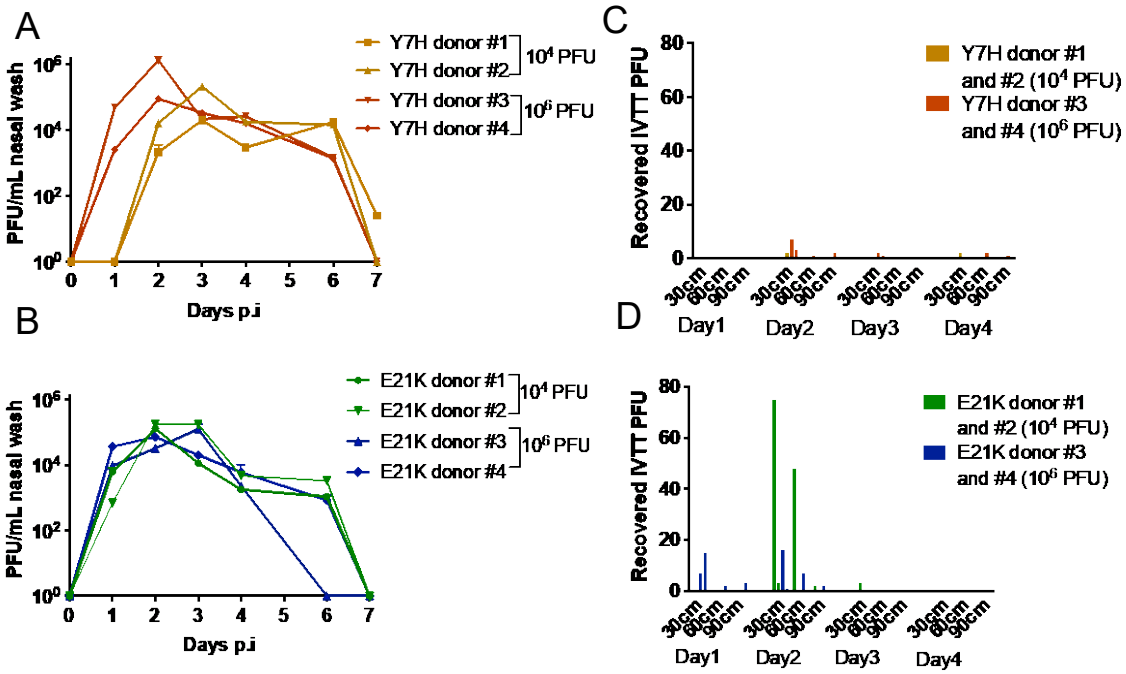

Figure 3.5 Virus emitted from ferrets infected with an acid stable virus retains infectivity in airborne droplets. Four ferrets were infected with either Y7H (orange/red) or E21K (green/blue) viruses. In each group donors #1 and #2 were infected with 10^4 PFU and donors #3 and #4 with 10^6 PFU. Viral titres in nasal wash samples were quantified by plaque assay for (A) Y7H and (B) E21K infected ferrets. Virus emitted in airborne droplets was collected from (C) Y7H and (D) E21K infected ferrets in the IVTT for 10 minutes on days 1 to 4 and detected on culture plates placed at 30cm, 60cm and 90cm along the tunnel.

3.2.3.2 Mutations that promote stability of haemagglutinin enhance virus survival in the air

Virus plaques collected from within the IVTT were picked and Sanger sequencing of the HA and M genes was performed. HA and M genes were selected for sequencing as these are the viral genes described to affect pH stability. Additionally, we carried out next-generation sequencing (NGS) of ferret nasal washes collected on days 1 to 4 post infection in order to detect any minority virus genotypes generated in the donor ferrets. A random selection of 25 plaques were picked that were exhaled from the 4 ferrets inoculated with E21K. There were no additional HA or M gene mutations detected in any of these IVTT plaques – all viral plaques retained the parental genotype. There were also no mutations detected in the nasal wash (at >5% frequency by NGS) from the four E21K-infected ferrets.

In contrast, HA mutations were detected from both airborne and nasal virus collected from the Y7H-infected donor animals that were not present on deep sequencing of the inoculum virus. The greatest number of viral plaques (n=15) was emitted by Y7H-infected donor #3, infected at 10^6 PFU. An assortment of HA mutations were detected upon sequencing of these plaques, including reversion at position 7 (H7Y) or additional HA mutations that are located around the HA stem (E47K-HA2, V55I-HA2 and V19I) (Figure 3.9A and 3.9B). Interestingly, all of these mutations have previously either been detected during ferret transmission events, arisen during natural evolution of pH1N1, or been described to be stabilising to pH1N1 HA in previous literature(134,138,206,207). All of the 15 virus plaques (propagated once only on MDCK cells) were found to have increased acid stability compared to the Y7H parent virus when tested in a pH inactivation assay (Figure 3.9C). One virus plaque emitted by donor #3 displayed a HA genotype unchanged from the parent

virus (Y7H) but was still found to be more pH stable. To understand this, we performed NGS of this virus to look for genotypic changes that might account for the phenotype observed. Surprisingly, NGS identified an additional A202T mutation in segment 8, the non-structural (NS) protein (Figure 3.6). This mutation was also detected in the nasal wash of the animal at a frequency of 1.5%-5.8% and was not present in the inoculum (Table 3.1). It may be that this NS mutation is contributing, via an as yet unknown mechanism, to the virus' ability to be exhaled and survive in airborne droplets. Intriguingly, NS1 has been previously described to facilitate airborne transmission of influenza viruses between ferrets(208) but the mechanism of this has not been clearly elucidated.

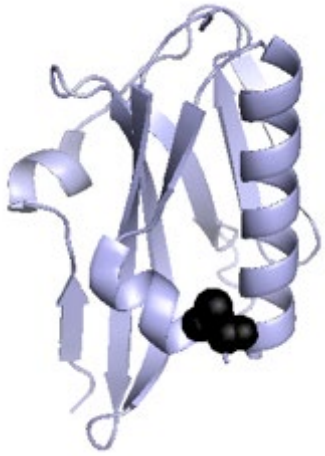

Figure 3.6. Location of NS mutation identified in virus plaque exhaled by Y7H-infected donor #3. The location of the mutation is shown in black spheres on the effector domain of NS1 (light purple). PDB structure 3RVC modelled using Pymol molecular visualisation tool.

In both donor #2 (Figure 3.8A) and donor #4 (Figure 3.10A), there was also evidence of survival of airborne virus with a pH stabilised phenotype and corresponding genotypic changes. The HA mutations detected in these virus plaques included I57F (exhaled by donor #2) and V16I/T61P (exhaled by donor #4). These mutations are positioned in regions of HA that are expected to impact on pH stability (Figure 3.8B and 3.10B). The viruses isolated were found to be significantly more pH stable than the parent virus when tested in a pH inactivation assay ($p<0.0001$ by one-way

ANOVA). Other plaques emitted by donors #2 and #4 that were isolated from the plate nearest to the ferret source did not show evidence of significantly increased stability. These were found to have retained the parental HA genotype (Y7H) or in the case of one plaque, had acquired only a T241I mutation located in the HA head with no mutations detected in the seven other genes (Figure 3.8C and 3.10C).

3.2.3.3 Minority populations of virus in the nasal tract of Y7H-infected ferrets gave rise to the majority of airborne infectious virus detected in the IVTT

In the nasal wash of the Y7H-infected ferrets, the mutations detected in exhaled plaques were present as minority populations including some existing as low frequency variants (<5% frequency) (Figures 3.7A, 3.8A, 3.9A, 3.10A). The predominant mutation detected was a reversion at position 7 (H7Y) which arose rapidly by day 1 in the nasal wash of donors #3 and #4 (infected at 10^6 PFU) and increased to 53% by day 4 (Figures 3.9A and 3.10A). This reversion mutation was also seen at 15% in the day 4 nasal wash from donor #1 (Figure 3.7A). Donor #2 did not accumulate a position 7 reversion but instead showed different mutations in HA on day 3 (Figure 3.8A).

All of the pH-stabilised plaques isolated from virus shed into the air carried HA mutations that were present in nasal washes, but these were detected as a minority population in several cases (for example T241I at 1% frequency in donor #2 and V19I at 2% frequency in donor #3). Several other mutations were present at various frequencies in nasal wash of the Y7H-infected ferrets that were not present in the plaques isolated from air (for example R45G from donor #1, L98M-HA2 from donor #2, N31S from donor #3) perhaps because these mutations were not adequately stabilising to preserve virus viability in droplets or that due to sampling constraints

these particular mutants were not detected as viral plaques. Taken together, these data show that virus mutants with more stable HA arose during replication in the ferret nasal tract and that increased pH stability can improve retention of infectivity in airborne droplets. A striking aspect of these results is that whilst only minority populations of pH stable viruses were detected in the donor ferret nasal tract, it is predominantly these rare mutants that are detected in the air.

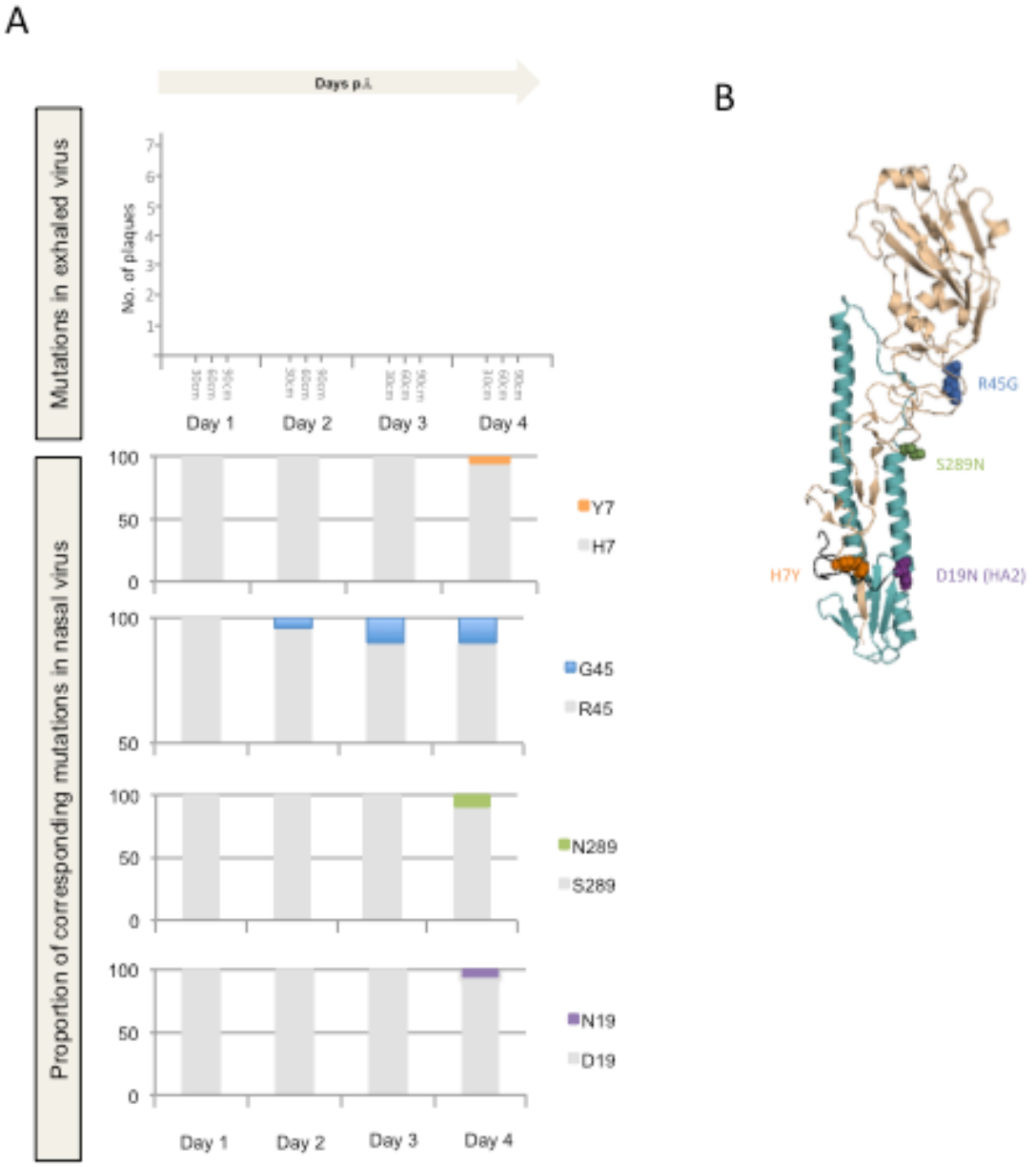

Figure 3.7 Sequencing of airborne and nasal virus isolated from Y7H-infected donor #1. (A) Upper panel: No virus was detected in the IVTT from Y7H-infected ferret donor #1 on days 1 to 4. Lower panel: Nasal wash from days 1 to 4 was next-generation sequenced and variants present at >5% frequency are shown in the bar graph: H7Y orange, R54G blue, S289N green and D19N in HA2 purple. In each of the bar graphs, the proportion of virus in nasal wash with sequence encoding the amino acid as in the parental virus (Y7H) is shown in grey. (B) HA mutations are modelled on a HA monomer using Pymol molecular visualization tool (PDB: 4jtv). H1 numbering using the mature HA sequence is used throughout(18). HA1 is shaded light brown, HA2 is teal and the fusion peptide is black.

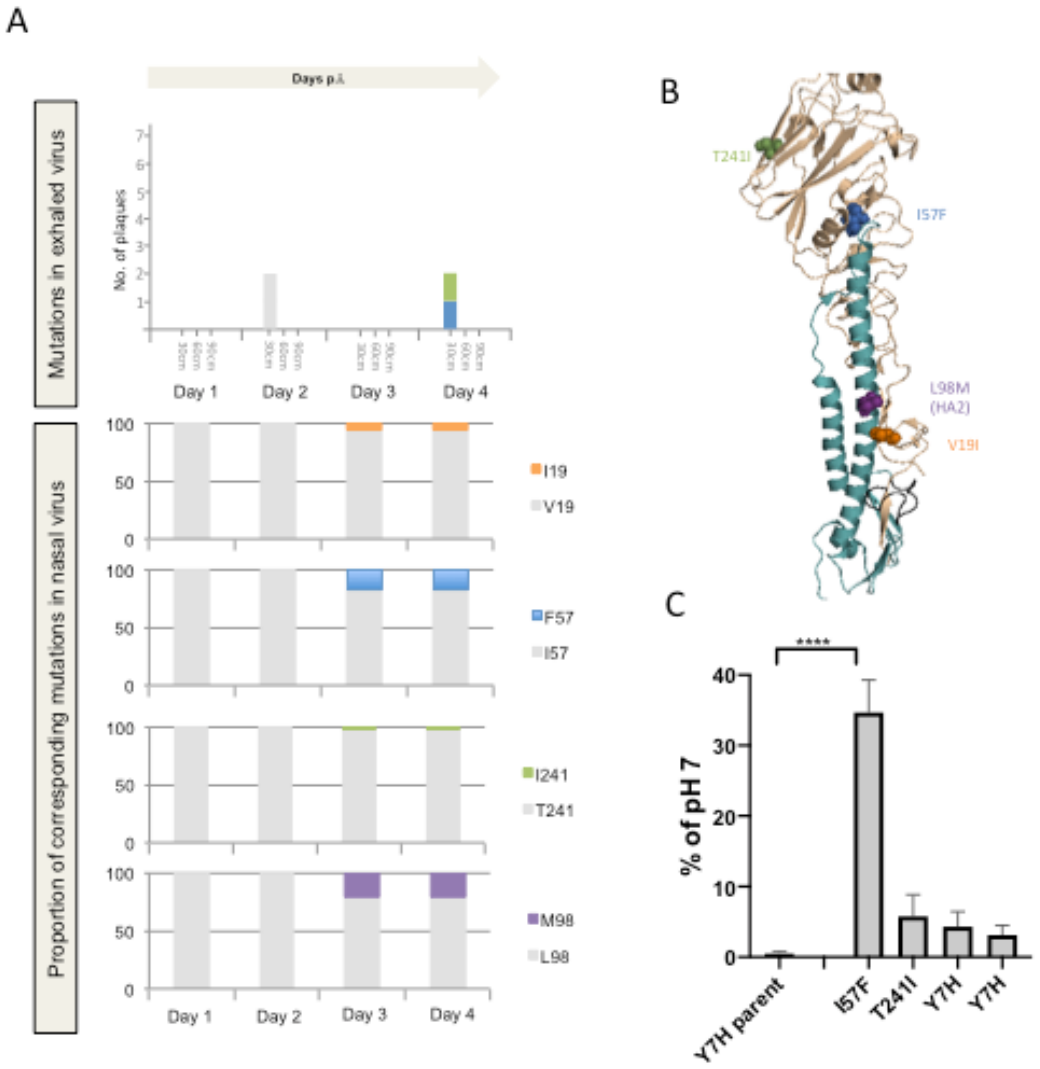

Figure 3.8 Sequencing of airborne and nasal virus isolated from Y7H-infected donor #2. (A) Upper panel: Virus emitted by Y7H-infected ferret donor #2 on days 1 to 4 was collected as plaques picked from plates 1 (30cm), 2 (60cm) and 3 (90cm) of the IVTT and viral RNA extracted. The haemagglutinin (HA) gene was Sanger sequenced. HA mutations identified in viral plaques are represented by the colours orange V19I, blue I57F, green T241I and purple L98M-HA2. Lower panel: The proportion of corresponding HA mutations on days 1 to 4 in the nasal wash was determined by next-generation sequencing. In each of the bar graphs, the proportion of virus in nasal wash with sequence encoding the amino acid as in the parental virus (Y7H) is shown in grey. (B) HA mutations are modelled on a HA monomer using Pymol molecular visualization tool (PDB: 4jtv). H1 numbering using the mature HA sequence is used throughout(18). HA1 is shaded light brown, HA2 is teal and the fusion peptide is black. (C) The acid stability of viruses in air emitted from donor #2 was tested by incubating virus propagated from IVTT plaques at low (pH 5.5) and neutral (pH 7) pH, in triplicate. The remaining infectivity detected at pH 5.5 is expressed relative to infectivity detected at pH 7. Stability of parental virus Y7H is shown on the left of the panel. Error bars represent standard deviation of three independent experiments. One-way ANOVA with Tukey post-test was used to compare each plaque with the Y7H parent virus. *p<0.05, **p<0.01 ***p<0.001 ****p<0.0001.

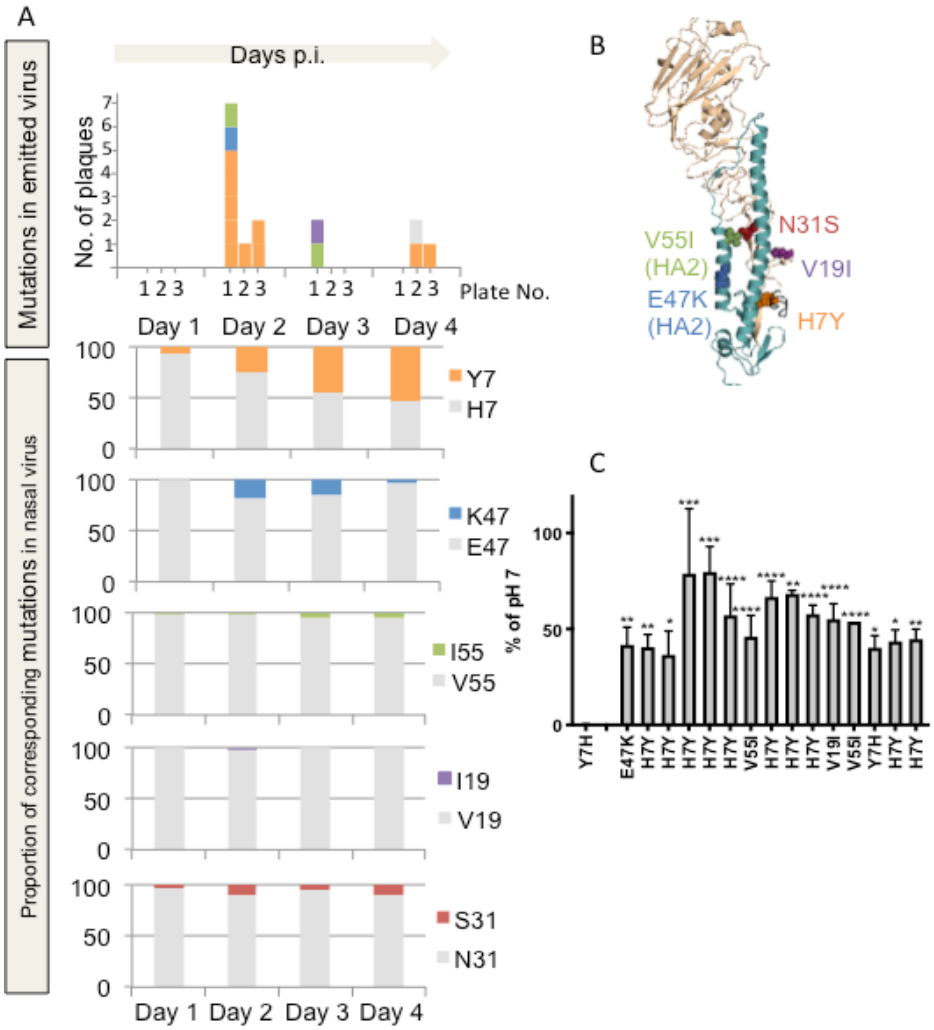

Figure 3.9 Mutations that promote stability of haemagglutinin enhance virus survival in the air. (A) Upper panel: Virus emitted by Y7H-infected ferret donor #3 on days 1 to 4 was collected as plaques picked from plates 1 (30cm), 2 (60cm) and 3 (90cm) of the IVTT and viral RNA extracted. The haemagglutinin (HA) gene was Sanger sequenced. HA mutations identified in viral plaques are represented by the colours orange H7Y, blue E47K-HA2, green V55I-HA2 and purple V19I. Lower panel: The proportion of corresponding HA mutations at positions 7 and 19 in HA1 and 47 and 55 in HA2 detected on days 1 to 4 in the nasal wash was determined by next-generation sequencing. An additional mutation detected in the nasal wash at >5% frequency but not in any picked plaques is also shown (N31S in red). In each of the bar graphs, the proportion of virus in nasal wash with sequence encoding the amino acid as in the parental virus (Y7H) is shown in grey. (B) HA mutations are modeled on a HA monomer using Pymol molecular visualization tool (PDB: 4jtv). H1 numbering using the mature HA sequence is used throughout(18). HA1 is shaded light brown, HA2 is teal and the fusion peptide is black. (C) The acid stability of viruses in air emitted from donor #3 was tested by incubating virus propagated from IVTT plaques at low (pH 5.5) and neutral (pH 7) pH, in triplicate. The remaining infectivity detected at pH 5.5 is expressed relative to infectivity detected at pH 7. Stability of parental virus Y7H is shown on the left of the panel. Error bars represent standard deviation of three independent experiments. One-way ANOVA with Tukey post-test was used to compare each plaque with the Y7H parent virus. *p<0.05, **p<0.01 ***p<0.001 ****p<0.0001.

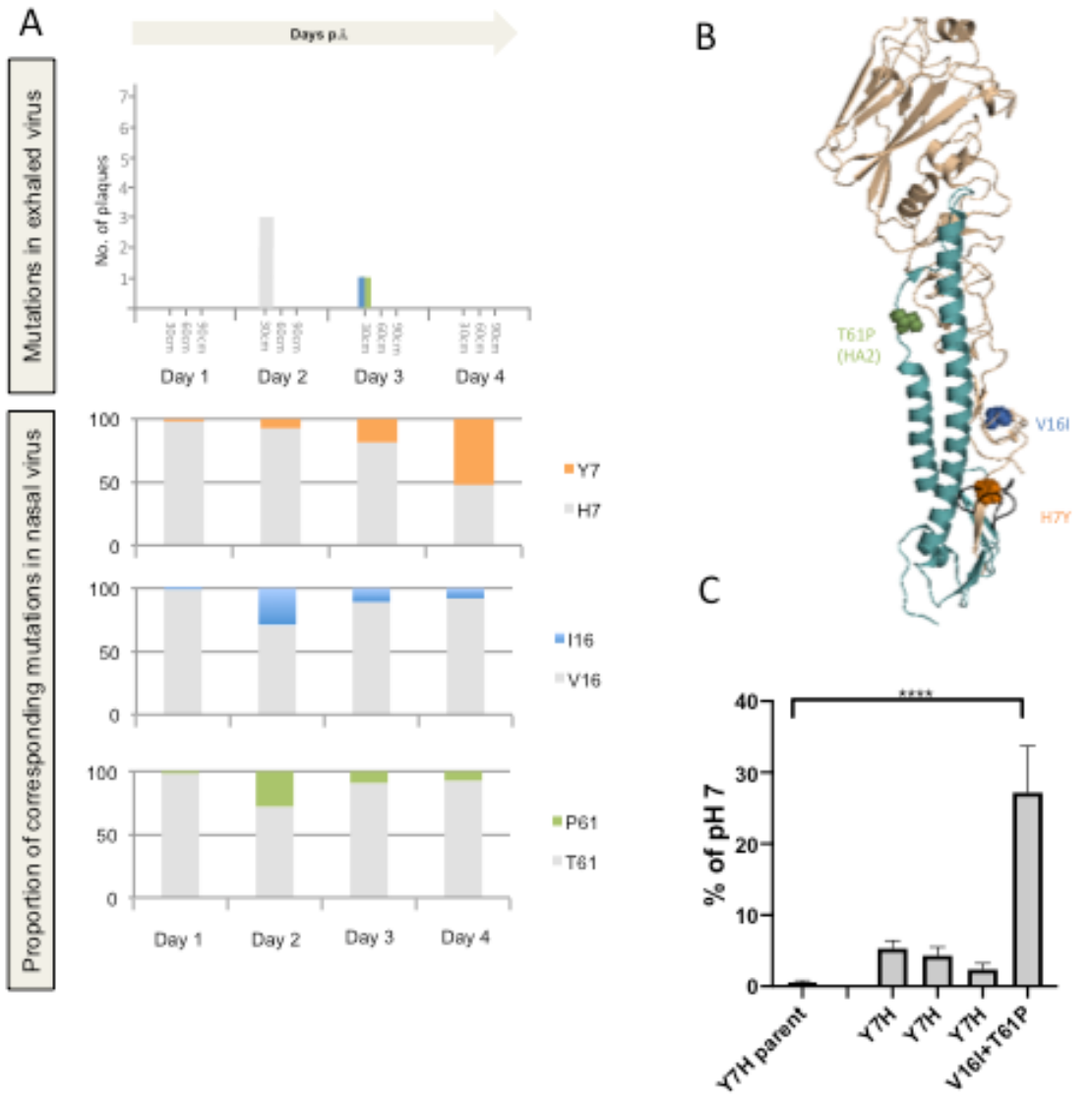

Figure 3.10 Sequencing of airborne and nasal virus isolated from Y7H-infected donor #4. (A) Upper panel: Virus emitted by Y7H-infected ferret donor #4 on days 1 to 4 was collected as picked plaques from plates 1 (30cm), 2 (60cm) and 3 (90cm) of the IVTT and viral RNA extracted. The haemagglutinin (HA) gene was Sanger sequenced. HA mutations identified in viral plaques are represented by the colours orange H7Y, blue V16I, green T61P in HA2. Lower panel: The proportion of corresponding HA mutations at positions 7 and 16 in HA1 and 61 in HA2 detected on days 1 to 4 in the nasal wash was determined by next-generation sequencing. No additional mutations were detected in the nasal wash at >5% frequency. In each of the bar graphs, the proportion of virus in nasal wash with sequence encoding the amino acid as in the parental virus (Y7H) is shown in grey. (B) HA mutations are modelled on a HA monomer using Pymol molecular visualization tool (PDB: 4jtv). H1 numbering using the mature HA sequence is used throughout(18). HA1 is shaded light brown, HA2 is teal and the fusion peptide is black. (C) The acid stability of viruses in air emitted from donor #4 was tested by incubating virus propagated from IVTT plaques at low (pH 5.5) and neutral (pH 7) pH, in triplicate. The remaining infectivity detected at pH 5.5 is expressed relative to infectivity detected at pH 7. Stability of parental virus Y7H is shown on the left of the panel. Error bars represent standard deviation of three independent experiments. One-way ANOVA with Tukey post-test was used to compare each plaque with the Y7H parent virus. *p<0.05, **p<0.01 ***p<0.001 ****p<0.0001.

3.2.3.4 Other mutations detected in exhaled plaques

Having identified an NS mutation in one plaque that retained the same HA genotype as the parental virus, we were interested to see if mutations or mixed populations had occurred in any other genes for the other virus plaques exhaled by Y7H-infected ferrets. Using NGS, we identified a PB2 mutation in 2 virus plaques (V504I in a plaque from donor #3 and F363L in a plaque from donor #2). These PB2 mutations were not detected in the inoculum or in the nasal washes taken from the animals, suggesting that they may have arisen during propagation of the plaque on MDCK cells. Similarly, another plaque exhaled by donor #3 had a A651T mutation in PA that could have arisen during cell culture propagation. However, one PA mutation (A448E) detected in a plaque exhaled by donor #4 was detected at 20.6% in the nasal wash and was absent in the inoculum, suggesting it arose during nasal replication. Another PA R269K mutation in a plaque exhaled by donor #3 was present at 1.5% frequency in the nasal wash. The significance of these PA mutations is uncertain (Table 3.1).

Day	Plate	Plaque	HA Mutation	Other gene mutation	Inoculum freq	Peak nasal wash freq
DONOR #2						
2	1	1	T241I			
2	1	2	I57F	PB2 F363L	<1%	<1%
4	1	1	Y7H			
4	1	2	Y7H			
DONOR #3						
2	1	1	E47K			
2	1	2	H7Y			
2	1	3	H7Y			
2	1	4	H7Y			
2	1	5	H7Y			
2	1	6	H7Y			
2	1	7	V55I	PA A651T	<1%	<1%
2	2	1	H7Y	PA R269K	<1%	**1.5% K269**
2	3	1	H7Y			
2	3	2	H7Y	PB2 V504I	<1%	<1%
3	1	1	V19I			
3	1	2	V55I			
4	2	1	Y7H	NS A202T	<1%	**5.8% T202**
4	2	2	H7Y			
4	3	1	H7Y			
DONOR #4						
2	1	1	Y7H			
2	1	2	Y7H			
2	1	3	Y7H			
3	1	1	V16I+T61P	PA A448E	<1%	**20.6% E448**

Table 3.1 Mutations in virus plaques exhaled by Y7H-infected ferrets detected by next-generation sequencing. The peak frequency of the corresponding mutation in the nasal wash on days 1-4 is shown.

3.2.3.5 pH stable influenza viruses have improved survival when nebulised into airborne droplets

To provide validation for our observations in ferrets that suggest a survival advantage in droplets is conferred by increased pH stability, we performed further studies *in vitro*. A 40:60% mixture of E21K and Y7H viruses (10^6PFU) was nebulised into the

IVTT and virus plaques collected over 10 minutes. Plaques from plates 2 (n= 70) and 3 (n=75) were picked and Sanger sequencing of the HA gene performed. There were too many plaques on plate 1 to enable plaque purification. The proportion of plaques with the pH stable E21K genotype was found to be significantly increased on plate 2 (65%, p=0.024 by Fishers exact test) and plate 3 (79%, p=0.0002 by Fishers exact test) compared to the inoculum (36%) (Figure 3.11A). To further confirm this finding, we repeated the experiment using a mixture containing a lower titre of inoculum virus to enable individual plaques to be isolated from plate 1, which is more representative of the distribution of plaques emitted in ferret exhaled breath. A 25:75% mixture of E21K and Y7H (total $5x10^4$ PFU) was nebulised into the IVTT [Figure 3.11B]. Virus plaques collected on plates 1 (n=70) and 2 (n=26) were picked and Sanger sequencing of the HA gene performed. There were too few plaques collected on plate 3 (<5 plaques). The proportion of plaques with the pH stable E21K genotype was again found to be significantly increased on plate 1 (72%, p<0.0001) and plate 2 (58%, p=0.001) compared to the proportion in the inoculum (22%). Finally, we attempted the same experiment using an even lower proportion of E21K to examine if the observation would hold true even when the stable virus was present in a minority. A 10:90% mixture of E21K and Y7H (total $5x10^4$ PFU) was nebulised into the IVTT [Figure 3.11C]. Virus plaques collected on plates 1 (n=71)) and 2 (n=22) were picked and Sanger sequencing of the HA gene performed. There were too few plaques collected on plate 3 (<5 plaques). The proportion of plaques with the pH stable E21K genotype was again significantly increased on plate 1 (55%, p<0.0001) and plate 2 (46%, p=0.02) compared to the proportion in the inoculum (13%) supporting the hypothesis that HA stability can enhance the ability of virus to remain infectious in airborne droplets.

If virus is being rendered non-infectious by premature triggering of HA within airborne droplets and this is disproportionately affecting the more fragile Y7H mutant, we hypothesised that the proportions of viral genetic material detected within the IVTT would be unchanged from that introduced in the inoculum. To investigate, in our first experiment (40%:60% mix) we collected depositing droplets into 500µL PBS placed in the central space between wells of each culture plates, extracted viral RNA from 140µL PBS and performed NGS of the HA gene in order to quantify the proportion of E21K/Y7H genomes present. Our results show, similarly to infectious virus, that the proportion of E21K genomes detected on the IVTT culture plates and from an air sample was higher than that detected in the inoculum ($p<0.0001$ for each plate compared to the inoculum by Chi-squared test) (Figure 3.11D). This might suggest that physical stress of the nebulisation process or the external challenges of existing in airborne droplets lead to disruption of the virus such that the virion is degraded, with Y7H being disproportionately affected due to its more pH sensitive surface protein.

A

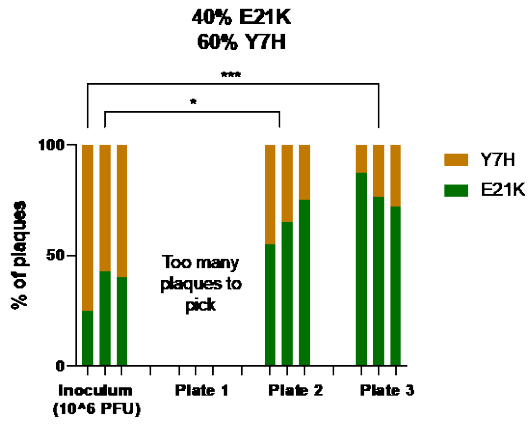

B

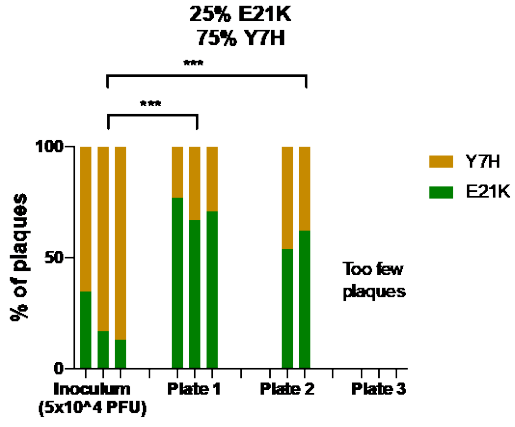

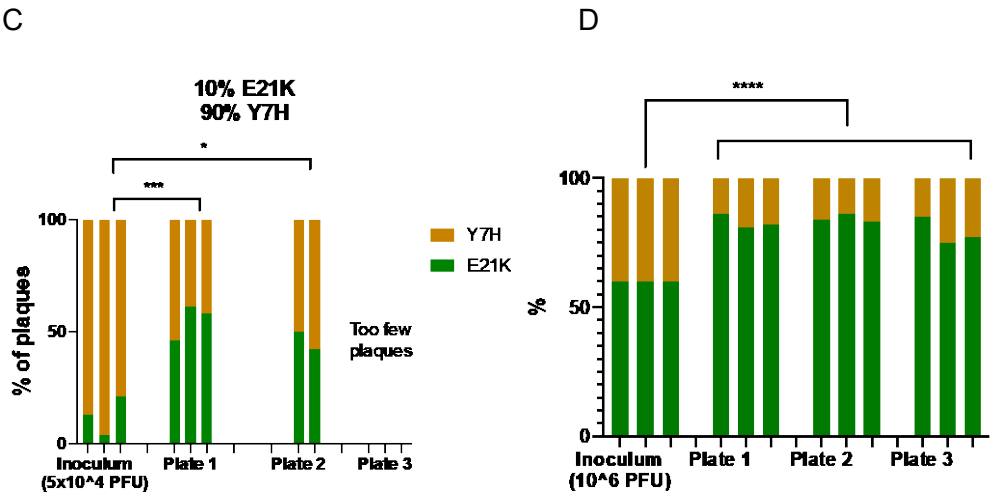

Figure 3.11. Increased acid stability enables virus to remain infectious in airborne droplets. (A) 40%:60% (B) 25%:75% (C) 10%:90% mixture of E21K and Y7H based on PFU/mL titres was nebulised into the IVTT in three independent experiments. Input viral titres were 10^6 PFU in (A) and $5x10^4$ PFU in (B) and (C). Plaques collected on IVTT plates and a smaple of plaques from the inoculum were picked and Sanger sequencing of the HA gene performed. Where the distribution of plaques was such that too few (n=<5) or too many plaques were collected to enable purification and/or analysis is indicated. (D) From the experiment detailed in (A), the proportion of E21K and Y7H viral genome copies detected on each culture plate and in the inoculum was quantified by next generation sequencing. Chi-squared test was used to compare the proportions of E21K/Y7H genotype detected on each plate. Fisher's exact test was used to compare the proportions of E21K/Y7H genotype detected on each plate. *p<0.05, ***p<0.001.

3.3 Discussion Part 1: key findings from studies on ferrets experimentally inoculated with pH1N1 virus

For virus to successfully transmit through the air between two hosts, it must be exhaled from the donor in sufficient quantities and retain infectiousness in the air. This aspect of transmission is poorly understood given prior lack of a satisfactory method of quantifying infectious virus from airborne particles. Using a novel technique of direct viral plaque isolation from airborne droplets, we were able to successfully collect infectious virus exhaled by infected ferret donors at a more

efficient rate than previously described. The unique aspect of the technique is the ability to isolate individual exhaled viruses and analyse their genotype and phenotype.

3.3.1 Sampling infectious virus exhaled by ferrets infected with wild-type pH1N1

We show that ferrets infected with pH1N1 Eng/09 virus exhaled a peak of infectious virus early after infection. We did not observe any coughing or sneezing by virus-infected ferrets whilst they were sampled in the IVTT during the peak of airborne virus detection. The quantity of infectious virus detected in the IVTT decreased over time after infection. This pattern correlates with previous reports of an early window of airborne contagiousness in ferrets, prior to the onset of fever and clinical signs(102,105,204). In these studies, contagiousness was found to decrease as infection progressed and clinical symptoms such as coughing, sneezing and nasal congestion became more apparent. This is in contrast to the commonly held assumption that coughing and sneezing promote influenza airborne transmission. Studies in humans are required to confirm the relevance of observations in ferrets for human disease. In a meta-analysis of experimental infection studies on human volunteers intranasally inoculated with influenza, the peak of nasal viral shedding was found to precede peak of clinical symptoms by one day. However, there have been no studies systematically investigating the timing or duration of contagiousness or the presence of exhaled infectious virus in experimentally- or naturally- infected humans. Previous studies on ferrets that have measured exhaled viral RNA showed no correlation between airborne RNA levels and contagiousness, actually detecting more airborne viral RNA during times of reduced contagiousness(102) and for

several days after infection(102,103,105). Measuring infectious virus appears to be a better correlate for contagiousness, although further work is required to confirm this and to investigate the relevance for other subtypes and strains of influenza. The reason that contagious virus is not being shed into the air at later time points despite high titres of virus detectable in ferret nasal washes and viral RNA detectable in exhaled air warrants further investigation. Perhaps other as yet uncharacterised inhibitory host factors limit survival of exhaled virus later in the course infection, for example the production of innate immune mediators or a change in the local environment of the URT, such as pH, viscosity, or mucous production.

3.3.2 pH stability confers a survival advantage for virus in airborne droplets

Typical ferret-to-ferret influenza transmission experiments assess the ability of the virus to replicate in a donor animal and its ability to initiate infection in a sentinel. Importantly, after virus enters and replicates in a sentinel animal, further selection limits the information that can be gained about the transmitted virus. For example, it is not possible to delineate whether selection of a transmitted mutant has occurred during replication in the donor, at the point of release from the donor, during travel in the air between animals, or during infection of the sentinel animal. Using the IVTT to sample virus can capture information about the genotype of viruses released into the air without the need for virus to infect and replicate in an onward host. We employed this technique to demonstrate a role for stability of influenza HA for retention of viability in airborne droplets. The more stable “human virus-like” E21K mutant was better able to retain infectivity when nebulised into droplets than the less stable “avian virus-like” Y7H mutant. Ferrets infected with E21K emitted more infectious

virus than ferrets infected with Y7H. Infectious virus recovered from air shed from ferrets inoculated with Y7H virus contained mutations that conferred restabilisation of HA. This extends the findings of Russier *et al.*(134) who detected a single stabilised mutant (HA H7Y+R106K) in 1 out of 4 sentinel ferrets exposed to donors infected with pH1N1/Y7H in a traditional ferret-to-ferret transmission experiment. 3 out of 4 sentinel ferrets did not become infected in this study. Using the IVTT has enabled to identify many more HA mutants and to gain a broader understanding of what is happening to virus travelling between hosts. An interesting aspect of our findings is that whilst only minority populations of pH stable viruses are detected in the Y7H-infected donor ferret nose, it is predominantly these rare mutants that are detected in the air.

3.3.3 Hypotheses to explain a role for pH stability for survival of airborne virus

Within airborne droplets, the viral envelope must withstand conditions quite distinct from the environment of the URT. Evaporation of water occurs rapidly (in < 1 second) after respiratory droplets are released from the URT(209). As a consequence of water evaporation, the concentration of free H+ ions in a droplet increases and lowers the pH. For example, Yang and Marr(210) calculated that at 60% relative humidity, similar to conditions during our IVTT experiments, a droplet will shrink to 0.17 of its initial diameter, reducing pH by 2.3 units. This effect might be compounded at the air/water interface at the surface of droplets(211). Human nasal mucosa is mildly acidic (ranging from 5.3 to 7.0)(30). A decrease in pH in droplets consisting of fluid derived from the nasal mucosa of up to 2.3 units would fall within the pH range that can trigger HA unfolding and have significant impact on virus

viability. Moreover, inhibitory substances incorporated into droplets formed from respiratory secretions may become more concentrated in droplet nuclei, which could contribute to infectivity losses. Of note, a recent study from the CDC has shown a correlation between loss of infectivity in aged aerosols and poor transmission(212). It has also been suggested that an increased concentration of salts and insoluble solutes in droplet nuclei(209,213), osmotic forces(214), or disruption of virions accumulating at the surface of droplets due to surface tension might explain infectivity losses(210). Our finding of a significantly greater proportion of E21K RNA than Y7H RNA detected in the IVTT when a mixture of the viruses were nebulised into the IVTT might support this theory, suggesting that Y7H is more susceptible to virion degradation.

3.3.4 Limitations of the IVTT

As with all methods employed to isolate influenza virus from the air, there are limitations to the design of the IVTT that must be considered.

(i) Lack of sampling of aerosols and small droplet nuclei

The IVTT is uniquely designed as a straightforward and sensitive method to sample infectious virus from airborne droplets, which has been of particular challenge in previous studies. Efficient collection of infectious virus from aerosols will require different methodology. Whilst studies have shown that a large proportion of exhaled particles are submicron in size, emerging data suggests that larger droplets may be important for transmission through the air in a ferret model(102,103).

(ii) Particle losses and limited sampling surface area

Using culture plates to sample virus means that droplets are only being collected on a limited surface area. Deposition of particles on the walls and floor of the

IVTT will occur. The technique aims to sample airborne virus rather than attempt to collect all airborne particles as has been the aspiration of the majority of previous studies using impactors or bioaerosol samplers. Nonetheless, our sampling approach is shown to be more efficient at collecting infectious virus than other techniques that propose to be collecting all airborne particles.

(iii) Limited sampling time

Ferrets are introduced into the IVTT ferret chamber while fully conscious (to allow for natural breathing). We believe this to be a strength of our study compared to other approaches that have administered anaesthetic to animals or collected exhaled particles from artificially induced coughs/sneezes. Administration of anaesthetic is likely to alter the rate and kinetics of respiration that affect the relevance of results for natural infection. Because ferrets are sampled while fully conscious, a maximum breath collection of 10 minutes is applied for animal welfare reasons but this does limit the efficiency of collection.

(iv) Difficulties collecting viral RNA from ferrets

Others in the Barclay laboratory have performed preliminary work to attempt collection of viral genome copies emitted by pH1N1-infected ferrets using the IVTT but this has so far been unsuccessful. This would be useful data to help understand whether virus is being shed into droplets but losing infectivity and only a proportion remains viable. Briefly, in these experiments, 500µL of PBS was placed in the space between the wells of the 6-well culture plates within the IVTT. Viral RNA was extracted from 140µL of PBS after the 10-minute ferret exposure period and subjected to RT-qPCR. It is possible that quantities of virus collected in this manner are below the limit of detection by RT-qPCR but confirmatory studies are still required. Based on previous studies, we might expect genome copies in the order of ~2 logs (10-20 fold greater than infectious virus) to be released by an infected ferret over 10 minutes in both sedimenting droplets and non-sedimenting aerosols(103). Taking into account various losses

that occur during air sampling and RNA extraction/processing, this likely falls below sensitivity for detection. To overcome this limitation, a longer ferret exposure time may be necessary to increase virus in the IVTT to a measureable quantity or adaption of the apparatus to improve its ability to collect viral RNA.

(v) Ferret-to ferret variability

We do note ferret-to-ferret variability in the quantities of airborne infectious virus detected in the IVTT. This has also been observed in previous studies on exhaled virus from ferrets(103) and humans(194). It is possible that this variability represents differences in individual ferret physiology or in how the timing of the 10-minute IVT sampling period relates to virus-host kinetics in the individual.

3.4 Results – Part 2

3.4.1 Lack of detection of infectious virus exhaled by experimentally-infected humans: results of a preliminary study

3.4.1.1 Review of the literature on sampling of infectious virus from human exhaled breath

The vast majority of studies on exhaled virus from influenza infected human subjects have used RT-qPCR for quantification of viral genome copies. The few studies (listed in Table 3.2) that have attempted to collect viable virus from human subjects have had poor success rates. Frequently, detection of any viable virus has required a secondary culture step, which abrogates quantification, and artificial breathing techniques such as forced coughs and exhalations, which are not a natural emission. In the largest study of exhaled breath collection, Yan *et al*.(194) collected 218

samples of exhaled breath from 142 college students with confirmed influenza using a bespoke device that aims to collect all particles exhaled over 30 minutes. 41 samples of fine aerosol particles (<5μm) collected using an impactor were positive for influenza, with a mean of 37 FFU collected over 30 minutes (=1.23 FFU/minute). The highest titre in a sample was 1100 FFU (=36.6 FFU/minute). However, contamination and delayed processing invalidated 84 of the 218 samples and it is not clear how many individual subjects yielded the 41 positive results versus how many were replicate samples from the same patient. A further caveat of this work is that quantification using FFU that assesses virus in a single round of replication, rather than a multicycle analysis such as PFU, would incorrectly score incomplete and defective viral particles as viable. Additionally, particles >5μm, which may have contained significant amounts of viable virus, were excluded from analysis due to sampling constraints related to inefficiency of the impactor used. Challenges in collecting viable virus from human exhaled breath contribute to significant gaps in knowledge about influenza transmission. For example, the quantity and timing of exhaled infectious virus, duration of human contagiousness and how this relates to timing of symptoms, and the relative contribution of different particle sizes and modes of transmission.

First author, year	**Emission**	**Mode of collection**	**Secondary culture step performed**	**Summary of results**
Lindsley, 2010 (215)	Forced coughing	SKC Biosampler OR Impactor	No	Viable virus (0.8 and 5 pfu/mL/cough) was detectable from only 2 out of 21 influenza-positive subjects
Milton, 2013 (195)	30 minutes breathing and forced coughing	Impactor	Yes	Viable virus collected from 2 out of 37 influenza-positive subjects
Hatagishi, 2014 (216)	Forced coughing	Gelatin membrane filter	No	Viable virus was detected in 3 samples from 56 patients (1.5,1.5, 8 PFU per cough)

				onto a gelatin membrane filter.
Lindsley, 2015 (202)	Forced coughing	SKC Biosampler	No	Viable virus from 17 out of 64 participants (range of 5 to 538 PFU detected)
Lindsley, 2016 (203)	Forced exhalations AND Forced coughing	SKC Biosampler	Yes	Viable virus was detected from forced exhalation aerosols from 28/53 subjects and forced cough aerosols from 22/53 subjects
Yan et al. 2018; (194)	30 minutes natural breathing and talking	Impactor	No	218 samples collected from 142 subjects with confirmed influenza. Quantification of infectious virus by FFU on 41 fine aerosol samples with a mean of 37 FFU in 30 minutes. 56 fine aerosol samples showed CPE when passaged on MDCK cells.

Table 3.2 Analysis of studies that reported collection of viable virus from human exhaled breath.

3.4.1.2 Collection of exhaled breath from experimentally-infected humans using the IVTT

Having demonstrated that the IVTT can successfully detect infectious virus exhaled by influenza-infected ferrets, we carried out a preliminary study to test the ability of the IVTT to detect virus exhaled by human volunteers that were experimentally infected with a pH1N1-like virus. Experimental infection of human volunteers with influenza virus dates back to the 1918 pandemic. The illness induced tends to be less severe than a natural infection(217), considered to be due to differences in the inoculated viruses and route of infection. Human challenge studies have largely been used to investigate antiviral drugs and vaccines and there has been very little research on viral transmissibility using challenge subjects. Killingley *et al*.(218) published a proof-of-concept study to assess the feasibility of using a human challenge model to assess influenza transmission. They exposed “recipient” volunteers to infected “donors” in shared accommodation for 30 hours commencing on day 2 post inoculation with a H3N2 influenza virus. This set up, which allowed for

all forms of natural influenza transmission (airborne, droplet, direct contact, fomite), demonstrated a secondary attack rate of 25% (3 of 12 infected recipients). However, the ability of human experimental infection to result in transmission through the air has never been tested.

A total of 17 healthy human adult volunteers were recruited for study between June and November 2016. This human challenge study was coordinated and performed by Dr Christopher Chiu and team from the National Heart and Lung Institute, Imperial College London, with a separate goal of investigating immune responses resulting from influenza challenge. Our study was opportunistically carried out in parallel to this work, with a primary aim of isolating influenza virus plaques from human exhaled breath using the IVTT apparatus. All volunteers were confirmed by the Chiu group to be sero-negative to the challenge pH1N1 strain and were isolated in a quarantine unit during the course of the study. Volunteers were intranasally inoculated with 10^6 PFU of A/California/04/2009 (pH1N1)-like virus, in 5 cohorts. The inoculum virus strain used was described by Watson *et al*.(219) to have been isolated from a healthy 3 year old boy in 2009. Prior to use in this study, the virus strain had undergone three passages in SPF eggs and was expanded to GMP standards.

10 out of 17 (59%) volunteers were confirmed to have become successfully infected by the challenge virus by real-time PCR and/or plaque assay performed on nasal wash samples. Each volunteer was asked to breathe naturally (tidal breathing) into the IVTT for 10 minutes. A portable low flow suction pump was attached to the end of the IVTT to encourage directional airflow. Figure 3.12 shows the set up of the IVTT for collection from human volunteers. Refinements to the collection method were carried out with each subsequent cohort, in an attempt to optimise the chance of virus collection. For cohort 1, each volunteer was asked to breathe via a disposable mouthpiece attached directly to the IVTT. For cohort 2, the mouthpiece was changed

to a facemask covering the nose and mouth, in an attempt to capture virus exhaled from both the nasal cavity and mouth. In cohorts 3 and 4, we sealed the IVTT after the 10 minute breath collection and exposed the cells for an additional 30 minutes, attempting to isolate any virus contained in smaller droplets that might take longer to settle within the IVTT. Cohort 5 were additionally asked to carry out 10 forced coughs after the 10 minute breath collection and air was pulled through the apparatus at a defined rate (2L/minute). Despite these multiple attempts, no virus plaques were isolated from any of the experimentally infected human subjects. For cohort 5, an additional two cell culture plates were place in the IVT and left to incubate to allow for viral replication. However, there was no evidence of cytopathic effect and the cell supernatant was negative by HA assay and plaque assay after 5 days.

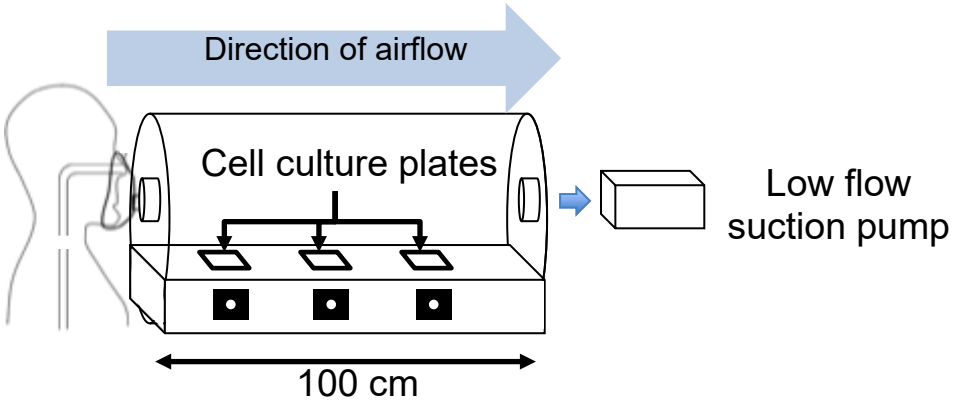

Figure 3.12 Schematic diagram of the IVTT adapted for collection of virus from air exhaled by human volunteers.

3.4.1.3 Hypotheses to explain the lack of infectious virus sampled from humans using the IVTT

There are several possible contributing factors to the failure to detect viable virus from the challenge subjects.

1) **Technical issues.** Operational issues of adapting the equipment for use in a patient isolation ward may have contributed to the lack of virus detected. It

was not possible to push air into the device using the bias flow pump whilst a human exhaled so a portable low flow pull pump was used instead, which will have altered the air flow dynamics. Additionally, human subjects exhaled into the IVTT whilst wearing a facemask. Substantial condensation was noted within the mask after each collection and it is possible that viable virus adhered to the interior of the facemask. Swabbing the mask for virus could have helped to understand this. Further refinement of our technique may be required to optimise the apparatus for virus isolation from humans.

2) **Droplet sizes.** Emerging data from ferret studies has indicated that the majority of viable influenza virus released into the air may exist in larger particles(102,103). However, the situation in humans is unclear. Although influenza is traditionally thought to transmit via large droplets, a contribution of aerosol transmission is being increasingly recognised(112,220). If humans exhale the majority of viable virus into small aerosols that do not sediment within the IVTT, this could explain the lack of detection. We did attempt to expose the cells for an additional 30 minutes to allow some smaller particles to settle but unfortunately did not attempt any air sampling for non-sedimenting aerosols in these experiments.
3) **Pre-existing immunity.** The complex pre-existing immune profile of humans means that artificial infection is harder to achieve than in immunologically naïve ferrets. It is well described that human experimental infection results in milder symptoms than natural infection(217). It may be that subjects are mounting a rapid immune response to the challenge virus that subverts its release into the air. One intriguing hypothesis is that secretory antibody or other immune mediators can become contained in droplets released early in infection and inhibit virus infectivity. Attempting quantification of viral RNA could have helped to understand this.

4) **Inoculating virus.** The virus used to inoculate the volunteers had been propagated in eggs. Changes in receptor binding or pH stability of the inoculating virus may have occurred during egg propagation could have resulted in a virus not optimally adapted to replicate in the human URT. Low URT viral titres are likely to correlate with less efficient shedding and transmission. In human influenza challenge, the intranasal route of inoculation and high inoculum dose (10^6 PFU) used, whilst akin to experiments on ferrets, is unlike natural human infection and may not be ideal for stimulating robust URT viral replication and shedding into the air. Indeed, previous human challenge studies have shown that infection by aerosol inhalation leads to more potent infection than instillation of nasal drops(221).

3.4.2 Nasal wash viral titres from experimentally-infected humans

We sought to understand if the failure to detect exhaled virus was a result of its poor replicative ability in the human URT. Viral titre was quantified by RT-qPCR from daily nasal wash samples for the 10 successfully infected subjects. This data, shown in Figure 3.13, was kindly provided by the Chiu laboratory. Viral RNA became detectable in the nose of the majority of patients between day 1 and 3 p.i.. One subject (4-2) only had detectable nasal virus from day 5 p.i.. Peak titres reached ~10^4-10^5 RNA copies/mL, which is similar to that previously described following human experimental inoculation(222). The day on which nasal wash titre peaked was found to be heterogeneous between study subjects: day 2 (n=2), day 3 (n=2), day 4 (n=1), day 5 (n=3), day 6 (n=1), day 7 (n=1). Watson *et al.*(219), using the same inoculum virus at a titre of ~10^6 $TCID_5$, detected a mean peak $TCID_{50}$ of $10^{5.16}$ from nasal samples with peak viral replication occurring 3-4 days after challenge. However, in a meta-analysis of 56 human challenge studies, peak shedding occurred

predominantly on day 2 p.i, similar to that seen in immunologically naïve ferrets(222).

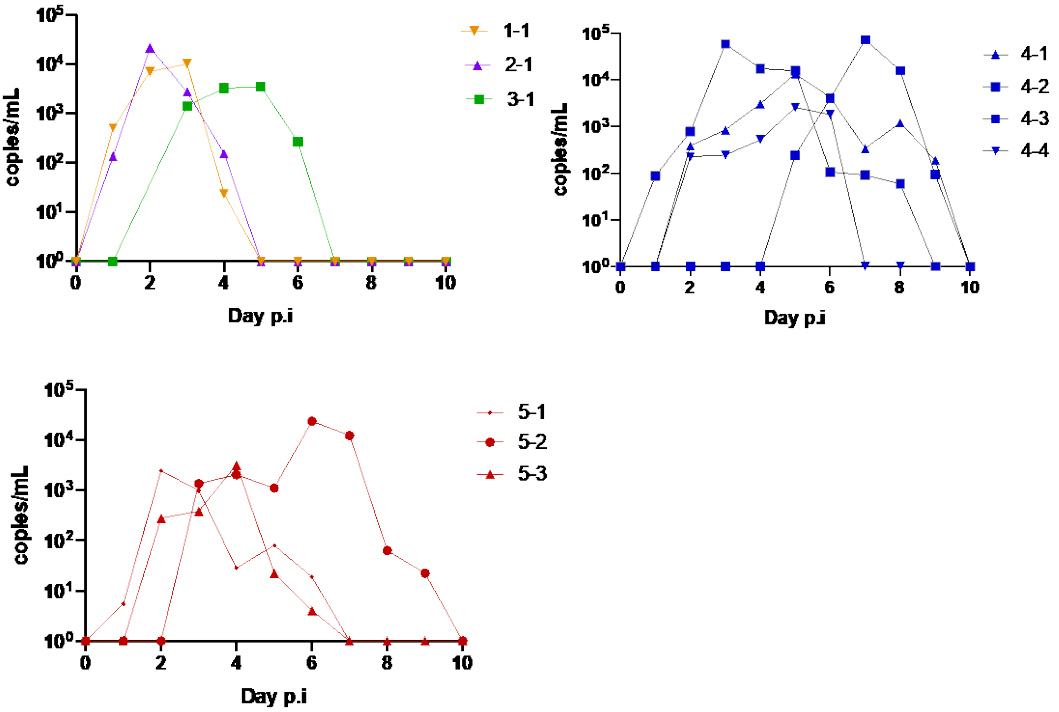

Figure 3.13. Nasal wash viral loads from experimentally infected human subjects. Virus titre was quantified daily over 10 days by RT-qPCR for A) cohorts 1,2, and 3 (n=3) B) cohort 4 (n=4), C) cohort 5 (n=3). Data is shown courtesy of Dr Christopher Chiu.

3.4.3 Mutations in the egg-adapted virus inoculum occur rapidly after infection

Deep sequencing of the "A/California/04/2009-like" inoculum virus identified that it differed from a reference A/California/04/2009 (Cal04) strain by several mutations - the non-synonymous mutations identified are listed in Table 3.3. HA mutations P83S, S203T, I321V and T197A have been described as variants that arose during the early antigenic drift of pH1N1(223), signifying that the inoculum virus strain was isolated later in the 2009 than the prototypic Cal04 strain and had already undergone some genetic drift. D127E, D222G and Q223R have been described as egg

adaptation mutations(224), which have likely arisen during the propagation of the inoculum virus.

Segment	1	2	3	4	5	6	7	8
Gene	PB2	PB1	PA	HA	NP	NA	M	NS
Non-synonymous mutations	R3K P302S		P224S	P83S D127D/E T197A S203T D222D/G Q223R/Q I321V	V100I G102R I353V L307L/I	S95N V106I N248D		

Table 3.3 Non-synonymous mutations identified in the inoculum A/California/04/2009-like virus compared to a reference A/California/04/2009 sequence. The HA mutations previously described to have arisen as genetic drift are coloured green and those that have been described as egg adaptations are coloured blue.

We analysed the virus sequence present in nasal wash samples obtained from the 10 infected subjects on days 1, 2 and 3 p.i. by NGS. Sequencing quality was variable and data is only shown where depth of >100 reads was obtained. None of the day 1 samples could be successfully sequenced. We saw rapid reversion of egg adaptation mutations in segment 4 (HA) and segment 5 (NP) in virus obtained from nasal washes compared with the inoculum virus that occurred by day 2/3 for multiple subjects.

HA mutations

Sequence data of adequate depth and quality for the HA gene was obtained from 5 subjects. Mixed populations were detected at positions 127, 222 and 223, which are

residues that have been previously described to be associated with egg adaptation. These positions are all located in the head of HA, in close proximity to the receptor binding domain or Sa antigenic site (Figure 3.14).

Figure 3.14. Location of mutations identified in sequencing of virus isolated from human nasal wash samples. The position of mutations are modelled on a HA monomer using Pymol molecular visualisation tool (PDB: 4jtv).

i) Position 223

A mixed population of R/Q at position 223 (226 in H3 numbering) was present in the inoculum virus (80% Q, 20% R), likely as a result of its propagation in eggs. In the nasal wash of subjects where virus was successfully sequenced, this rapidly reverted back to 100% of the “human-like” Q (Figure 3.15). Position 223 is located in the receptor-binding site and is well described to play a key role in receptor binding specificity in numerous influenza virus subtypes and strains. Q223R was previously shown to switch receptor binding preference in pH1N1 from α2,6- to α2,3- linked

sialic acid. Q223R resulted in abolition of respiratory droplet transmission in guinea pigs and decreased transmission efficiency in ferrets. When introduced in combination with the mammalian-adapting PB2 mutation T271A, Q223R resulted in abolition of RD transmission in ferrets(225).

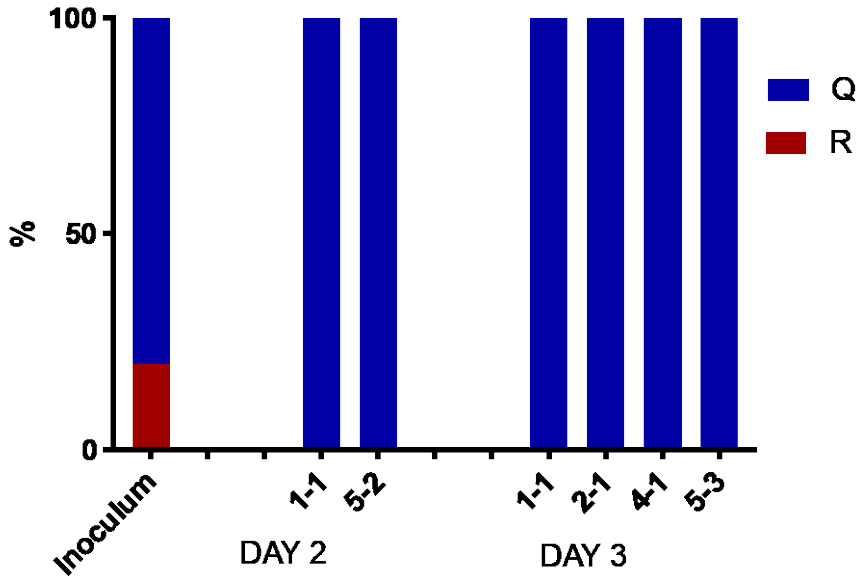

Figure 3.15. Deep sequencing of HA position 223. Proportions of amino acids detected by NGS at position 223 in the HA gene of virus obtained from nasal wash samples acquired on day 2 or day 3 post inoculation, in comparison to the inoculum. Sequencing from all day 1 samples was unsuccessful.

ii) Position 222 and 127

Mixed populations at positions 222 (225 in H3 numbering) and 127 (131 in H3 numbering) were also detected in the inoculum virus. The reference Cal04 virus has a D at position 222 and D at position 127. The inoculum virus was found to contain 89% D/11% G at position 222 and 30% D/70% E at position 127, which may be a consequence of egg adaptation.

Following early replication in the URT of challenge volunteers, the proportion of D222 and E127 increased to >90% in 3 of the 5 subjects (1-1, 5-1 and 5-2). In the remaining 2 subjects (2-1 and 4-1), a population of G222 and D127 persisted (Figure 3.16). We could hypothesise that differences in the baseline immunity of the adult challenge subjects may underlie the differing selection pressures that we have seen during this early stage of replication in the human nose.

D222G was reported in both 2009 pandemic H1N1 and 1918 pandemic H1N1 to result in receptor binding specificity switch from α2,6 to dual (α2,6/α2,3) receptor binding (82,226). D222G was also associated with cases of severe human pH1N1 infection, viraemia and lower respiratory tract involvement(227–230) and was associated with airborne transmissibility of pH1N1 in ferrets(231). Position 127 is located near the Sa antigenic site and D127E mutation has been characteristic of a small proportion of the 6B.2 clade of pH1N1 that emerged through antigenic drift in 2015/16(232).

In this human challenge study, 3 volunteers consented to lower airway examination by bronchoscopy – subjects 1-1, 2-1 and 4-4. Interestingly, subject 2-1 was the only subject with a detectable viral load from lower airway sampling. One hypothesis is that the G222 and/or D127 mutation in subject 2-1 increased binding to LRT-prevalent α2,3-linked SA receptors, enabling viral replication at this site. Sequencing virus obtained from lower airway sampling to ascertain the population of virus prevalent at this site could help to understand this. Furthermore, it would be interesting to investigate if any host factors specific to subjects 2-1 and 4-1 could have lead to enrichment of G222/D127. For example, suboptimal immune responses or any association with compromised lung function (e.g. asthma, smoking history). Future work might aim to understand if humans pre-disposed to severe infection are more tolerant of expanding populations of virus with G222.

A

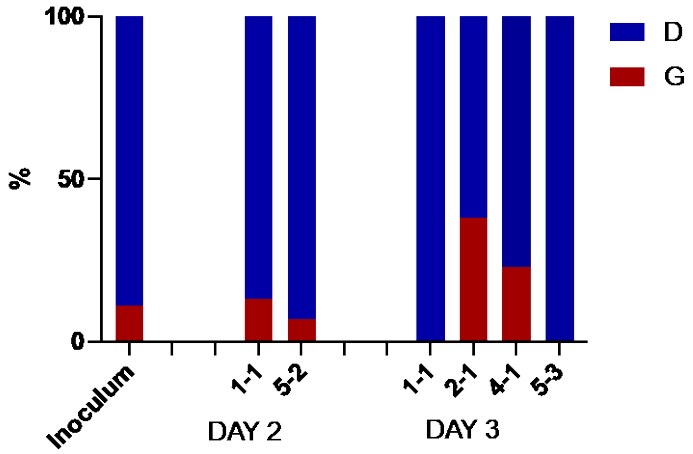

B

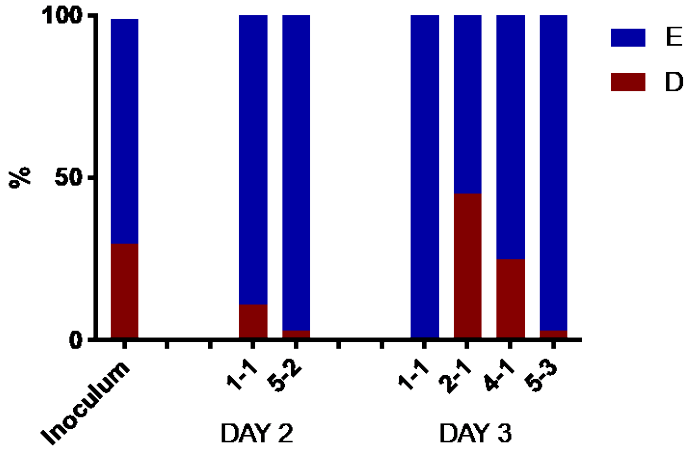

Figure 3.16. Deep sequencing of HA positions 222 and 127. Proportions of amino acids detected by NGS at position (A) 222 or (B) 127 in the HA gene of virus obtained from nasal wash samples acquired on day 2 or day 3 post inoculation, in comparison to the inoculum. Sequencing from all day 1 samples was unsuccessful.

Nucleoprotein (NP) mutations:

Adequate sequencing of the NP gene was obtained from the nasal washes of 7 patients. In all these patients, an R to G mutation was detected at position 102. Sequencing of the inoculum revealed 90% R102, whereas the reference Cal09 had G at position 102 (Figure 3.17A). R102 has likely arisen as a consequence of egg propagation(224). Mutations in this region of NP (Figure 3.17B) have previously been

suggested to contribute to altered use of importin-α isoforms or escape from the antiviral effect of the IFN-induced antiviral factor MxA(233). We hypothesise that the G102R mutation is selected for during growth in eggs to enable use of importin-α3 (rather than α7 in human cells)(234) and/or that resistance to MxA is not required in this system. Indeed, chicken Mx has been shown to be inactive against influenza(235). In support of this, NP G102R resulted increased MxA sensitivity in a polymerase assay using recombinant RNPs in one recent study(236). MxA resistance has been linked to impaired viral fitness and therefore may be easily lost in the absence of selective pressure(233,237).

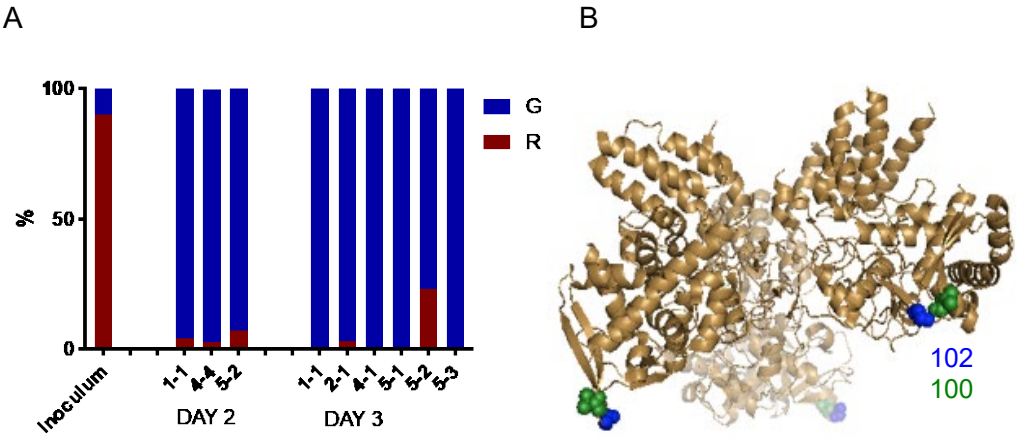

Figure 3.17. Deep sequencing of NP position 102. (A) Proportions of amino acids detected by NGS at position 102 in the NP gene of virus obtained from nasal wash samples acquired on day 2 or day 3 post inoculation, in comparison to the inoculum. Sequencing from day 1 samples was unsuccessful. (B) Location of residues 102 (blue) and 100 (green) in the base of the body domain modelled onto the trimeric NP using Pymol molecular visualisation tool (PDB: 2IQH).

3.5 Discussion Part 2: key findings from human volunteers experimentally inoculated with pH1N1 virus

59% of human volunteers became successfully infected with a pH1N1-like virus. Viral replication in the order of 10^4-10^5 RNA copies/mL was detected from nasal wash specimens. No exhaled viable virus was detected using the IVTT

NGS enabled us to measure the genetic diversity in the inoculating virus and after its early replication in the human nose. We identified that egg propagation selected for viral variants that likely provided a fitness advantage in this system, but probably carried a fitness cost for replication in the human URT.

Intra-host adaptation occurred rapidly (by day 2/3) at specific sites when humans were infected with this suboptimally adapted viral strain. The residues detected in HA are previously described to be important for receptor binding and/or antigenicity. The residue detected in NP is previously described to be important for importin-α specificity and resistance to the antiviral restriction factor MxA. It would be interesting to directly investigate whether the egg adaptation mutations in the inoculum virus led to any change in its pH stability that could have contributed to an inability to be shed efficiently into the air and have contributed to the lack of detection of IVTT plaques from human volunteers.

Chapter 4. The significance of HA stability for effectiveness of the live attenuated influenza vaccine

4.1 Introduction

Two types of influenza vaccines are available for annual vaccination programmes against circulating seasonal H1N1, H3N2 and influenza B viruses: the injectable inactivated vaccine and the nasally-administered LAIV. LAIVs are needle-free, more straightforward to manufacture and can induce mucosal, cellular and humoral immune responses, mimicking natural immunity. LAIV viruses have cold adapted (*ca*), temperature sensitive (*ts*) and attenuated (*att*) internal viral genes from master donor viruses (MDV) and surface antigens (HA and NA) from the circulating influenza H1N1, H3N2 and influenza B subtypes. The cold-adapted nature of the internal viral genes results in mild and self-limiting infection when administered intranasally, since the virus cannot replicate at the higher temperature of the lower respiratory tract. Two types of LAIV have been independently developed. FluMist®/Fluenz® (AstraZeneca) is derived using the A/Ann Arbor/6/60 or B/Ann Arbor/1/66 MDV and has been introduced into seasonal influenza vaccination programmes in the US, UK, Canada and Finland. The other product, developed and used in Russia, is derived using the A/Leningrad/134/57 or B/USSR/60/69 MDV and is primarily targeted to low- and middle- income countries as part of a WHO-driven pandemic preparedness initiative aiming to increase global pandemic vaccine production capability (238).

LAIV is predominantly targeted as a vaccine for children. RCTs performed in the early 2000s demonstrated that LAIV was highly efficacious in this patient group (85% efficacy on meta-analysis (239)). However, in recent years, controversies have

arisen about LAIV effectiveness, in particular against pH1N1 viruses that have circulated since 2009. In years when pH1N1 circulated as the predominant seasonal virus, very low pH1N1 VE was reported from the USA – 15% in 2010/11, 17% in 2013/14 and -21% (i.e. no effectiveness) in 2015/16 (240). These findings led to a temporary stalling on the use of LAIVs in the USA between 2016 and 2018 and highlighted significant unknowns on how to optimise their effectiveness (240).

The immunity induced by LAIV requires adequate viral replication in the human URT and the leading hypothesis for reduced VE is poor replicative ability of the pH1N1 strain. As discussed in Chapter 2, when pH1N1 viruses emerged in 2009, they had a pH of fusion of around 5.5, which is higher than that reported for the other human seasonal viruses, and retained binding to α2,3-linked SA receptors. Over the subsequent years of its circulation amongst humans, a decrease in the pH of fusion (134,138) and α2,3 SA binding and concomitant increase in α2,6 SA binding (241) has been detected. In contrast, the extent of adaptation of H3N2 viruses (that have circulated in humans since 1968) and B viruses (that are human-specific) to replication in the human nasal tract is likely to be much greater than for pH1N1. We hypothesised that poor replicative ability of the novel pH1N1 virus in the human nasal tract might underlie the poor VE observed. In Chapter 2, we demonstrated that viruses with different HA pH stability had differing replication kinetics in pHNECs. A pH of fusion >5.5 was attenuating for replication in pHNECs, likely due to increased inactivation in the extracellular environment. Although WT pH1N1 (pH of fusion of ~5.5) replicated efficiently in our experiments in pHNECs detailed in Chapter 2, O'Donnell *et al*.(34) showed that when viruses were reassorted to contain the Ann Arbor MDV internal genes they can become less pH stable than their wild-type counterparts due to cold-adapting mutations in the viral M gene. Any reduction in stability could have a greater impact on the infectivity of pH1N1 in human nasal epithelium by increasing its pH of fusion above the threshold for beneficial survival in

the extracellular environment and tip the delicate balance out of favour of the virus. Compounding this, as part of a multivalent product, the pH1N1 component might struggle to compete with the other better adapted influenza strains for host cells and substrates.

LAIV manufacturers have historically used eggs or continuous cell cultures (MDCK cells) to grow and/or titrate viruses. Based on our findings in Chapter 2, which demonstrated that the replicative ability of viruses with varying pH of fusion in MDCK cells and pHNECs can be inconsistent, we aimed to investigate whether pHNECs can offer a more useful model for vaccine manufacturers to assess the replicative ability of viral strains selected for inclusion in the vaccines of the future.

4.2 Results

4.2.1 Growth of monovalent cold-adapted vaccine viruses on primary human nasal epithelium

Influenza vaccines produced between 2009/10 and 2017/18 included the pH1N1 A/California/07/2009-like virus as per WHO recommendations, based on a virus isolated at the start of the 2009 pandemic. As discussed above, LAIV effectiveness against pH1N1 during this time was reported to be poor. The key hypothesis that we sought to explore is poor replicative ability of this early pH1N1 strain in the human nose. Because of antigenic changes in the pH1N1 virus, the WHO recommended use of an updated pH1N1 strain in influenza vaccines for the 2017/18 season. We aimed to compare if this updated strain, isolated from more recent circulation, had improved replicative ability in the human nose.

To investigate, monovalent cold-adapted vaccine viruses were kindly provided by Serum Institute of India Pvl Ltd (SIIPL). As part of a WHO-led initiative to increase global pandemic vaccine preparedness, SIIPL manufactures Leningrad-backbone LAIV (Nasovac-S®). The cold-adapted monovalent vaccine strain viruses provided included:

- A/17/California/2009/38 (pH1N1, “Cal09”)
- A/17/New York/15/5364 (pH1N1, “NY15”)
- A/17/Hong Kong/2014/8296 (“H3N2”)
- B/Texas/02/2013 (B/Victoria lineage, “B/Vic”)
- B/60/Phuket/2013/26 (B/Yamagata lineage, “B/Yam”)

The Leningrad-backbone LAIV produced by SIIPL in 2017/18 includes A/17/New York/15/5364 (“NY15”) - a pH1N1 strain isolated 6 years later than Cal09. We hypothesised that this more “human-adapted” strain might have increased pH stability which could contribute, at least in part, to improved replication in the human URT. Whether any improved replicative ability translates to improved VE remains to be seen from real-world data. In the 2017/18 season, H3N2 virus predominated and there is therefore no data on pH1N1 VE. pH1N1 co-circulated with H3N2 in 2018/19 and data on LAIV VE is not yet out in the public domain.

To compare the replicative fitness of Cal09 and NY15 as well as the other vaccine viruses, we inoculated pHNECs with each monovalent virus at equal MOI (determined by plaque assay of the monovalent stock). Viral titre (PFU/mL) was quantified by plaque assay on MDCK cells (or MDCK-SIAT cells for H3N2) from apical washings taken daily post inoculation. All viruses replicated well initially; however, by 72 hours, titres of Cal09 diminished whilst titres of the other viruses continued to increase. The area under the curve for NY15 was significantly greater

than Cal09 ($p<0.05$) (Figure 4.1A). For comparison, the replication kinetics of monovalent H3N2 and influenza B strains were also tested (Figure 4.1B). These viruses replicated robustly, although the kinetics of replication are noted to be different from NY15, which peaks earlier after infection.

We also tested the pH stability of Cal09 and NY15 by exposing the viruses to pH-adjusted buffers and quantifying the remaining infectivity. The data demonstrate NY15 was more resistant to inactivation at low pH than Cal09 ($p<0.0001$ at pH 5.3) (Figure 4.1C), which may be contributing to its improved replicative ability in human nasal cells.

A

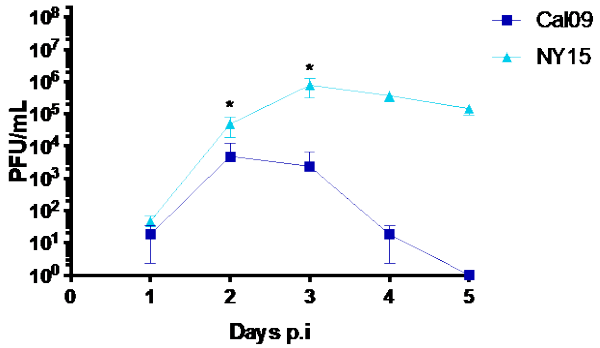

B

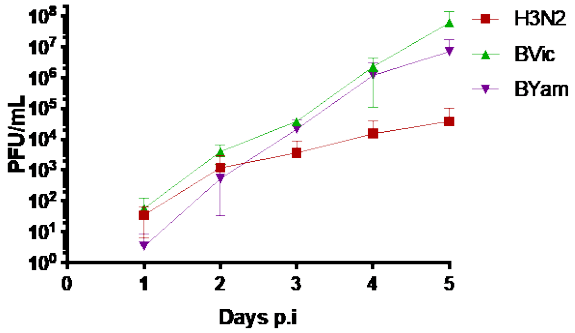

C

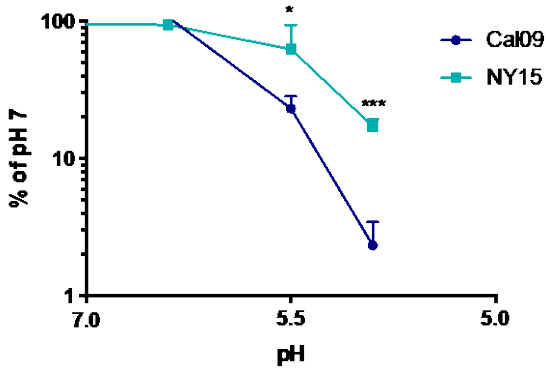

Figure 4.1 Replicative ability of monovalent live attenuated vaccine viruses. (A and B) Primary human nasal epithelial cells were infected at MOI 0.01 (calculated by PFU/mL) in triplicate with each monovalent virus. Time points were taken daily and virus titre quantified by plaque assay on MDCK cells (or MDCK-SIAT cells for H3N2 virus). (C) The pH stability of Cal09 versus NY15 was tested by incubating each virus in low pH MES buffers and titrating remaining infectivity by plaque assay on MDCK cells. Mean +/-SD is shown and students t test used to compare viruses at each time point. *p<0.05, ***p<0.001.

4.2.2 Growth of cold-adapted viruses from the multivalent vaccine on primary human nasal epithelium

We obtained Leningrad-backbone LAIV (Nasovac-S®) produced for the 2016/17 and 2017/18 influenza seasons. These are trivalent vaccines that contain A/17/Hong Kong/2014/8296 (H3N2), B/Texas/02/2013 (B/Victoria lineage, "B/Vic") and either A/17/California/2009/38 (pH1N1, "Cal09") in the 2016/17 vaccine or A/17/New York/15/5364 (pH1N1, "NY15") in the 2017/18 vaccine.

4.2.2.1 Replicative ability of vaccine viruses

We sought to investigate how the vaccine viruses replicate in pHNECs when inoculated simultaneously from the multivalent product. One hypothesis is that pH1N1 may be outcompeted in the presence of other viral strains and that this could be contributing to the poor VE reported. Investigating viral replication using the vaccine product itself rather than an artificial mix of viruses was felt to be most clinically relevant as it is not possible to reproduce the exact combination of viruses. We inoculated pHNECs with each vaccine mix at MOI of 0.01 (based on the plaque assay titre of the vaccine) in triplicate. Time points were taken daily for 5 days p.i. and the quantity of each vaccine component was assessed by RT-qPCR using specific primers targeted to the HA gene. The raw data obtained (presented as 1/Ct value) is shown in Figure 4.2A and Figure 4.3A. Additionally, we derived a standard curve consisting of 10-fold dilutions of each of the monovalent viruses obtained from the same vaccine manufacturer based on their titre in PFU/mL determined by plaque assay. This standard curve was used to convert the Ct values to a PFU-equivalent titre (Fig 4.2B and 4.3B). One caveat of this approach is that we cannot be certain

that the monovalent virus stock provided by SIIPL has the same PFU:particle ratio as that used to derive the vaccine mix.

With the 2016/17 vaccine, replication of pH1N1 Cal09, was low. The H3N2 strain was also observed to replicate poorly. B/Vic replicated the most efficiently. This pattern could be seen in both the raw RT-qPCR (Figure 4.2A) data and also when converted to a PFU equivalent titre (Figure 4.2B). Comparing PFU equivalents, the area under the curve for B/Vic was significantly higher than for Cal09 or H3N2 ($p<0.05$). When the difference between the viruses at each time point was assessed by 2-way ANOVA, significance was reached for Cal09 versus B/Vic and H3N2 versus B/Vic day 3 ($p<0.01$) and day 4. ($p<0.0001$) p.i but the difference between Cal09 and H3N2 was not significant.

On the other hand, from the 2017/18 vaccine, pH1N1 NY15 replicated to high titres. Unexpectedly, however, we saw attenuation of the B/Vic component (Figure 4.3A and Figure 4.3B), which had replicated robustly when pHNECs were inoculated with the 2016/17 vaccine mix and on its own. By 2-way ANOVA, the difference between H3N2 and B/Vic versus NY15 reached significance only on day 5 p.i..

Next, we measured the quantity of each viral component in the 2016/17 and 2017/18 Leningrad trivalent mixes by RT-qPCR and used our standard curve of known PFU/mL titres to convert Ct values to PFU-equivalents. With this method, we quantified ~1 log less Cal09 PFU-equivalents in the 2016/17 vaccine mixture than the other two viruses (Figure 4.2D). It is tempting to speculate that this could have contributed to the poor replication noted. On the other hand, the quantity of NY15 PFU-equivalents in the 2017/18 vaccine was more comparable to H3N2 and B/Vic (Figure 4.3D). Interestingly, in the 2017/18 vaccine the quantity of B/Vic by PFU/mL was significantly higher than NY15 so this is unlikely to account for the poor replication noted in Fig 4.3A and 4.3B.

However, comparing raw Ct values obtained by RT-qPCR gave a different picture whereby the relative of quantities of the three components was similar in both vaccines with pH1N1>H3N2>B (Figure 4.2C and 4.3C). This may suggest that there are virus particles in the LAIV vaccine mix that are non-infectious and that this phenomenon disproportionately affects the pH1N1 component, particularly Cal09. Gould et al.(242) reported the presence of defective interfering particles in preparations of Ann Arbor LAIV and it would be of interest to perform a similar analysis of the Leningrad vaccine. However, we cannot rule out that the monovalent virus stock used for deriving the PFU-equivalent standard curve had a different PFU:particle ratio than that included in the vaccine and it is not possible to determine the quantity of infectious units for individual viruses in a trivalent mixture. In addition, we do note that the Ct values for all strains (Figure 4.2C and Figure 4.3C) and PFU equivalents/mL (Figures 4.2D and 4.3D) for H3N2 and B/Vic in the vaccine were higher in 2017/18 than in 2016/17. Unfortunately, the 2016/17 vaccine could only be obtained after the influenza season had finished and experiments were performed on a vaccine vial that was therefore just outside expiry. It is possible, as a result of this, that a loss of viral infectivity in the 2016 vaccine vial had occurred, which may have disproportionately affected infectivity of the pH1N1 component in 2016/17 and is a caveat of this work.

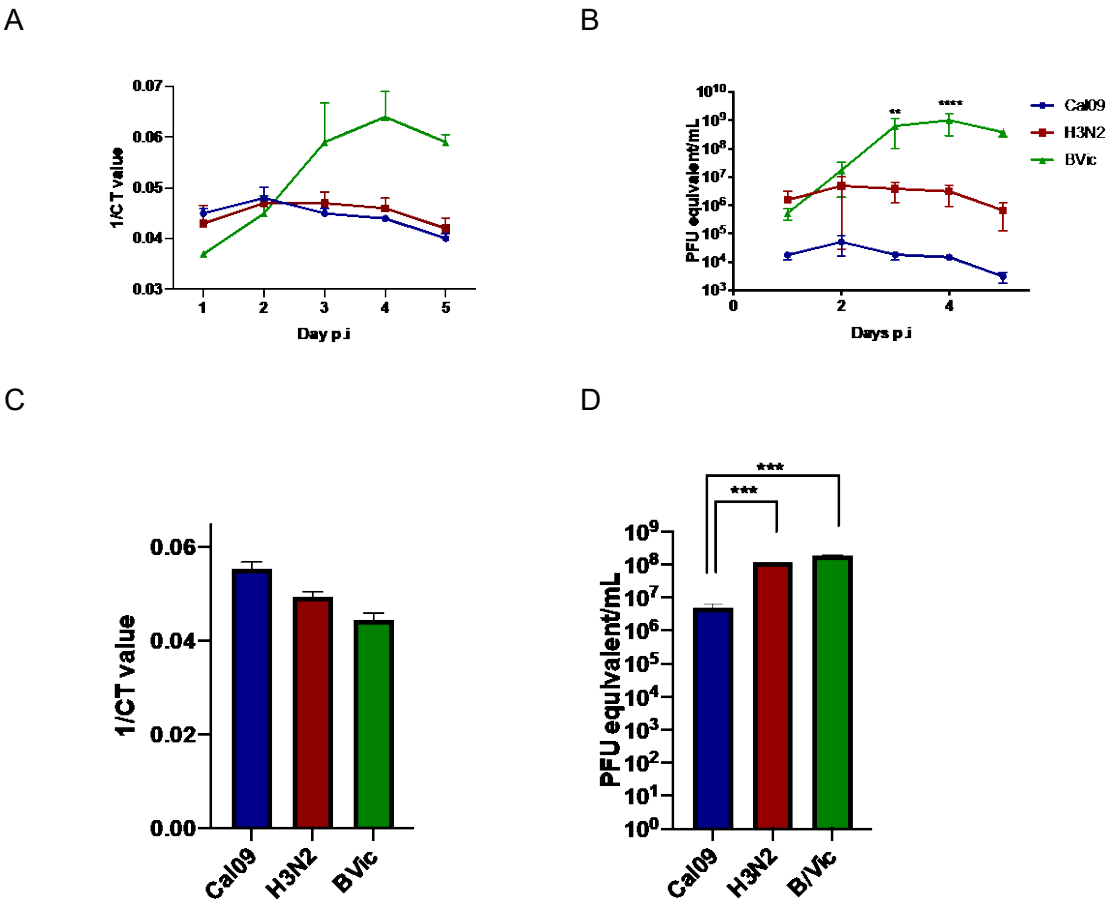

Figure 4.2 Replicative ability and quantification of viral strains in the 2016/17 season LAIV. (A) and (B) Primary human nasal epithelial cells were infected with 2016/17 season Nasovac-S® vaccine at MOI 0.01 in triplicate. Time points were taken daily and each viral component quantified by RT-qPCR. (C) and (D) The amount of each virus in the 2016/17 vaccine was quantified by RT-qPCR. Raw 1/CT values are shown in (A) and (C) and Ct values converted to PFU equivalents based on a standard curve consisting of 10-fold dilutions of each monovalent virus at known PFU/mL in (B) and (D). Error bars represent standard deviations. Two-way ANOVA (B) or one-way ANOVA (D) was used to compare Cal09 to H3N2 and B/Vic ** p<0.01 ***p<0.001, ****p<0.0001

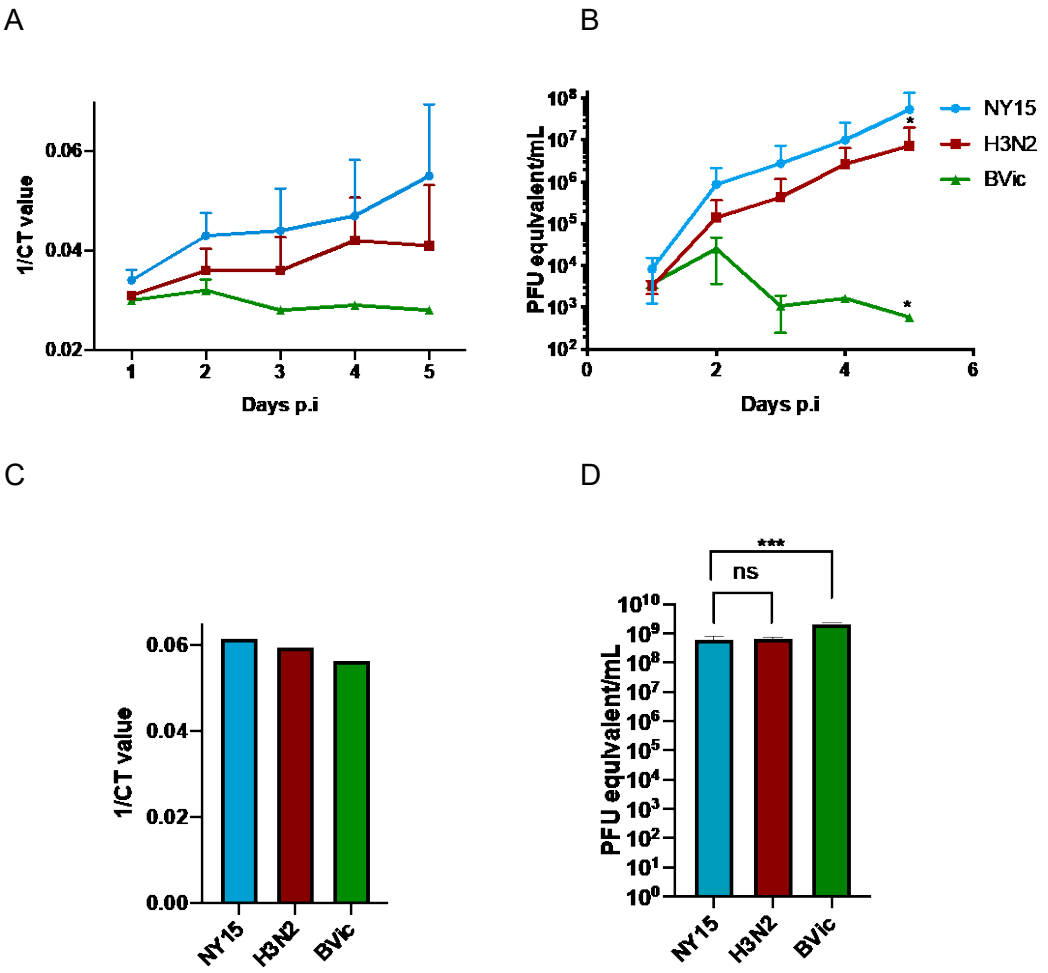

Figure 4.3 Replicative ability and quantification of viral strains in the 2017/18 season LAIV. (A) and (B) Primary human nasal epithelial cells were infected with 2017/18 season Nasovac-S® vaccine at MOI 0.01 in triplicate. Time points were taken daily and each viral component quantified by RT-qPCR. (C) and (D) The amount of each virus in the 2017/18 vaccine was quantified by RT-qPCR. Raw 1/CT values are shown in (A) and (C) and Ct values converted to PFU equivalents based on a standard curve consisting of 10-fold dilutions of each monovalent virus at known PFU/mL in (B) and (D). Error bars represent standard deviations. Two-way ANOVA (B) or one-way ANOVA (D) was used to compare NY15 to H3N2 and B/Vic * $p<0.05$ ***$p<0.001$

4.3 Discussion

It is of paramount importance to understand the underlying reasons for the low effectiveness of pH1N1 within LAIV, to aid in improving vaccines and in making public health decisions. Based on data accrued prior to 2016 showing poor VE of LAIV against pH1N1, the US Advisory Committee for Immunization Practices (ACIP)

withdrew its recommendation for use of LAIV in the US market for the 2016/17 and 2017/18 seasons. This decision had far reaching impact for vaccine manufacturers, public health officials and the public. Importantly, real-world LAIV VE data is now not available for analysis from the US in 2016-2018, which will have impact for evidence based public health decision-making across the world over forthcoming years. At the time of the ACIP decision, the underlying reason for poor pH1N1 VE was unclear and the issue highlighted significant gaps in understanding about virological, immunological and epidemiological aspects of making and using LAIVs and how to assess their effectiveness(240). Here, we have attempted to address and discuss some of these issues

4.3.1 Poor replicative ability of pH1N1 strain

We hypothesised that pH1N1 may have lower replicative ability in the human URT than H3N2 and influenza B virus strains. Since viral replication is critical to immunogenicity of live vaccines, any reduction in replication could translate to a reduction in VE(240). We demonstrated poor replication of the prototypic Cal09 pH1N1 strain in the 2016/17 Leningrad-backbone LAIV. An updated pH1N1 NY15 strain in the 2017/18 vaccine had improved replicative ability and increased acid stability. These data have been included in a recently published paper, Lindsey *et al*.(243). Our coauthors assessed *in vivo* viral shedding and immunogenicity in children in The Gambia following vaccination with the 2016/17 and 2017/18 season Leningrad-backbone LAIV. In line with our results in pHNECs, the data demonstrated poor replicative fitness and low immunogenicity of the Cal09 virus in Gambian children vaccinated with 2016/17 Leningrad LAIV, whereas NY15 virus in the 2017/18 vaccine was shed to higher titres and induced enhanced immune responses.(243). In this study, VE was not assessed; when available, data from real-

world use of LAIV containing updated pH1N1 component during a season when pH1N1 is predominant will provide further clarification about whether this strain substitution can translate to improved VE. In support of our findings, a recent report from the CDC using Leningrad-backbone LAIV strains also demonstrated that replicative ability of Cal09 LAIV strain was poor in pHNECs. The authors also showed that same virus replicated robustly on MDCK cells, highlighting that the same virus can behave differently in different experimental systems(244). In recent years, vaccine manufacturers have responded to these findings in real-time. Data presented to the ACIP meeting in 2018 also showed that using eggs and MDCK cells was not predictive of replication of pH1N1 Ann Arbor LAIV viruses in primary human nasal cells. Consequently, there has been a recent move to evaluate replicative fitness of LAIV candidate strains in pHNECs(245).

4.3.2 Reduced quantity of infectious pH1N1 in the LAIV

Our data also suggested a reduced titre of infectious pH1N1 virus in the 2016/17 vaccine; an issue that appears to be rectified in the 2017/18 mix. Possible explanations for this include (i) the presence of Cal09 defective interfering particles in the vaccine(242,246), (ii) a consequence of the assay used by manufacturers to quantify viruses for inclusion in the vaccine, or (iii) an artefact of the method we used here for quantification. Regardless, it raises interesting points for discussion. The viral strains used in Leningrad LAIV are highly egg adapted and are quantified by EID_{50}. Data from SIIPL previously reported that titres of LAIV viruses in Vero and MDCK cells could be up to 2 logs lower than when titrated in eggs and this phenomenon varied from strain to strain(247). This issue may also apply to the USA/UK-product, the Ann Arbor-backbone LAIV, which is titrated by focus forming assay (FFA). FFA quantifies virus in a single round of replication, which could

mistakenly score defective particles as viable and also may be prone to strain-to-strain variability. In Chapter 2, we saw that HA mutants with high pH of fusion that scored highly in the “UpLUC” reporter assay had reduced replicative ability in pHNECs. The UpLUC assay, similar to the FFU, quantifies virus in a single round of replication. Indeed, more recent evaluation of pH1N1 viruses used in the 2013/14 and 2015/16 vaccines by the Ann Arbor vaccine manufacturer revealed that viral titres obtained via $TCID_{50}$ (a multicyle assay) were substantially lower than those obtained via FFU. The vaccine manufacturer subsequently reported to ACIP in 2018 that they have moved to quantifying vaccine viruses for inclusion in the LAIV using both $TCID_{50}$ and FFU in combination(245). These findings are consistent with our data.

4.3.3 Viral interference in the multivalent LAIV vaccine

A further observation that may compound the problem of poor pH1N1 VE is the multivalent nature of LAIV. As viral strains replicate at the same site in the nose, the least efficient virus could become suppressed by lack of target cells or overwhelmed by an innate immune response induced by the faster replicating strains (248–250). Indeed, Laurie *et al*. previously demonstrated viral interference in wild type virus infections of ferrets exposed to different influenza types and subtypes (251,252). For example, pH1N1 replication in ferrets induced a temporary state of refractoriness to subsequent infection with influenza B (250). Similarly, we saw in pHNEC cultures that robust replication of the NY15 pH1N1 LAIV strain may have adversely affected replication of B/Vic. It would be interesting to mix different quantities of NY15 and B/Vic and explore in more detail if interference is occurring. Whether or not this observation translates to human shedding or VE data is unclear. Lindsey *et al*.(243) did not observe any decline in viral shedding or immunogenicity of the B/Vic

component using the 2017/18 Leningrad vaccine in The Gambia. This discrepancy in our *in vitro* findings and those of Lindsey *et al.* may indicate an artefact of cell culture experiments. Within the restricted environment of a well of pHNECs, viral interference from the pH1N1 NY15 strain that is replicating robustly and perhaps inducing an early interferon response or using up the limited number of cells within a pHNEC culture well may have greater impact on the replication of other viruses. Indeed, comparing Figure 4.1A and 4.1B, we can see that the replication kinetics of monovalent NY15 and B/Vic differ, with NY15 reaching higher titres early in infection (by day 3) whereas the peak of B/Vic occurs later. The relevance of this phenomenon for replication in human upper respiratory tract where there is a larger surface area and far greater number of target cells, is unclear. Nonetheless, the data raise the possibility of a limitation of pHNECs as a model for viral interference in the human URT. An *in vivo* model such as ferrets could provide a more useful means to understand the delicate balance that needs to be struck when viruses are delivered in combination in order to enable adequate replication of each strain and induction of effective immunity against each strain. Future work must focus on improving our understanding of viral hierarchies and competition in the context of LAIV. For example, it may be that vaccine manufacturers could consider including different quantities of viral components or stagger their delivery to optimise the replicative ability and immunogenicity of each strain.

To conclude, the problem with pH1N1 in LAIV demonstrates that the HA surface protein has a significant impact on the performance of LAIV strains. Strain selection for inclusion into LAIV needs to be much more considered than has occurred to date. In general, the WHO recommends strains for inclusion in the inactivated influenza vaccines based on antigenicity of circulating strains and this has been directly applied to LAIV. However, it has become clear that selection of LAIV viruses requires a deeper understanding of virological aspects of influenza strains that affect their

infectivity in the human URT including receptor binding characteristics, pH and temperature stability, HA:NA balance and the generation of defective particles.

In addition to the potential for improving the effectiveness of seasonal influenza vaccines, our findings may have relevance to other LAIVs under development, including those aimed for use in a pandemic. Pandemic LAIVs including against H5 and H7 viruses were found to be highly restricted in replication and poorly immunogenic in phase 1 trials in healthy adults (253,254). Improved understanding of the viral genetic basis for good infectivity in the nasal tract and immune correlates for protection would improve the ability to select and engineer appropriate strains in the future. For example, engineering mutations into the HA stalk that alter pH stability without affecting antigenicity may be an interesting strategy to pursue. Overall, understanding how to make and use a live attenuated influenza vaccine that protects against emerging influenza viruses is of public health priority.

Chapter 5. Conclusions and Future Directions

The pH-dependent uncoating of influenza A viruses as they enter cells is a critical step in the viral life cycle. Virions that do not trigger HA conformational change will be trafficked for degradation in lysosomes. The pH stability of influenza viruses can vary, affecting their ability to uncoat efficiently in endosomes and release their genomes to the host cell nucleus. The evolution of a virus' acid stability could depend on a variety of selective pressures including sites of replication, target cells, host species, ecology and routes of transmission. Opposing pressures from both extracellular and intracellular environments encountered may limit HA pH of fusion to an optimal range that can shift depending on viral and host factors or ecology.

5.1 Increased pH sensitivity can advantage virus uncoating intracellularly

Having generated a panel of pH1N1 viruses with varying HA pH stability, we found that increased pH sensitivity (high pH of fusion) conferred a replicative advantage in continuous cell cultures. We demonstrated that the underlying reason for this replicative advantage related to more efficient virion uncoating in endosomes. When mutant pH1N1 viruses were triggered to fuse at the cell surface and enter via the cytoplasm, increased pH sensitivity did not advantage replication. The ability to uncoat more efficiently in endosomes was not related to escape from IFITM 3 but may result from fewer virions being trafficked to degradative lysosomes.

5.2 Increased pH sensitivity disadvantages virus depositing on the upper respiratory tract

Studies have shown that the human upper respiratory tract is mildly acidic. Virions must successfully traverse this hostile environment in order to reach their target cells. Virus with more fragile HA protein may be rendered non-infectious if HA conformational change is triggered in the extracellular environment, before virions reach their target cells. We generate evidence to support this hypothesis using different experimental model systems. In primary human nasal epithelial cells cultured at air-liquid interface, virus with more pH sensitive HA was attenuated for replication. When the acidic environment of the apical surface was pH neutralised, this attenuation was abrogated. A similar pattern was seen when mice were inoculated with our panel of pH1N1 mutants, with the most pH sensitive virus causing limited weight loss and lower lung viral titre on day 2 p.i. than its more pH stable counterparts.

5.3 Increased pH sensitivity disadvantages virus in airborne droplets

pH stability is a critical property for between-host transmission. In addition to survival outside of target cells once a virus deposits on the URT, a stable HA can facilitate virus survival as it travels between hosts in airborne droplets. Using a novel method for directly isolating and characterising infectious virus from airborne droplets, we found that ferrets infected with a more stable pH1N1 mutant exhaled more infectious virus into the air. Virus exhaled by ferrets infected with a more fragile mutant had

acquired mutations to stabilised the HA protein. When the two mutant viruses were nebulised into the IVTT apparatus together, the more stable mutant was found to better retain infectivity in airborne droplets. Unfortunately, when we applied the same apparatus to attempt collection of virus exhaled by experimentally-infected humans, we were unable to detect any infectious virus in the air.

5.4 Implications for pandemic potential and antiviral treatment

A schematic diagram of our understanding of the relationship between HA stability, virulence and transmission is shown below (Figure 5.1). In order to infect and replicate in humans (blue line) or mice (purple line) influenza viruses have an optimum pH of fusion that is lower than in domestic poultry (green line). This becomes important when assessing for zoonotic influenza viruses with pandemic potential. For an influenza virus to become a successful human pathogen, it must be able to sustain human-to-human airborne transmission, which requires a more stable HA. Avian viruses that circulate in poultry and have raised pandemic concern such as H7N9 and H5N1 are not transmissible via the airborne route. They must therefore evolve to become more pH stable in order to be efficient and infecting and transmitting amongst humans. Interestingly, as part of a risk assessment of H7N9 viruses, Sun *et al*.(135) showed that two highly pathogenic H7N9 viruses isolated from human cases in the “fifth wave” in 2016/2017 were more acid stable (pH of fusion 5.4) than low pathogenic human isolates (pH of fusion 5.7-5.8). This increased stability was found to be mediated by a K64 mutation in HA2 but the highly pathogenic fifth wave viruses were no more transmissible in a ferret model – additional viral adaptive changes were perhaps still required. Systematic monitoring

of the acid stability of emerging influenza viruses may be informative in the future as part of pandemic risk assessment. Conversely, anti-influenza therapeutics that target the fusogenic ability of the influenza HA may drive virus to evolve an increased pH of fusion, with consequences on the balance we describe, between viral pathogenicity and transmissibility.

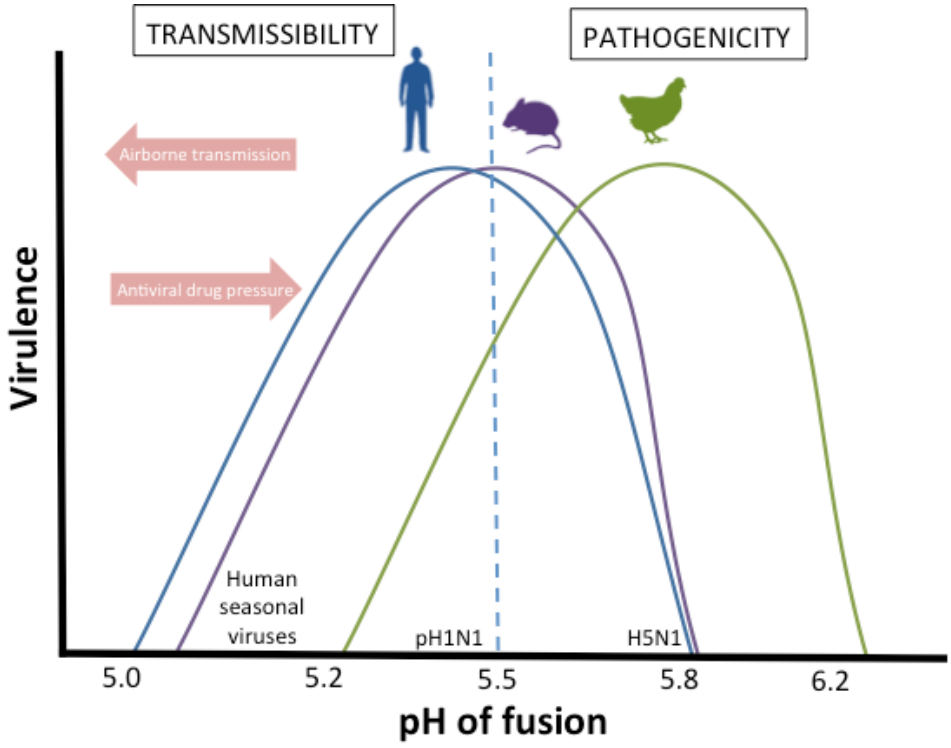

Figure 5.1. Schematic diagram of the relationship between HA pH of fusion, virulence and airborne transmissibility.

5.5 Implications for optimising live attenuated vaccines

Understanding the implications of HA stability for viral growth and titration in different experimental systems, where the balance between extracellular and intracellular conditions may be weighed differently has proven critical for optimising LAIV production and delivery. The poor effectiveness of pH1N1 in LAIV may be partially

explained by its pH sensitivity impacting on reduced growth in the human URT and/or reduced quantity of infectious units in the vaccine. As part of LAIV strain selection, it may be prudent to test HA stability, growth in pHNECs and use an appropriate multi-cycle growth assay for titrating virus for inclusion in the vaccine. Optimising the pH stability of vaccine virus strains by genetic manipulation of residues in the HA stem region that do not impact on antigenicity is a potential avenue for improving live attenuated vaccines.

5.6 Future work

5.6.1 Chapter 2

1. We did not detect any differential effect of IFITM3 on our panel of mutant viruses with varying pH of fusion. However, another study(157) did detect that viruses with higher pH of fusion can escape restriction by IFITM 3. It would be prudent to perform further testing to confirm our result, for example using an IFITM2/3 knock-out cell line to exclude any effect of intrinsic cellular IFITMs.
2. To neutralise the acidic pH on the apical surface of pHNECs we submerged the cells in DMEM (pH 7.4). However, we cannot be certain that this pH was maintained throughout the apical space, for example on the cell surface. pHNECs have a layer of mucous, cilia and ion channels that may be acting to regulate extracellular pH. It would be interesting to perform a growth curve with our panel of viruses submerged in mildly acidic media, in both pHNECs and MDCKs. Furthermore infecting pHNECs and staining en face for virus NP would help to confirm our hypothesis that Y7H virus was becoming inactivated extracellularly and infecting fewer cells.

3. Deep sequencing of Y7H virus after 5-7 days replication in pHNECs would be valuable to analyse if any evolution has occurred as was observed in the ferret URT in experiments described in Chapter 3.
4. Analysis of cytokine profiles and lung histology from mice infected with our panel of HA mutants would be of interest to delineate whether the HA mutations had any additional effects during mouse infection.
5. Measurement of the pH of the mouse upper respiratory and lower respiratory tract would help to understand comparison of the model to what is known about the human respiratory tract.
6. Deep sequencing of Y7H virus after 5-7 days replication in mice would also be valuable to analyse if any evolution has occurred as was observed in the ferret URT. In particular, we observed an increase in the lung viral titre on day 5 in some Y7H-infected mice and it would be interesting to see if any viral mutations had occurred.
7. To confirm our hypothesis of increased degradation in lysosomes of viruses with more pH stable HA, direct visualisation using immunofluorescence or single particle tracking techniques would be worthwhile.
8. It would be of interest to perform cell culture passaging studies of pH1N1 in the presence of drugs targeting the fusogenic ability of HA such as stem-targeting monoclonal antibodies to understand how virus might escape such drugs.
9. Our studies were restricted to 3 mutant viruses plus the wild type pH1N1 virus. With more time, testing more virus mutants and additional virus subtypes/strains would help to broaden the significance of our findings. In particular it would be interesting to analyse if the same patterns could be observed in seasonal H3N2 viruses as well as emerging avian/swine viruses of pandemic concern.

5.6.2 Chapter 3

1. A major caveat of the IVTT is that we have not been able to successfully quantify viral RNA emitted by infected ferrets. It is likely that refinement of the methodology is required to achieve this. Measuring exhaled viral RNA would be instrumental in assessing our hypothesis that virus released into the air becomes inactivated. The data would help to understand how much virus is exhaled and thereby what proportion is remaining infectious.
2. In our experiments on ferrets infected with Y7H or E21K we did not include sentinel animals. Although use of the IVTT in Y7H-infected ferrets enabled us to detect many more exhaled mutant viruses, it would be of interest to identify which, if any, virus mutant could initiate infection in a respiratory droplet sentinel animal housed in an adjacent cage.
3. Sampling viral RNA from the air using devices such as the NIOSH Biosampler or Anderson impactor, which can be placed in the animal's room to collect viral RNA from air over a prolonged period of time (e.g. 24 hours) may have yielded some interesting data for analysis.
4. Furthermore, it could have been valuable to have directly monitored clinical signs in ferrets during these experiments such as timing of fever, coughs, sneezes and mucous production and how these relate to the amount of infectious virus that was exhaled. However, based on the findings of Roberts *et al*.(204), we do not anticipate there to be much in the way of quantifiable clinical signs in ferrets at the time that the peak of exhaled virus was detected using the IVTT.
5. Measurement of the pH of the ferret upper respiratory tract and respiratory secretions would help to understand comparison of the model to what is known about the human respiratory tract.

6. Further analysis of the composition of ferret secretions and how they change during infection would be of great interest but will require development of novel techniques. This could be an important area for future research, to understand why it is that the amount of infectious virus released decreases over the course of infection – for example, whether this is related presence of immune mediators, a change in pH or other factors.
7. Further analysis of the NS1 mutation that was identified in one exhaled plaque that had increased pH stability should be performed. For example, it would be worthwhile generating a reverse genetics virus with this mutation included and testing if the mutation can confer increased pH stability or is conferring some other advantage to virus existing in respiratory droplets.
8. Our studies were restricted to 3 mutant viruses plus the wild type pH1N1 virus. With more time, testing more virus mutants and additional virus subtypes/strains would help to broaden the significance of our findings. In particular it would be interesting to analyse if the same patterns could be observed in seasonal H3N2 viruses as well as emerging avian/swine viruses of pandemic concern.
9. Future studies in ferrets using the IVT to increase our understanding of the transmission bottleneck for other known viral determinants of airborne transmissibility should be performed. For example, the IVT could be used to investigate whether the bottleneck is at the point of virus release from the donor, as virus travels through the air in droplets or at the point of entry and replication in the sentinel host. Viral properties such as receptor binding specificity, NA stalk length or virus morphology could be the subject of future studies.
10. It would also be of interest to sample exhaled virus from a sentinel ferret to understand if the kinetics of virus detection differed in a ferret infected by a

more “natural” method than the intranasal instillation used to infect the donor ferrets.

11. We were unable to detect any infectious virus exhaled by humans experimentally infected with pH1N1. It is likely that further refinement of the IVT technique is required for isolation of airborne virus from humans. It would be particularly useful to attempt detection of viral RNA from air in the IVTT to assess whether virus-laden droplets are able to pass into the IVT tunnel.
12. Testing the pH stability of the inoculum virus used to inoculate human volunteers in this study would be prudent. The egg adaptation mutations could have increased the pH of fusion of the inoculum that impaired its ability to remain infectious in airborne droplets.
13. Future studies applying the IVT in naturally infected humans or in LAIV recipients to assess whether infectious +/- non-infectious virus can be detected would be valuable. Furthermore, experimental infection with a virus strain that has not been passaged in eggs may yield more fruitful data.

5.6.3 Chapter 4

1. pHNECs have been adopted for use in strain selection for LAIV. However, our data point to some potential caveats of this system. Further experiments in pHNEC to understand why the growth of some strains appears to be impaired when viruses are infected in combination would be of use.
2. Further, investigations into the role of interference with LAIV viruses using an in vivo model such as ferrets could help to understand this issue.
3. If we had further viral stock and time available, we would plan to assess monovalent LAIV viruses using other assays such as UpLUC, FFA and to investigate their growth in MDCK cells and eggs.

4. We were only able to procure Leningrad-backbone vaccine. However the majority of real-world VE data is from use of the Ann Arbor-backbone LAIV. Ideally, similar experiments in pHNECs using the Ann Arbor vaccine should be performed to assess if similar observations can be made.

5.7 Summary statement

To conclude, our data show that mutations that alter the HA pH of activation have marked effects on virus behavior in different experimental systems and point toward an optimum pH of activation for influenza viruses to infect, replicate and transmit in humans. This appears to be denoted by a balance between a virus' need to withstand external conditions (environmental and extracellular) while maintaining adequate sensitivity to trigger viral uncoating intracellularly. Understanding the consequences of changes in HA pH stability on viral phenotypes has implications for the rational use of antiviral drugs, improvement of vaccines, and monitoring of pandemic risk.

Chapter 6. Materials and Methods

6.1 Materials

6.1.1 Cell lines

Name	Cell Type	Source
Madin Darby canine kidney (MDCK)	Canine kidney epithelial cells	GlaxoSmithKline
MDCK-SIAT1	MDCK cells expressing increased levels of α2,6-linked sialic acid(255)	WHO CC London
293T	Human embryonic kidney cells	GlaxoSmithKline
A549	Human lung adenocarcinoma epithelial cells	ATCC
pHNEC	Highly differentiated primary human nasal epithelial cells cultured at air-liquid interface	Epithelix Sàrl

Table 6.1 Cell lines used in this study.

6.1.2 Animals

Species	Age, sex	Comment
BALB/c mice	6-8 weeks, female	Virus infection and pathogenicity
Ferrets	14-16 weeks, female	Virus infection and transmission

Table 6.2 Animal species used in this study.

6.1.3 Viruses

Virus	Details	Source
A/England/195/2009 (H1N1)	First fully sequenced pH1N1/09 virus from the UK. Derived by reverse genetics.	R Elderfield, Barclay Laboratory
A/England/195/2009 E21K	Reverse genetics virus with E21K point mutation in haemagglutinin	This study
A/England/195/2009 A9T	Reverse genetics virus with A9T point mutation in haemagglutinin	

A/England/195/2009 Y7H	Reverse genetics virus with Y7H point mutation in haemagglutinin	
A/England/195/2009 D112G	Reverse genetics virus with D112G point mutation in haemagglutinin	
A/England/195/2009 N114K	Reverse genetics virus with N114K point mutation in haemagglutinin	
A/England/195/2009 S113F	Reverse genetics virus with S113F point mutation in haemagglutinin	
A/England/195/2009 E103H	Reverse genetics virus with E103H point mutation in haemagglutinin	
A/England/195/2009 H72D	Reverse genetics virus with H72D point mutation in haemagglutinin	
A/England/195/2009 H72N	Reverse genetics virus with H72N point mutation in haemagglutinin	
A/England/195/2009 T49S	Reverse genetics virus with T49S point mutation in haemagglutinin	
A/England/195/2009 K75R	Reverse genetics virus with K75R point mutation in haemagglutinin	
A/California/04/2009 (H1N1) GMP virus	Inoculum virus for human challenge subjects, expanded to GMP standards	Dr C Chiu, Imperial College
A/17/California/2009/38 (H1N1)	Live attenuated vaccine virus. 6 internal genes (PB1, PB2, PA, NP, NS, M) from A/Leningrad/134/57 and HA and NA genes from A/California/04/2009-like virus. Used in monovalent form and included the trivalent 2016/17 vaccine.	Serum Institute of India Pvl. Ltd. (SIIPL)
A/17/New York/15/5364 (H1N1)	Live attenuated vaccine virus. 6 internal genes (PB1, PB2, PA, NP, NS, M) from A/Leningrad/134/57 and HA and NA genes from A/Michigan/45/2015-like virus. Used in monovalent form and included the trivalent 2016/17 vaccine.	
A/17/Hong Kong/2014/8296 (H3N2)	Live attenuated vaccine virus. 6 internal genes (PB1, PB2, PA, NP, NS, M) from A/Leningrad/134/57 and HA and NA genes from A/Hong Kong/4801/2014-like virus. Used in monovalent form and included the trivalent 2016/17 vaccine.	
B/Texas/02/2013 (Victoria lineage)	Live attenuated vaccine virus. 6 internal genes (PB1, PB2, PA, NP, NS, M) from B/USSR/60/69 and HA and NA genes from B/Brisbane/60/2008-like virus. Used in monovalent form and included the trivalent 2016/17 vaccine.	

Table 6.3 Influenza viruses used in this study.

6.1.4 Plasmids

Plasmid name	Details	Source
PCAGGS-Renilla luciferase	Transfection control – constitutive expression of Renilla luciferase	O Moncorge, Barclay Laboratory
pHPOM1-358-Firefly	Directs production of a virus-like minigenome encoding Firefly luciferase and with mutations G3A, U5C and C8U in the 3' end promoter region that allow amplification by polymerase from infecting virus.	
PCAGGS-IFITM3	Control plasmid	A Vaughan, Barclay Laboratory
PCAGGS-empty	Expression plasmid expressing IFITM3	
pPol1-E195-PB1	Rescue plasmid encoding A/England/195/2009 PB1	Barclay Laboratory stock
pPol1-E195-PB2	Rescue plasmid encoding A/England/195/2009 PB2	
pPol1-E195-PA	Rescue plasmid encoding A/England/195/2009 PA	
pPol1-E195-NP	Rescue plasmid encoding A/England/195/2009 NP	
pPol1-E195-M	Rescue plasmid encoding A/England/195/2009 M	
pPol1-E195-NS	Rescue plasmid encoding A/England/195/2009 NS	
pPol1-E195-NA	Rescue plasmid encoding A/England/195/2009 NA	
pPol1-E195-HA	Rescue plasmid encoding A/England/195/2009 HA	
pCMV-Victoria-PB1	Expression plasmid for A/Victoria/3/75 PB1	
pCMV-Victoria-PB2	Expression plasmid for A/Victoria/3/75 PB2	
pCMV-Victoria-PA	Expression plasmid for A/Victoria/3/75 PA	

pCMV-Victoria-NP	Expression plasmid for A/Victoria/3/75 NP	
pPol1-E195-HA E21K	Rescue plasmid encoding A/England/195/2009 mutant HA	This study
pPol1-E195-HA A9T		
pPol1-E195-HA Y7H		
pPol1-E195-HA D112G		
pPol1-E195-HA N114K		
pPol1-E195-HA S113F		
pPol1-E195-HA E103H		
pPol1-E195-HA H72D		
pPol1-E195-HA H72N		
pPol1-E195-HA T49S		
pPol1-E195-HA K75R		

Table 6.4 Plasmids used in this study.

6.1.5 Oligonucleotides

Name	Sequence (5' – 3')	Use	Source
HA-F	AGCAAAAGCAGGGGAAAACAAAAGC	Sequencing	This study
HA-R	AGTAGAAACAAGGGTGTTTTTTCTCATGC		
HA-short-R	GCTTGCTGTGGAGAGTGATTCAC		
M-F	AGCAAAAGCAGGTAGATATTTAAAGATGAG		
M-R	AGTAGAAACAAGGTAGTTTTTTACTCTAGC		
HA E21K-F	CAGACACTGTAGACACAGTACTAAAAAAGAATGTAACAGTAACAC	Site-directed mutagenesis	J Long, Barclay laboratory
HA E21K-R	GTGTGTTACTGTTACATTCTTTTTTAGTACTGTGTCTACAGTGTC		
HA A9T-F	GTATAGGTTATCATACGAACAATTCAACAG		This study
HA A9T-R	CTGTTGAATTGTTCGTATGATAACCTATAC		
HA Y7H-F	CATTATGTATAGGTCATCATGCGAACAATTCAAC		
HA Y7H-R	GTTGAATTGTTCGCATGATGACCTATACATAATG		
HA D112G-F	GACTACCACGGTTCAAATGTGAAGA		
HA D112G-R	TCTTCACATTTGAACCGTGGTAGTC		
HA N114K-F	CTACCACGATTCAAAAGTGAAGAACTTATATG		
HA N114K-R	CATATAAGTTCTTCACTTTTGAATCGTGGTAG		

HA S113F-F	CTACCACGATTTTAATGTGAAG AACTTATATG		
HA S113F-R	CATATAAGTTCTTCACATTAAAA TCGTGGTAG		
HA E103H-F	GATTATGAGGAGCTAAGACATC AATTGAGCTCAG		
HA E103H-R	CTGAGCTCAATTGATGTCTTAG CTCCTCATAATC		
HA H72D-F	GTAGGTAAAGAGTTCAACGACC TGGAAAAAAG		
HA H72D-R	CTTTTTTCCAGGTCGTTGAACT CTTTACCTAC		
HA H72N-F	GTAGGTAAAGAGTTCAACAACC TGGAAAAAAG		
HA H72N-R	CTTTTTTCCAGGTTGTTGAACT CTTTACCTAC		
HA T49S-F	GVVATTGACGAGATTTCTAACA AAGTAAATTCTG		
HA T49S-R	CAGAATTTACTTTGTTAGAAATC TCGTCAATGGC		
HA K75R-F	CAACCACCTGGAAAGAAGAATA GAGAAT		
HA K75R-R	ATTCTCTATTCTTCTTTCCAGGT GGTTG		
M-qPCR-F	AAGACAAGACCAATYCTGTCAC CTCT	qPCR primer	R Frise, Barclay Laboratory
M-qPCR-R	TCTACGYTGCAGTCCYCGCT		
M-Probe	6FAM – TYACGCTCACCGTGCCCAGTG -MGB	qPCR probe	
ca-H1-F	TGGACTTACAATGCCGAACT	qPCR primer	A Meijer, RIVM
ca-H1-R	CAGCCGTTTCCAATTTCCTT		
ca-H3-F	CRATGTRTACAGGGATGAAGC WTTAAACA		
ca-H3-R	TAGGATCCAATCTTTGTACCCT GACTT		
ca-B-HA-F	ACCCTACARAMTTGGAACCTCA GG		
ca-B-HA-R	ACRGCCCAAGCCATTGTTG		
H1IVT-probe	FAM-TGC AGT CCT CGC TCA CTG GGC ACG-BHQ1	qPCR probe	J Zhou, Barclay Laboratory
H1IVT-F	GACCRATCCTGTCACCTCTGA C	qPCR primer	
H1IVT-R	AGGGCATTYTGGACAAAKCGTC TA		
DNAIVT-F	AGTAACCCGACACGAAGCAG		
DNAIVT-R	GGAACCAACGTCCCAGGAAT		

Table 6.5 Primers used in this study.

6.1.6 Compounds and chemicals

Name	Details	Source
Arbidol hydrochloride	Small molecule fusion inhibitor. Licensed to treat influenza in Russia and China	Carbosynth Ltd.
FI6	Broadly neutralising monoclonal antibody targeting the HA stem	Davide Corti, Humabs
Bafilomycin A1	Vacuolar ATP-ase inhibitor	Sigma
Amphoteracin B	Anti-mycotic drug, prevents IFITM3 mediated restriction of influenza	Gibco
NasovacS 2016/17 season	Leningrad-backbone LAIV from 2016/17 influenza season	Serum Institute of India Pvt. Ltd. (SIIPL)
NasovacS 2017/18 season	Leningrad-backbone LAIV from 2017/18 influenza season	
Dimethyl sulfoxide (DMSO)	Polar aprotic solvent	Sigma
Geneticin (G418)	Selection antibiotic for MDCK-SIAT cells	Gibco
Type 1 interferon	Recombinant human interferon α hybrid protein	PBL Assay Science
Lipofectamine 3000	Transfection reagent	Invitrogen

Table 6.6 Compounds and chemicals used in this study.

6.1.7 Buffers and culture media

Name	Details	Use
DNA loading buffer (6x)	0.25% Bromophenol blue 40% (w/v) sucrose in TAE	Loading samples for DNA gel electrophoresis
TAE buffer	40mM Tris acetate pH 8 1mM EDTA	Buffer for DNA gel electrophoresis
Lysogeny Broth (LB)	1% Tryptone 0.5% Yeast extract 0.5% NaCl 0.1% Glucose dH2O	Culturing bacteria for plasmid production
SOC	2% Tryptone 0.5% Yeast extract 10mM NaCl	Culturing bacteria for plasmid selection

	2.5mM KCl 10mM $MgCl_2$ 10mM $MgSO_4$.7H2O 20mM Glucose	
Cell culture media	Dulbecco's modified Eagle's medium containing L-glutamine and sodium pyruvate (Gibco) 1 % non-essential amino acids (NEAA) (Sigma) 1% penicillin/streptomycin (P/S) (Gibco) 10% Foetal calf serum (FCS) (Biosera) For MDCK-SIAT cells: Plus 1mg/mL G418	Cell line maintenance media
MucilAir culture media	Serum free media purchased from Epithelix Sàrl, contains growth factors and Phenol Red.	Culture media for primary human nasal epithelial cells
Virus infection media	Dulbecco's modified Eagle's medium containing 1% L-glutamine and sodium pyruvate 1 % NEAA 1% P/S 1µg/mL TPCK-treated trypsin (Worthington Biochemcals)	For virus infections
Plaque assay overlay media	100ml 10x MEM 28ml 7.5% fraction V BSA 10ml 100x L-glutamine 20ml 7.5% $NaHCO_3$ 10ml 1M HEPES 2ml 1% dextran 10ml 10x penicillin/streptomycin dH_2O up to 700ml 1µg/mL TPCK-treated trypsin 2% agarose is added prior to use	For plaque assay titration of viruses
Crystal violet	100 ml Crystal violet stock solution 300 ml ethanol 1.6L water	Cell staining for plaque assay
Giemsa stain	Diluted 1:20 with dH_2O	Cell staining for syncytia formation assay
MES buffer	100mM MES, 150mM NaCl, 0.9mM $CaCl_2$, 0.5mM $MgCl_2$ pH adjusted with 4M NaOH	For syncytia formation assay and pH inactivation assay

Table 6.7 Buffers and culture media used in this study.

6.2 Methods

6.2.1 Cell maintenance and transfection

6.2.1.1 Cell lines

MDCK, 293T and A549 were maintained in DMEM supplemented with 10% FCS, 1% NEAA and 1% PS. MDCK-SIAT cells were maintained in DMEM supplemented with 10% FCS, 1% NEAA, 1% PS and 1mg/mL G418 to maintain stable expression of the 2,6-sialyltransferase gene (255). All cells were cultured at 37°C in 5% CO_2 atmosphere.

pHNEC cultures were purchased from Epithelix Sàrl. Upon arrival, inserts were transferred into 700µL pre-warmed MucilAir culture media under sterile conditions. MucilAir culture medium was refreshed twice weekly. The apical surface of pHNEC cultures was washed with serum-free DMEM once weekly to remove excess mucous. Cells were cultured at 37°C in 5% CO_2 atmosphere.

6.2.1.2 Cell transfections

Transfections for the virus-driven luciferase assay were performed using Lipofectamine 3000 reagent (Invitrogen) according to manufacturer's instructions. DNA: reagent ratios were scaled as required. DNA and lipofectamine were diluted in OptiMEM (Invitrogen). Transfection of plasmids for recombinant virus generation was carried out using Xtreme gene 9 (Sigma).

6.2.2 Molecular techniques

6.2.2.1 Viral RNA extraction and reverse transcription

RNA was extracted from 140µL of cell supernatant using Qiagen viral RNA mini kit (Qiagen) according to manufacturer's instructions and eluted into 40µL of dH_2O. Reverse transcription was performed using SuperScript III (Invitrogen) and random hexamers according to manufacturer's instructions.

6.2.2.2 Polymerase chain reaction

PCR amplification was performed with K.O.D Taq polymerase (Novagen). A 50uL PCR mix was made containing 5µL 10x buffer, 3µL MgSO4, 0.15µL forward and reverse primers (at 100pmol/µL), 5µL 2mM dNTPs, 1µL KOD polymerase, 10-100ng cDNA template and nuclease free water up to 50µL

6.2.2.3 Agarose gel electrophoresis and DNA purification

DNA fragments were separated on1% agarose gels diluted with 0.5XTAE buffer and supplemented with 1x gel red (Cambridge Bioscience). DNA was loaded with 5x loading dye (Qiagen). A 1kb DNA ladder (Invitrogen) was run alongside samples. Gels were run in 0.5X TAE buffer at 100V until the bands had adequately separated. DNA was visualised using an ultraviolet trans illuminator and cut from the agarose gel. DNA was extracted using QIAquick Gel extraction kit (Qiagen) according to manufacturers instructions and eluted into 35µL sterile water.

6.2.2.4 Real-time quantitative PCR (RT-qPCR)

6.2.2.4.1 pH1N1 viral RNA copy number (for PFU:particle ratio)

RT-qPCR for viral M gene was performed with TaqMan probe 5'FAM – TYACGCTCACCGTGCCCAGTG –MGBNFQ 3' (Life Technologies). Primer sequences were AAGACAAGACCAATYCTGTCACCTCT (FWD) and TCTACGYTGCAGTCCYCGCT (REV). Data was analysed on the Applied Biosystems® ViiATM Real-Time PCR System.

6.2.2.4.2 RT-qPCR for LAIV viruses

RT-qPCR was performed with Sybr green PCR mix (Applied Biosystems) using primers specific for the HA gene of each viral component. Primer sequences, kindly provided by Adam Meijer (RIVM), were TGGACTTACAATGCCGAACT (FWD) and CAGCCGTTTCCAATTTCCTT (REV) for pH1N1, CRATGTRTACAGGGATGAAGCWTTAAACA (FWD) and TAGGATCCAATCTTTGTACCCTGACTT (REV) for H3N2 and ACCCTACARAMTTGGAACCTCAGG (FWD) and ACRGCCCAAGCCATTGTTG (REV) for influenza B. Data was analysed on the Applied Biosystems® ViiATM Real-Time PCR System. The PFU equivalent of cycle threshold values was calculated against a standard curve generated from serial 10 fold dilutions of monovalent viral stocks.

6.2.2.4.3 RT-qPCR in IVTT experiments

RT-qPCR was used to quantify the amount of plasmid DNA or viral RNA deposited on each culture plate and from an air sample collected using a SKC Biosampler. Viral

RNA was extracted using the QIAamp viral RNA mini it (Qiagen) from 140µL samples and eluted into 40µL water. RT-qPCR of the viral M gene or DNA plasmid was performed using AgPath-ID One-Step RT-PCR Reagents (Thermo Fisher Scientific)(256) with probe 5' FAM-TGC AGT CCT CGC TCA CTG GGC ACG-BHQ1-3'. Primer sequences were GACCRATCCTGTCACCTCTGA C (FWD) and AGGGCATTYTGGACAAAKCGTCTA (REV). Primer sequences for the DNA plasmid were AGTAACCCGACACGAAGCAG (FWD) and GGAACCAACGTCCCAGGAAT (REV). Data was analysed on the QuantStudio 7 Flex Real-Time PCR System. The plasmid copy number was calculated against a standard curve generated from serial 10-fold dilutions from $2x10^8$ to $2x10^0$ copies/µL.

6.2.2.5 Site directed mutagenesis

Site directed mutagenesis was carried out on the Eng09 HA rescue plasmid using QuikChange Lightening Site-Directed Mutagenesis Kit according to manufacturers instructions (Agilent Technologies).

6.2.2.6 Transformation of competent bacterial cells

XL10-Gold competent cells (Agilent Technologies) were thawed on ice then mixed with ~50ng of plasmid. After incubated on ice for 15 minutes, cells were heat shocked for 30 seconds at 42°C and replaced on ice for 2 minutes. 250µl of pre-warmed SOC media (Invitrogen) was added and the mixture incubated with shaking for 1 hour at 37°C. A suitable volume was plated onto LB agar plates containing 1% Ampicillin and incubated overnight at 37°C.

6.2.2.7 Plasmid purification

Single colonies were grown overnight at 37°C with shaking in 5ml LB containing 100µg/ml Ampicillin then pelleted by centrifugation at 3000 rpm for 10 minutes at 4°C. The supernatant was discarded and plasmids were isolated using the QIAprep Spin Miniprep kit (QIAGEN) according to manufacturer's instructions. DNA was eluted into 50µl nuclease free water and stored at 20°C. DNA concentration was measured using a NanoDrop® ND-1000 spectrophotometer.

6.2.2.8 Sanger sequencing

Sanger sequencing (plasmids, virus HA and M genes) was carried out at GATC Services, Eurofins Genomics and results analysed using Geneious v6.1.8.

6.2.2.9 Next-generation sequencing

Next generation sequencing (NGS) of ferret and human nasal washes was performed on the NGS pipeline at the Respiratory Virus Unit, Public Health England, Colindale, by Dr Shahjahan Miah and Dr Monica Galiano. Total RNA was extracted directly from 150µL of nasal wash sample using Easymag, according to manufacturer instructions. Multisegment reverse transcription-PCR (M-RTPCR)(257) was used to amplify influenza virus-specific segments. Reverse-transcription and amplification was performed using One-step RT-PCR system with Superscript III and Platinum Taq HiFi polymerase (Life Technologies). The M-RTPCR products were cleaned, diluted to required concentration and submitted for Nextera library preparation for Illumina short-read sequencing with a MiSeq instrument. Sequence data generated using the Illumina MiSeq was processed using BWA-MEM to map the reads to appropriate reference sequences. Samtools(258) was used to post-process the

reference assembly and an in-house C++ program (QuasiBam) used to quality filter, trim and generate two outputs: a consensus sequence for the influenza genomes and a table with the frequency of each nucleotide and depth at every position. Positions in the consensus genome showing greater than 20% variance were assigned an ambiguity code. Variant calling required a minimum of 100 reads and a minimum read frequency cutoff of 5% was set.

NGS of the HA gene was performed to analyse the proportion of E21K and Y7H RNA depositing in the IVTT after nebulisation in a mixture. cDNA samples were prepared using NebNext Ultra II (NEB) according to manufacturer's instructions and sequencing performed on an Illumina MiSeq machine at Molecular Diagnostics Unit, Imperial College London by Dr Steve Kaye. Data was analysed using Geneious v6.1.8.

6.2.3 *In vitro* infectious studies

6.2.3.1 Growth of virus stocks

MDCK cells grown to 80% confluency in T75 flasks were infected with virus at low multiplicity and incubated for one hour at 37°C 5% CO_2. The inoculum was removed, cells washed twice with PBS and 12 ml serum free DMEM containing 1 µg/ml TPCK-treated trypsin added. Flasks were incubated at 37°C 5% CO_2 and the media harvested once cytopathic effect was observed. Cultures were centrifuged at 2000 rpm for 10 minutes and aliquots of supernatant stored at -80°C. All viruses were used at low passage, virus titre confirmed by plaque assay and sequence confirmed prior to use.

6.2.3.3 Rescue of recombinant influenza virus by 12 plasmid transfection

12 plasmids (8 Pol1 plasmids and 4 expression plasmids) were transfected into 293T cells grown to 80% confluency. To prepare the transfection mix, 20µl Xtreme gene 9 was added to 250µL Opti-MEM and incubated for 5 minutes at room temperature. The plasmid mix (500ng of each Pol1 plasmid, 500ng PB1 and PB2 expression plasmids, 250ng PA expression plasmid and 1000ng NP expression plasmid) was added and incubated for a further 20 minutes at room temperature. Media on the 293T cells was changed to pre-warmed Opti-MEM and transfection mix added drop-wise to the cell monolayer before incubating at 37°C overnight. The next day transfected 293T cells were resuspended in 1mL DMEM with 10% FBS. The resuspended 293T cells were transferred into T25 flask of MDCK cells (at 70% confluency) containing 4mL DMEM+10% FBS. Cells were allowed to adhere for 6 hours at 37 °C then washed gently in serum-free DMEM. 5ml virus infection medium was added (see 6.1.7) and cultures incubated at 37°C for 2-3 days until CPE was observed, or haemagglutination activity was observed by a haemagglutination assay. Virus was harvested, cell debris removed by centrifugation at 2000 rpm for 10 minutes, and aliquots stored at -80°C. A positive control (wild type virus plasmids) and negative control (HA plasmid excluded) were included in all experiments.

6.2.3.4 Virus titration

6.2.3.4.1 Haemagglutination assay

Two-fold serial dilution of virus in PBS was performed in 96 well V-bottomed plates. 50µL of 0.5% turkey red blood cell suspension (diluted in PBS) was added to each well. The plate was incubated on ice for 1 hour then HA titre determined as the well prior to the first well displaying a blood pellet.

6.2.3.4.2 Plaque assay

A 10-fold serial dilution of virus was prepared in serum-free DMEM. 12 well plates of confluent MDCK cells were washed with PBS and 100ul of each virus dilution added to a well of MDCKs. Plates were incubated for 1 hour at 37°C and 5% CO_2 (for Eng09 and Eng09 mutants) or 32°C and 5% CO_2 (for LAIV viruses). The medium was then removed and 1mL overlay medium containing 2% agarose and 1 µg/ml trypsin was added to each well. After the agarose mix was set, plates were incubated at 37°C 5% CO_2 for 3 days (for Eng09 and Eng09 mutants) and 32°C 5% CO_2 (for LAIV viruses). Plaque assays for the H3N2 LAIV virus were performed on MDCK-SIAT cells. Plaques were visualised by crystal violet staining.

6.2.3.5 Plaque picking

Individual viral plaques were picked using a Gilson pipette and propagated in a 24 well plate of MDCK cells until cytopathic effect was observed.

6.2.3.6 Virus growth kinetics in MDCK and A549 cells

12 well plates of MDCK cells were washed with PBS then infected with virus at the indicated MOI diluted in 100µL serum-free DMEM. For multi-cycle growth analysis, cells were infected at low multiplicity (MOI 0.0001-0.01 PFU/cell) and for single-cycle growth analysis cells were infected at high multiplicity (MOI 3 PFU/cell), in triplicate. The plate was incubated at 37°C, 5% CO_2 for 1 hour. The inoculum was then removed, cells washed twice with PBS and 1mL virus infection media added before incubating at 37°C, 5% CO_2. At desired time points post-infection, a 200µl aliquot of supernatant was removed and stored at -80°C. Samples were titrated by plaque assay on MDCK cells.

6.2.3.7 Virus infection of pHNECs

The apical surface of pHNECs was washed with 200µL DMEM to remove excess mucous. For experiments with Eng09 and Eng09 mutants, cells were infected at MOI of 0.001, in triplicate, for 1h at 37ºC and 5% CO_2. For experiments with LAIV viruses, cells were infected at MOI 0.01 PFU/cell, in triplicate, for 1h at 32ºC and 5% CO_2. The apical surface was then washed twice with serum free medium before re-incubating at 37ºC/32ºC. At indicated time points, 200µL of DMEM was added to the apical surface, incubated for 30 minutes, removed and stored at -80ºC before being titrated by plaque assay. For experiments on Eng09 and Eng09 mutants with a DMEM overlay, 200µL of DMEM was left on the apical surface between time points.

6.2.3.8 Virus driven replicon assay

A549 or 293T cells were transfected with pHSP1-3,5,8-Firefly and *Renilla* luciferase expression plasmids. 16 hours later, cells were infected with viruses at MOI of 1 PFU/cell for 1 hour, in triplicate. Inoculum was removed and cells washed gently with PBS before incubating in 10% DMEM for the indicated time at 37ºC and 5% CO_2. For experiments with IFITM3, the indicated amount of PCAGGS-IFITM3 and/or PCGASS-empty was added to the 10% DMEM. The same total amount of PCAGGS plasmid was added to each well. For experiments with type 1 IFN and amphotericin B, the indicated amount was added to the 10% DMEM. The levels of firefly luciferase (indicating viral replication in the nucleus) and *Renilla* luciferase (a marker of cellular polymerase) were quantified using a FLUOstar Omega plate reader (BMG Labtech).

6.2.3.9 Acid bypass assay

A549 cells were transfected with pHSP1-3,5,8-Firefly and *Renilla* luciferase expression plasmids. 16 hours later, influenza viruses at MOI of 1 PFU/cell were bound to A549 cells for 1 hour at 4ºC, in triplicate. Cells were washed twice with chilled (4ºC) PBS to remove any unbound virus particles, and then incubated with pre-warmed MES buffer pH-adjusted to 5.0 at 37ºC for 2 min to induce virus fusion at the cell surface. Cells were washed twice with chilled PBS and then incubated for 24 hours at 37ºC with DMEM + 20mM NH_4Cl + 50mM HEPES to block viral entry via the endocytic pathway. The levels of firefly and *Renilla* luciferase were quantified using a FLUOstar Omega plate reader. A negative (no fusion) control treating with pH 7.4 buffer followed by DMEM+NH_4Cl+HEPES and a positive (endosomal fusion) control treating with pH 7.4 buffer followed by DMEM+50mM HEPES were carried out simultaneously.

6.2.4 Assays to measure HA stability

6.2.4.1 Syncytia formation assay

MDCK cells at 60% confluence were inoculated with viruses at MOI of 10 PFU/cell for 1 hour at 37ºC and 5% CO_2 in duplicate. The inoculum was removed, cells were washed three times with PBS and incubated in DMEM + 2% FCS for 16 hours at 37ºC. Cells were treated with 10µg/mL TPCK-treated trypsin for 15 minutes at 37ºC then exposed to pH-adjusted MES buffers for 5 minutes at 37ºC. Buffers were replaced with DMEM + 10% FCS for 3 hours at 37ºC, fixed with methanol/acetone (1:1) and stained with Giemsa stain. Visual inspection for syncytia was performed under light microscopy.

6.2.4.2 Acid inactivation assay

Virus was mixed with pH-adjusted MES buffer (100mM MES, 150mM NaCl, 0.9mM $CaCl_2$, 0.5mM $MgCl_2$) in triplicate and incubated for 15 minutes at 37°C 5% CO_2 for Eng09 and Eng09 mutants, or 32°C 5% CO_2 for LAIV viruses. The buffer was inactivated with a 10-fold dilution in DMEM and samples titrated by plaque assay on MDCK cells.

6.2.4.3 Thermostability assay

64 haemagglutinating units of each virus was incubated for 30 minutes at 54°C in triplicate. The HA titre remaining after incubation was tested by haemagglutination assay.

6.2.4.4 Drug sensitivity

MDCK cells at 70% confluence were infected with each virus at MOI 0.01 PFU/cell in triplicate and incubated for 1 hour at 37°C and 5% CO_2. The inoculum was removed, cells washed twice with PBS, and 1mL of virus infection media with drug at the stated dose (or no drug control) added, before incubating cells for 24 hours. Drugs tested included the vacuolar ATPase inhibitor bafilomycin, the HA stalk-targeting fusion inhibitor arbidol hydrochloride and the HA-stem targeting monoclonal antibody FI6. Remaining infectivity was titrated by plaque assay on MDCK cells.

6.2.5 *In vivo* infectious studies

6.2.5.1 Ethics

All work was approved by the local genetic manipulation (GM) safety committee of Imperial College London, St. Mary's Campus (centre number GM77), and the Health and Safety Executive of the United Kingdom. Animal work was performed under United Kingdom Home Office License, PPL 70/7501 in accordance with the approved guidelines, under the Animals (Scientific Procedures) Act 1986 (ASPA).

6.2.5.2 Studies on mice

BALB/c mice (6-8 weeks old) were anaesthetised with nebulised isofluorane and intranasally inoculated with $2x10^5$ PFU of each virus in 40µL of PBS, or a mock control. Mice were weighed daily and would be sacrificed if >20% weight loss occurred. At day 2 and day 5 post-infection, 5 mice from each group were sacrificed and lungs harvested and weighed. Lungs were homogenised in 500uL PBS (Minilys, Bertin Instruments) and titrated by plaque assay on MDCK cells. Results were normalised to lung weight.

6.2.5.2 Studies on ferrets

Female ferrets (14–16 weeks old) weighing 500–1000g were used. After acclimatization, ferrets were lightly anaesthetized with ketamine (22 mg/kg) and xylazine (0.9 mg/kg) and inoculated intranasally with Eng09/wild type (10^4 PFU), Eng09/E21K or Eng09/Y7H virus (10^4 or 10^6 PFU as stated) diluted in phosphate

buffered saline (PBS) (0.1 ml per nostril). Post inoculation ferrets were returned to their cages, placed in the recovery position and monitored until they returned to full consciousness. Body weight was measured daily with any animal losing >20% body weight culled via a Schedule one method for welfare reasons. Ferrets were monitored for any adverse signs or symptoms. All animals were nasal washed daily, while conscious, by instilling 2 ml PBS into the nostrils and the expectorate collected in modified 250 ml centrifuge tubes on ice. Infectious virus was titrated immediately by plaque assay of the nasal wash on MDCK cells.

6.2.6 Studies using the influenza virus transmission tunnel (IVTT)

The influenza virus transmission tunnel (IVTT) was designed in house (J Ashcroft, R Elderfield and W Barclay) and manufactured by EMMS systems (Hampshire, UK). The system consists of a bias flow pump (EMMS) connected to a 37.5cm (height) x 25cm (diameter) ferret chamber. The ferret chamber is connected to the IVTT (a 100cm (length) x 18cm (width) x 9cm (height) half-cylindrical clear acrylic exposure tunnel) by a 1.5 cm (diameter) aperture allowing free passage of air. Sentinel cell plates are centred at 30, 60 and 90 cm from the tunnel opening and can be accessed via drawers from the side of the IVTT. Air is channelled from the exit port of the IVTT toward a downflow bench or microbiological safety cabinet filter to provide a low level draw. For air sampling, an SKC Biosampler (SKC Inc.) is connected to the exit port of the IVTT, with air pulled through at a rate of 12.5L/min. The ferret chamber is replaced by a 10cm (height) x 9cm (diameter) nebulisation chamber (EMMS) attached to an Aerogen Pro nebuliser (Aerogen), which generates droplets with a volume mean diameter (VMD) of 4 to 6μm, for *in vitro* experiments. All experiments were conducted with minimal-to-no UV light exposure.

6.2.6.1 Nebulised virus

Viruses (and/or plasmid DNA) under study were diluted in PBS and nebulised using the Aerogen Pro nebuliser into the nebuliser chamber attached to the IVT tunnel. Airflow at a rate of 1L/minute was introduced via two ports into the nebuliser chamber, which connects to the IVTT. Sentinel MDCK cells overlaid with 0.5mL overlay medium were exposed for 10 minutes per nebulisation and after exposure the plates were incubated for one hour at 37°C, 5% CO_2 prior to the addition of 1.5mL of semi-solid agarose overlay medium containing 1µg/mL TPCK treated trypsin and incubated for a further 3 days to allow formation of viral plaques. Viral RNA or tracer DNA were collected from1120µL PBS supplemented with 0.375% BSA-V placed in the central space between the wells of the three 6-well IVTT culture plates. Where air sampling was undertaken, after the 10 minute collection window, air remaining in the IVTT tunnel was pulled through a SKC Biosampler (SKC Inc.) at a rate of 12.5L/minute (calibrated as per manufacturer's instructions), for a further 10 minutes. Air samples were collected into 15mL PBS and quantified immediately by plaque assay on MDCK cells. RNA was extracted from 140µL for RT-qPCR or next generation sequencing. Temperature and humidity were monitored throughout experiments and were 21+/-1°C and 50+/-10% respectively. All experiments were performed with the IVTT placed within a class II biological safety cabinet at containment level 2. The IVTT was disinfected after use with a 1% virucidal disinfectant solution.

6.2.6.2 Ferret infection studies

Infected ferrets were placed into the ferret chamber for 10 minutes per exposure. Ferrets were not sedated during the exposure period and therefore, for well being, exposure was restricted to 10 minutes. Airflow of 7.5L/minute was introduced using

the bias flow pump via three ports into the ferret chamber (2.5L/minute into each port), which connects to the IVTT during the exposure period. Sentinel 6-well plates containing a confluent monolayer of MDCK cells overlaid with 0.5mL overlay medium were added to the tunnel for the duration of the exposure period. The plates were incubated for one hour at 37°C, 5% CO_2 prior to the addition of 1.5mL of semi-solid agarose overlay medium containing 2.5µg/mL of amphotericin B and 1µg/mL TPCK treated trypsin and incubated for a further 3 days to allow for formation of viral plaques. Between exposures for each donor ferret, sentinel cells were replaced and the collection chamber and cell tunnel cleaned to remove any surface deposited virus. Ferrets were nasal washed after IVTT exposures had been carried out. Temperature and humidity were monitored throughout experiments and observed to be 21+/-1°C and 50+/-10% respectively. The IVTT was disinfected after use with a 1% virucidal disinfectant solution. All experiments were conducted at containment level 2.

6.2.6.3 Human infection studies

Healthy adult volunteers were recruited for participation in a human influenza challenge study between June and November 2016 by Dr Christopher Chiu and team from the National Heart and Lung Institute Imperial College London. All volunteers were confirmed by the Chiu group to be sero-negative to the challenge virus and were isolated in a quarantine unit during the course of the study. Volunteers were intranasally inoculated with 10^6 PFU of A/California/04/2009 (pH1N1)-like virus, in 5 cohorts, by the Chiu team. Daily nasal washing and RT-qPCR of the samples was performed by the Chiu team.

Each volunteer was asked to breathe naturally (tidal breathing) into the IVTT for 10 minutes. A portable low flow suction pump was attached to the end of the IVTT to encourage directional airflow. Refinements to the collection method were carried out with each subsequent cohort, in an attempt to optimise the chance of virus collection. For cohort 1, each volunteer was asked to breathe via a disposable free flow mouthpiece attached directly to the IVTT (Figure 6.1A). For cohort 2, the mouthpiece was changed to a facemask covering the nose and mouth (Figure 6.1B), in an attempt to capture virus exhaled from both the nasal cavity and mouth. In cohorts 3 and 4, we sealed the IVTT after the 10 minute breath collection and exposed the cells for an additional 30 minutes, attempting to isolate any virus contained in smaller droplets that might take longer to settle within the IVTT. Cohort 5 were additionally asked to carry out 10 forced coughs after the 10 minute breath collection and air was pulled through the apparatus at a defined rate (2L/minute). Sentinel 6-well plates containing a confluent monolayer of MDCK cells overlaid with 0.5mL overlay medium were added to the tunnel for the duration of the exposure period. The plates were incubated for one hour at 37°C, 5% CO_2 prior to the addition of 1.5mL of semi-solid agarose overlay medium containing 2.5µg/mL of amphotericin B and 1µg/mL TPCK treated trypsin and incubated for a further 3 days to allow for formation of viral plaques. Between exposures for each human volunteer, sentinel cells were replaced and the collection chamber and cell tunnel cleaned to remove any surface deposited virus. A new sterile facemask was used for each volunteer. The IVTT was disinfected after use with a 1% virucidal disinfectant solution. All experiments were conducted at containment level 2.

A B

Figure 6.1. Devices used for experiments using the IVTT on human subjects. (A) shows free flow mouthpiece used for cohort 1, which attaches directly to the IVTT. (B) shows facemask used for cohorts 2-5, which attaches directly to the IVTT.

6.2.6.4 Conversion calculations of virus detection in the IVTT.

Viral plaque counts were taken from 6-well plates centred at 30cm (plate 1), 60cm (plate 2) and 90cm (plate 3). Plaque counts from the 6 wells were divided by the measured surface area to obtain an estimate for the viral plaques per square metre, or plaque density, at that recorded point. As the results were taken in triplicate, this then allowed for a set of upper, lower and mean values at each site. The decay in plaque numbers between subsequent sites was somewhere between linear and exponential across all ferrets. An exponential or linear regression fit was adopted accordingly to model the viral plaque densities, *N*, at a distance *x*. By integrating the plaque density over definite limits we formed an estimate for the total number of plaques, *P*, within a given area, *A*:

$$P = \int_A N \; dA = L_z \int_{x_1}^{x_2} N \; dx$$

where x_1 and x_2 represent axial distances along the tube, and L_z is the spanwise width. This calculation was performed by Dr L Nicolaou, Department of Mechanical Engineering, Imperial College London.

6.2.7 Structural modelling and statistical analysis

Modeling was performed using Pymol molecular visualization tool (Schrödinger, Inc.) and structures downloaded from RCSB Protein Data Bank (www.rcsb.org). All data analysis and graphs were prepared using GraphPad Prism 8 (GraphPad Software, San Diego, CA). Data are presented as mean +/- SD of three or more.

Chapter 7. References

1. Knipe DM HP. Fields Virology. 6th ed. 2013.
2. US Centre for Disease Control and Presenvtion. Types of Influenza Viruses [Internet]. [cited 2019 Jul 22]. Available from: https://www.cdc.gov/flu/about/viruses/types.htm
3. Ma W, García-Sastre A, Schwemmle M. Expected and Unexpected Features of the Newly Discovered Bat Influenza A-like Viruses. PLoS Pathog. 2015 Jun;11(6):e1004819.
4. Webster RG, Bean WJ, Gorman OT, Chambers TM, Kawaoka Y. Evolution and ecology of influenza A viruses. Microbiol Rev. 1992 Mar;56(1):152–79.
5. Harris A, Cardone G, Winkler DC, Heymann JB, Brecher M, White JM, et al. Influenza virus pleiomorphy characterized by cryoelectron tomography. Proc Natl Acad Sci. 2006 Dec 12;103(50):19123–7.
6. Badham MD, Rossman JS. Filamentous Influenza Viruses. Curr Clin Microbiol Reports. 2016 Sep 2;3(3):155–61.
7. Dou D, Revol R, Östbye H, Wang H, Daniels R. Influenza A Virus Cell Entry, Replication, Virion Assembly and Movement. Front Immunol. 2018 Jul 20;9:1581.
8. Hutchinson EC, Charles PD, Hester SS, Thomas B, Trudgian D, Martínez-Alonso M, et al. Conserved and host-specific features of influenza virion architecture. Nat Commun. 2014 Sep 16;5:4816.
9. Takemoto DK, Skehel JJ, Wiley DC. A surface plasmon resonance assay for the binding of influenza virus hemagglutinin to its sialic acid receptor. Virology. 1996 Mar;217(2):452–8.
10. Wiley DC, Skehel JJ. The Structure and Function of the Hemagglutinin Membrane Glycoprotein of Influenza Virus. Annu Rev Biochem. 1987

Jun;56(1):365–94.

11. Edinger TO, Pohl MO, Stertz S. Entry of influenza A virus: host factors and antiviral targets. J Gen Virol. 2014 Feb 1;95(Pt_2):263–77.
12. Blaas D, Patzelt E, Kuechler E. Identification of the cap binding protein of influenza virus. Nucleic Acids Res. 1982 Aug 11;10(15):4803–12.
13. Boulo S, Akarsu H, Ruigrok RWH, Baudin F. Nuclear traffic of influenza virus proteins and ribonucleoprotein complexes. Virus Res. 2007 Mar;124(1–2):12–21.
14. Takeda M, Leser GP, Russell CJ, Lamb RA. Influenza virus hemagglutinin concentrates in lipid raft microdomains for efficient viral fusion. Proc Natl Acad Sci. 2003 Dec 9;100(25):14610–7.
15. Palese P, Tobita K, Ueda M, Compans RW. Characterization of temperature sensitive influenza virus mutants defective in neuraminidase. Virology. 1974 Oct;61(2):397–410.
16. Daidoji T, Watanabe Y, Arai Y, Kajikawa J, Hirose R, Nakaya T. Unique Infectious Strategy of H5N1 Avian Influenza Virus Is Governed by the Acid-Destabilized Property of Hemagglutinin. Viral Immunol. 30(6):398–407.
17. Gamblin SJ, Skehel JJ. Influenza Hemagglutinin and Neuraminidase Membrane Glycoproteins. J Biol Chem. 2010 Sep 10;285(37):28403–9.
18. Burke DF, Smith DJ. A recommended numbering scheme for influenza A HA subtypes. PLoS One. 2014;9(11):e112302.
19. Wilson IA, Skehel JJ, Wiley DC. Structure of the haemagglutinin membrane glycoprotein of influenza virus at 3 Å resolution. Nature. 1981;289(5796):366–73.
20. Bullough PA, Hughson FM, Skehel JJ, Wiley DC. Structure of influenza haemagglutinin at the pH of membrane fusion. Nature. 1994 Sep;371(6492):37–43.
21. Caton AJ, Brownlee GG, Yewdell JW, Gerhard W. The antigenic structure of

the influenza virus A/PR/8/34 hemagglutinin (H1 subtype). Cell. 1982 Dec;31(2 Pt 1):417–27.

22. Shi Y, Wu Y, Zhang W, Qi J, Gao GF. Enabling the “host jump”: structural determinants of receptor-binding specificity in influenza A viruses. Nat Rev Microbiol. 2014 Nov 10;12:822.
23. Chen J, Lee KH, Steinhauer DA, Stevens DJ, Skehel JJ, Wiley DC. Structure of the hemagglutinin precursor cleavage site, a determinant of influenza pathogenicity and the origin of the labile conformation. Cell. 1998 Oct;95(3):409–17.
24. Liu STH, Behzadi MA, Sun W, Freyn AW, Liu W-C, Broecker F, et al. Antigenic sites in influenza H1 hemagglutinin display species-specific immunodominance. J Clin Invest. 2018 Nov 1;128(11):4992–6.
25. Carr CM, Chaudhry C, Kim PS. Influenza hemagglutinin is spring-loaded by a metastable native conformation. Proc Natl Acad Sci U S A. 1997 Dec 23;94(26):14306–13.
26. Floyd DL, Ragains JR, Skehel JJ, Harrison SC, van Oijen AM. Single-particle kinetics of influenza virus membrane fusion. Proc Natl Acad Sci. 2008 Oct 7;105(40):15382–7.
27. Ivanovic T, Choi JL, Whelan SP, van Oijen AM, Harrison SC. Influenza-virus membrane fusion by cooperative fold-back of stochastically induced hemagglutinin intermediates. Elife. 2013 Feb 19;2.
28. Forgac M. Structure and Properties of the Vacuolar (H+)-ATPases. J Biol Chem. 1999;274(19):12951–4.
29. Lipsitch M, Barclay W, Raman R, Russell CJ, Belser JA, Cobey S, et al. Viral factors in influenza pandemic risk assessment. Elife. 2016 Nov 11;5.
30. Russell CJ, Hu M, Okda FA. Influenza Hemagglutinin Protein Stability, Activation, and Pandemic Risk. Trends Microbiol. 2018 Oct;26(10):841–53.
31. Mair CM, Ludwig K, Herrmann A, Sieben C. Receptor binding and pH stability

- how influenza A virus hemagglutinin affects host-specific virus infection. Biochim Biophys Acta. 2014 Apr;1838(4):1153–68.

32. Daniels R, Daniels FS, Downie JC, Hay AJ, Knossow M, Hill M. Fusion mutants of the influenza virus hemagglutinin glycoprotein. Cell. 1985 Feb;40(2):431–9.

33. Su B, Wurtzer S, Rameix-Welti M-A, Dwyer D, van der Werf S, Naffakh N, et al. Enhancement of the Influenza A Hemagglutinin (HA)-Mediated Cell-Cell Fusion and Virus Entry by the Viral Neuraminidase (NA). Geraghty RJ, editor. PLoS One. 2009 Dec 30;4(12):e8495.

34. O'Donnell CD, Vogel L, Matsuoka Y, Jin H, Subbarao K. The matrix gene segment destabilizes the acid and thermal stability of the hemagglutinin of pandemic live attenuated influenza virus vaccines. J Virol. 2014 Nov;88(21):12374–84.

35. Scholtissek C. Stability of infectious influenza A viruses at low pH and at elevated temperature. Vaccine. 1985 Sep;3(3):215–8.

36. Otterstrom J, van Oijen AM. Visualization of Membrane Fusion, One Particle at a Time. Biochemistry. 2013 Mar 12;52(10):1654–68.

37. Hamilton BS, Whittaker GR, Daniel S. Influenza virus-mediated membrane fusion: Determinants of hemagglutinin fusogenic activity and experimental approaches for assessing virus fusion. Viruses. 2012 Jul;4(7).

38. Suddala KC, Lee CC, Meraner P, Marin M, Markosyan RM, Desai TM, et al. Interferon-induced transmembrane protein 3 blocks fusion of sensitive but not resistant viruses by partitioning into virus-carrying endosomes. Whelan SPJ, editor. PLOS Pathog. 2019 Jan 14;15(1):e1007532.

39. Padilla-Parra S, Matos PM, Kondo N, Marin M, Santos NC, Melikyan GB. Quantitative imaging of endosome acidification and single retrovirus fusion with distinct pools of early endosomes. Proc Natl Acad Sci. 2012 Oct 23;109(43):17627–32.

40. Paules C, Subbarao K. Influenza. Lancet (London, England). 2017 Aug;390(10095):697–708.
41. de Francisco Shapovalova N, Donadel M, Jit M, Hutubessy R. A systematic review of the social and economic burden of influenza in low- and middle-income countries. Vaccine. 2015 Nov;33(48):6537–44.
42. Troeger CE, Blacker BF, Khalil IA, Zimsen SRM, Albertson SB, Abate D, et al. Mortality, morbidity, and hospitalisations due to influenza lower respiratory tract infections, 2017: an analysis for the Global Burden of Disease Study 2017. Lancet Respir Med. 2019 Jan;7(1):69–89.
43. Cassini A, Colzani E, Pini A, Mangen M-JJ, Plass D, McDonald SA, et al. Impact of infectious diseases on population health using incidence-based disability-adjusted life years (DALYs): results from the Burden of Communicable Diseases in Europe study, European Union and European Economic Area countries, 2009 to 2013. Euro Surveill. 2018 Apr;23(16).
44. Iuliano AD, Roguski KM, Chang HH, Muscatello DJ, Palekar R, Tempia S, et al. Estimates of global seasonal influenza-associated respiratory mortality: a modelling study. Lancet. 2018 Mar;391(10127):1285–300.
45. Chen R, Holmes EC. Avian influenza virus exhibits rapid evolutionary dynamics. Mol Biol Evol. 2006 Dec;23(12):2336–41.
46. European Centre for Disease Prevention and Control (ECDC). Questions and Answers on influenza pandemics [Internet]. [cited 2019 Jul 22]. Available from: https://ecdc.europa.eu/en/pandemic-influenza/facts/questions-and-answers
47. Taubenberger JK, Morens DM. 1918 Influenza: the mother of all pandemics. Emerg Infect Dis. 2006 Jan;12(1):15–22.
48. Morens DM, Taubenberger JK, Fauci AS. Predominant role of bacterial pneumonia as a cause of death in pandemic influenza: implications for pandemic influenza preparedness. J Infect Dis. 2008 Oct;198(7):962–70.
49. Taubenberger JK, Reid AH, Krafft AE, Bijwaard KE, Fanning TG. Initial genetic

characterization of the 1918 “Spanish” influenza virus. Science. 1997 Mar;275(5307):1793–6.

50. Kobasa D, Takada A, Shinya K, Hatta M, Halfmann P, Theriault S, et al. Enhanced virulence of influenza A viruses with the haemagglutinin of the 1918 pandemic virus. Nature. 2004 Oct;431(7009):703–7.

51. Kobasa D, Jones SM, Shinya K, Kash JC, Copps J, Ebihara H, et al. Aberrant innate immune response in lethal infection of macaques with the 1918 influenza virus. Nature. 2007 Jan;445(7125):319–23.

52. Tumpey TM, Basler CF, Aguilar P V., Zeng H, Solórzano A, Swayne DE, et al. Characterization of the reconstructed 1918 Spanish influenza pandemic virus. Science. 2005 Oct 7;310(5745):77–80.

53. Kash JC, Tumpey TM, Proll SC, Carter V, Perwitasari O, Thomas MJ, et al. Genomic analysis of increased host immune and cell death responses induced by 1918 influenza virus. Nature. 2006 Oct 5;443(7111):578–81.

54. Steinhauer DA. Role of Hemagglutinin Cleavage for the Pathogenicity of Influenza Virus. Virology. 1999 May;258(1):1–20.

55. Watanabe T, Kawaoka Y. Pathogenesis of the 1918 pandemic influenza virus. PLoS Pathog. 2011 Jan;7(1):e1001218.

56. Worobey M, Han G-Z, Rambaut A. Genesis and pathogenesis of the 1918 pandemic H1N1 influenza A virus. Proc Natl Acad Sci U S A. 2014 Jun;111(22):8107–12.

57. Antonovics J, Hood ME, Baker CH. Molecular virology: was the 1918 flu avian in origin? Nature. 2006 Apr;440(7088):E9; discussion E9-10.

58. Taubenberger JK, Reid AH, Lourens RM, Wang R, Jin G, Fanning TG. Characterization of the 1918 influenza virus polymerase genes. Nature. 2005 Oct;437(7060):889–93.

59. Belshe RB. The Origins of Pandemic Influenza — Lessons from the 1918 Virus. N Engl J Med. 2005 Nov 24;353(21):2209–11.

60. Zakstelskaja LJ, Yakhno MA, Isacenko VA, Molibog E V, Hlustov SA, Antonova I V, et al. Influenza in the USSR in 1977: recurrence of influenzavirus A subtype H1N1. Bull World Health Organ. 1978;56(6):919–22.

61. Nakajima K, Desselberger U, Palese P. Recent human influenza A (H1N1) viruses are closely related genetically to strains isolated in 1950. Nature. 1978 Jul;274(5669):334–9.

62. Krammer F, Smith GJD, Fouchier RAM, Peiris M, Kedzierska K, Doherty PC, et al. Influenza. Nat Rev Dis Prim. 2018 Dec 28;4(1):3.

63. Mena I, Nelson MI, Quezada-Monroy F, Dutta J, Cortes-Fernández R, Lara-Puente JH, et al. Origins of the 2009 H1N1 influenza pandemic in swine in Mexico. Elife. 2016;5.

64. Neumann G, Noda T, Kawaoka Y. Emergence and pandemic potential of swine-origin H1N1 influenza virus. Nature. 2009 Jun 14;459(7249):931–9.

65. Sekkides O. Pandemic influenza-a timeline. Lancet Infect Dis. 2010 Oct;10(10):663.

66. Elderfield R, Barclay W. Influenza pandemics. Adv Exp Med Biol. 2011;719:81–103.

67. Simonsen L, Spreeuwenberg P, Lustig R, Taylor RJ, Fleming DM, Kroneman M, et al. Global Mortality Estimates for the 2009 Influenza Pandemic from the GLaMOR Project: A Modeling Study. Hay SI, editor. PLoS Med. 2013 Nov 26;10(11):e1001558.

68. Dawood FS, Iuliano AD, Reed C, Meltzer MI, Shay DK, Cheng P-Y, et al. Estimated global mortality associated with the first 12 months of 2009 pandemic influenza A H1N1 virus circulation: a modelling study. Lancet Infect Dis. 2012 Sep;12(9):687–95.

69. World Health Organisation (WHO). Influenza (Avian and other zoonotic) [Internet]. 2018 [cited 2019 Jul 22]. Available from: https://www.who.int/news-room/fact-sheets/detail/influenza-(avian-and-other-zoonotic)

70. Ozawa M, Kawaoka Y. Cross talk between animal and human influenza viruses. Annu Rev Anim Biosci. 2013 Jan;1:21–42.

71. World Health Organisation (WHO). Avian Influenza Weekly Update Number 695. 2019.

72. WHO. Tool for Influenza Pandemic Risk Assessment (TIPRA). 2016;

73. Cox NJ, Trock SC, Burke SA. Pandemic preparedness and the Influenza Risk Assessment Tool (IRAT). Curr Top Microbiol Immunol. 2014;385:119–36.

74. Matrosovich MN, Matrosovich TY, Gray T, Roberts NA, Klenk H-D. Human and avian influenza viruses target different cell types in cultures of human airway epithelium. Proc Natl Acad Sci. 2004 Mar 30;101(13):4620–4.

75. Shinya K, Ebina M, Yamada S, Ono M, Kasai N, Kawaoka Y. Avian flu: influenza virus receptors in the human airway. Nature. 2006 Mar 23;440(7083):435–6.

76. Kuchipudi S V, Nelli R, White GA, Bain M, Chang KC, Dunham S. Differences in influenza virus receptors in chickens and ducks: Implications for interspecies transmission. J Mol Genet Med. 2009 Jan;3(1):143–51.

77. Walther T, Karamanska R, Chan RWY, Chan MCW, Jia N, Air G, et al. Glycomic Analysis of Human Respiratory Tract Tissues and Correlation with Influenza Virus Infection. Pekosz A, editor. PLoS Pathog. 2013 Mar 14;9(3):e1003223.

78. Chandrasekaran A, Srinivasan A, Raman R, Viswanathan K, Raguram S, Tumpey TM, et al. Glycan topology determines human adaptation of avian H5N1 virus hemagglutinin. Nat Biotechnol. 2008 Jan 6;26:107.

79. Imai M, Kawaoka Y. The role of receptor binding specificity in interspecies transmission of influenza viruses. Curr Opin Virol. 2012 Apr;2(2):160–7.

80. Rogers GN, Paulson JC, Daniels RS, Skehel JJ, Wilson IA, Wiley DC. Single amino acid substitutions in influenza haemagglutinin change receptor binding specificity. Nature. 1983 Jul;304(5921):76–8.

81. Matrosovich M, Tuzikov A, Bovin N, Gambaryan A, Klimov A, Castrucci MR, et al. Early alterations of the receptor-binding properties of H1, H2, and H3 avian influenza virus hemagglutinins after their introduction into mammals. J Virol. 2000 Sep;74(18):8502–12.

82. Tumpey TM, Maines TR, Van Hoeven N, Glaser L, Solorzano A, Pappas C, et al. A Two-Amino Acid Change in the Hemagglutinin of the 1918 Influenza Virus Abolishes Transmission. Science (80-). 2007 Feb 2;315(5812):655–9.

83. Pappas C, Viswanathan K, Chandrasekaran A, Raman R, Katz JM, Sasisekharan R, et al. Receptor specificity and transmission of H2N2 subtype viruses isolated from the pandemic of 1957. PLoS One. 2010 Jun;5(6):e11158.

84. Subbarao EK, London W, Murphy BR. A single amino acid in the PB2 gene of influenza A virus is a determinant of host range. J Virol. 1993 Apr;67(4):1761–4.

85. Steel J, Lowen AC, Mubareka S, Palese P. Transmission of Influenza Virus in a Mammalian Host Is Increased by PB2 Amino Acids 627K or 627E/701N. Baric RS, editor. PLoS Pathog. 2009 Jan 2;5(1):e1000252.

86. Gao Y, Zhang Y, Shinya K, Deng G, Jiang Y, Li Z, et al. Identification of amino acids in HA and PB2 critical for the transmission of H5N1 avian influenza viruses in a mammalian host. PLoS Pathog. 2009 Dec;5(12):e1000709.

87. Long JS, Giotis ES, Moncorgé O, Frise R, Mistry B, James J, et al. Species difference in ANP32A underlies influenza A virus polymerase host restriction. Nature. 2016 Jan 7;529(7584):101–4.

88. Seladi-Schulman J, Steel J, Lowen AC. Spherical influenza viruses have a fitness advantage in embryonated eggs, while filament-producing strains are selected in vivo. J Virol. 2013 Dec;87(24):13343–53.

89. Blumenkrantz D, Roberts KL, Shelton H, Lycett S, Barclay WS. The short stalk length of highly pathogenic avian influenza H5N1 virus neuraminidase limits

transmission of pandemic H1N1 virus in ferrets. J Virol. 2013 Oct;87(19):10539–51.

90. Yen H-L, Liang C-H, Wu C-Y, Forrest HL, Ferguson A, Choy K-T, et al. Hemagglutinin-neuraminidase balance confers respiratory-droplet transmissibility of the pandemic H1N1 influenza virus in ferrets. Proc Natl Acad Sci U S A. 2011 Aug 23;108(34):14264–9.

91. Rajsbaum R, Albrecht RA, Wang MK, Maharaj NP, Versteeg GA, Nistal-Villan E, et al. Species-specific inhibition of RIG-I ubiquitination and IFN induction by the influenza A virus NS1 protein. PLoS Pathog. 2012;8(11):e1003059.

92. Herfst S, Schrauwen EJ a., Linster M, Chutinimitkul S, de Wit E, Munster VJ, et al. Airborne Transmission of Influenza A/H5N1 Virus Between Ferrets. Science (80-). 2012;336(6088):1534–41.

93. Imai M, Watanabe T, Hatta M, Das SC, Ozawa M, Shinya K, et al. Experimental adaptation of an influenza H5 HA confers respiratory droplet transmission to a reassortant H5 HA/H1N1 virus in ferrets. Nature. 2012;486(7403):420–8.

94. Killingley B, Nguyen-Van-Tam J. Routes of influenza transmission. Influenza Other Respi Viruses. 2013 Sep;7:42–51.

95. Grayson ML, Melvani S, Druce J, Barr IG, Ballard SA, Johnson PDR, et al. Efficacy of soap and water and alcohol-based hand-rub preparations against live H1N1 influenza virus on the hands of human volunteers. Clin Infect Dis. 2009 Feb 1;48(3):285–91.

96. Thomas Y, Boquete-Suter P, Koch D, Pittet D, Kaiser L. Survival of influenza virus on human fingers. Clin Microbiol Infect. 2014 Jan;20(1):O58–64.

97. Bean B, Moore BM, Sterner B, Peterson LR, Gerding DN, Balfour HH. Survival of influenza viruses on environmental surfaces. J Infect Dis. 1982 Jul;146(1):47–51.

98. von Braun A, Thomas Y, Sax H. Do high-touch surfaces in public spaces pose

a risk for influenza transmission? A virologic study during the peak of the 2009 influenza A(H1N1) pandemic in Geneva, Switzerland. Am J Infect Control. 2015 Dec 1;43(12):1372–3.

99. Ikonen N, Savolainen-Kopra C, Enstone JE, Kulmala I, Pasanen P, Salmela A, et al. Deposition of respiratory virus pathogens on frequently touched surfaces at airports. BMC Infect Dis. 2018 Aug 29;18(1):437.

100. Killingley B, Greatorex J, Cauchemez S, Enstone JE, Curran M, Read RC, et al. Virus shedding and environmental deposition of novel A (H1N1) pandemic influenza virus: interim findings. Health Technol Assess. 2010 Oct;14(46):237–354.

101. Boone SA, Gerba CP. The occurrence of influenza A virus on household and day care center fomites. J Infect. 2005 Aug;51(2):103–9.

102. Zhou J, Wei J, Choy K-T, Sia SF, Rowlands DK, Yu D, et al. Defining the sizes of airborne particles that mediate influenza transmission in ferrets. Proc Natl Acad Sci U S A. 2018;115(10):E2386–92.

103. Gustin KM, Belser JA, Wadford DA, Pearce MB, Katz JM, Tumpey TM, et al. Influenza virus aerosol exposure and analytical system for ferrets. Proc Natl Acad Sci U S A. 2011 May 17;108(20):8432–7.

104. Lakdawala SS, Lamirande EW, Suguitan AL, Wang W, Santos CP, Vogel L, et al. Eurasian-origin gene segments contribute to the transmissibility, aerosol release, and morphology of the 2009 pandemic H1N1 influenza virus. PLoS Pathog. 2011 Dec;7(12):e1002443.

105. Koster F, Gouveia K, Zhou Y, Lowery K, Russell R, MacInnes H, et al. Exhaled aerosol transmission of pandemic and seasonal H1N1 influenza viruses in the ferret. Guan Y, editor. PLoS One. 2012 Apr 3;7(4):e33118.

106. Nicas M, Nazaroff WW, Hubbard A. Toward Understanding the Risk of Secondary Airborne Infection: Emission of Respirable Pathogens. J Occup Environ Hyg. 2005 Mar 17;2(3):143–54.

107. Fabian P, Brain J, Houseman EA, Gern J, Milton DK. Origin of exhaled breath particles from healthy and human rhinovirus-infected subjects. J Aerosol Med Pulm Drug Deliv. 2011 Jun 1;24(3):137–47.

108. Bake B, Larsson P, Ljungkvist G, Ljungström E, Olin AC. Exhaled particles and small airways. Vol. 20, Respiratory Research. BioMed Central Ltd.; 2019. p. 8.

109. Infectious Diseases Society of America (ISDA). Preventing Transmission of Pandemic Influenza and Other Viral Respiratory Diseases. Update 201. Washington, D.C.: National Academies Press; 2011.

110. Tellier R, Li Y, Cowling BJ, Tang JW. Recognition of aerosol transmission of infectious agents: a commentary. BMC Infect Dis. 2019 Jan 31;19(1):101.

111. Bourouiba L, Dehandschoewercker E, Bush JWM. Violent expiratory events: on coughing and sneezing. J Fluid Mech. 2014 Apr 25;745:537–63.

112. Cowling BJ, Ip DKM, Fang VJ, Suntarattiwong P, Olsen SJ, Levy J, et al. Aerosol transmission is an important mode of influenza A virus spread. Nat Commun. 2013;4:1935.

113. Brankston G, Gitterman L, Hirji Z, Lemieux C, Gardam M. Transmission of influenza A in human beings. Lancet Infect Dis. 2007 Apr;7(4):257–65.

114. Belser JA, Barclay W, Barr I, Fouchier RAM, Matsuyama R, Nishiura H, et al. Ferrets as Models for Influenza Virus Transmission Studies and Pandemic Risk Assessments. Emerg Infect Dis. 2018 Jun;24(6):965–71.

115. Belser JA, Eckert AM, Tumpey TM, Maines TR. Complexities in Ferret Influenza Virus Pathogenesis and Transmission Models. Microbiol Mol Biol Rev. 2016 Sep;80(3):733–44.

116. van Riel D, Munster VJ, de Wit E, Rimmelzwaan GF, Fouchier RAM, Osterhaus ADME, et al. Human and avian influenza viruses target different cells in the lower respiratory tract of humans and other mammals. Am J Pathol. 2007 Oct;171(4):1215–23.

117. Buhnerkempe MG, Gostic K, Park M, Ahsan P, Belser JA, Lloyd-Smith JO. Mapping influenza transmission in the ferret model to transmission in humans. Elife. 2015 Sep 2;4.

118. Frise R, Bradley K, van Doremalen N, Galiano M, Elderfield RA, Stilwell P, et al. Contact transmission of influenza virus between ferrets imposes a looser bottleneck than respiratory droplet transmission allowing propagation of antiviral resistance. Sci Rep. 2016 Jul 19;6(1):29793.

119. Andrewes CH, Glover RE. Spread of Infection from the Respiratory Tract of the Ferret. I. Transmission of Influenza A Virus. Br J Exp Pathol. 1941 Apr;22(2):91–7.

120. Mubareka S, Lowen AC, Steel J, Coates AL, García-Sastre A, Palese P. Transmission of influenza virus via aerosols and fomites in the guinea pig model. J Infect Dis. 2009 Mar 15;199(6):858–65.

121. Parker L, Wharton SA, Martin SR, Cross K, Lin Y, Liu Y, et al. Effects of egg-adaptation on receptor-binding and antigenic properties of recent influenza A (H3N2) vaccine viruses. J Gen Virol. 2016;97(6):1333–44.

122. Forrest BD, Pride MW, Dunning AJ, Capeding MRZ, Chotpitayasunondh T, Tam JS, et al. Correlation of cellular immune responses with protection against culture-confirmed influenza virus in young children. Clin Vaccine Immunol. 2008 Jul;15(7):1042–53.

123. Hoft DF, Babusis E, Worku S, Spencer CT, Lottenbach K, Truscott SM, et al. Live and Inactivated Influenza Vaccines Induce Similar Humoral Responses, but Only Live Vaccines Induce Diverse T-Cell Responses in Young Children. 2011 Sep 15;204(6):845–53.

124. Mohn KG-I, Brokstad KA, Pathirana RD, Bredholt G, Jul-Larsen Å, Trieu MC, et al. Live Attenuated Influenza Vaccine in Children Induces B-Cell Responses in Tonsils. J Infect Dis. 2016 Sep 1;214(5):722–31.

125. Fleming DM. Managing influenza: amantadine, rimantadine and beyond. Int J

Clin Pract. 2001 Apr;55(3):189–95.

126. Lackenby A, Hungnes O, Dudman SG, Meijer A, Paget WJ, Hay AJ, et al. Emergence of resistance to oseltamivir among influenza A(H1N1) viruses in Europe. Euro Surveill. 2008;13(5).

127. Abed Y, Pizzorno A, Bouhy X, Rheaume C, Boivin G. Impact of potential permissive neuraminidase mutations on viral fitness of the H275Y oseltamivir-resistant influenza A(H1N1)pdm09 virus in vitro, in mice and in ferrets. J Virol. 2014 Feb;88(3):1652–8.

128. Goldhill DH, Te Velthuis AJW, Fletcher RA, Langat P, Zambon M, Lackenby A, et al. The mechanism of resistance to favipiravir in influenza. Proc Natl Acad Sci U S A. 2018 Nov 6;115(45):11613–8.

129. Omoto S, Speranzini V, Hashimoto T, Noshi T, Yamaguchi H, Kawai M, et al. Characterization of influenza virus variants induced by treatment with the endonuclease inhibitor baloxavir marboxil. Sci Rep. 2018 Dec 25;8(1):9633.

130. Leneva I a., Russell RJ, Boriskin YS, Hay AJ. Characteristics of arbidol-resistant mutants of influenza virus: Implications for the mechanism of anti-influenza action of arbidol. Antiviral Res. 2009;81(2):132–40.

131. Galloway SE, Reed ML, Russell CJ, Steinhauer DA. Influenza HA subtypes demonstrate divergent phenotypes for cleavage activation and pH of fusion: implications for host range and adaptation. PLoS Pathog. 2013;9(2):e1003151.

132. Shelton H, Roberts KL, Molesti E, Temperton N, Barclay WS. Mutations in haemagglutinin that affect receptor binding and pH stability increase replication of a PR8 influenza virus with H5 HA in the upper respiratory tract of ferrets and may contribute to transmissibility. J Gen Virol. 2013 Jun 1;94(Pt 6):1220–9.

133. Baumann J, Mounogou Kouassi N, Foni E, Klenk H-D, Matrosovich M. H1N1 Swine Influenza Viruses Differ from Avian Precursors by a higher pH Optimum

of Membrane Fusion. J Virol. 2016;90(3):1569–77.

134. Russier M, Yang G, Rehg JE, Wong S-S, Mostafa HH, Fabrizio TP, et al. Molecular requirements for a pandemic influenza virus: An acid-stable hemagglutinin protein. Proc Natl Acad Sci. 2016 Feb 9;113(6):1636–41.

135. Sun X, Belser JA, Pappas C, Pulit-Penaloza JA, Brock N, Zeng H, et al. Risk assessment of fifth-wave H7N9 influenza A viruses in mammalian models. J Virol. 2018 Oct 10;pii: JVI.01740-18.

136. DuBois RM, Zaraket H, Reddivari M, Heath RJ, White SW, Russell CJ. Acid stability of the hemagglutinin protein regulates H5N1 influenza virus pathogenicity. PLoS Pathog. 2011;7(12):1–11.

137. Reed ML, Bridges O a, Seiler P, Kim J-K, Yen H-L, Salomon R, et al. The pH of activation of the hemagglutinin protein regulates H5N1 influenza virus pathogenicity and transmissibility in ducks. J Virol. 2010;84(3):1527–35.

138. Cotter CR, Jin H, Chen Z. A single amino acid in the stalk region of the H1N1pdm influenza virus HA protein affects viral fusion, stability and infectivity. PLoS Pathog. 2014;10(1):e1003831.

139. Klein EY, Blumenkrantz D, Serohijos A, Shakhnovich E, Choi J-M, Rodrigues J V, et al. Stability of the Influenza Virus Hemagglutinin Protein Correlates with Evolutionary Dynamics. mSphere. 2018;3(1):pii: e00554-17.

140. Pulit-Penaloza JA, Pappas C, Belser JA, Sun X, Brock N, Zeng H, et al. Comparative In Vitro and In Vivo Analysis of H1N1 and H1N2 Variant Influenza Viruses Isolated from Humans between 2011 and 2016. J Virol. 2018 Nov 15;92(22).

141. Zaraket H, Bridges O a, Russell CJ. The pH of activation of the hemagglutinin protein regulates H5N1 influenza virus replication and pathogenesis in mice. J Virol. 2013;87(9):4826–34.

142. Zaraket H, Bridges O a., Duan S, Baranovich T, Yoon S-W, Reed ML, et al. Increased acid stability of the hemagglutinin protein enhances H5N1 influenza

virus growth in the upper respiratory tract but is insufficient for transmission in ferrets. J Virol. 2013;87(17):9911–22.

143. Thoennes S, Li Z, Lee B-J, Langley WA, Skehel JJ, Russell RJ, et al. Analysis of residues near the fusion peptide in the influenza hemagglutinin structure for roles in triggering membrane fusion. Virology. 2008 Jan 20;370(2):403–14.

144. Byrd-Leotis L, Galloway SE, Agbogu E, Steinhauer D a. Influenza hemagglutinin (HA) stem region mutations that stabilize or destabilize the structure of multiple HA subtypes. J Virol. 2015 Apr;89(8):4504–16.

145. Krenn BM, Egorov A, Romanovskaya-Romanko E, Wolschek M, Nakowitsch S, Ruthsatz T, et al. Single HA2 mutation increases the infectivity and immunogenicity of a live attenuated H5N1 intranasal influenza vaccine candidate lacking NS1. PLoS One. 2011;6(4):e18577.

146. Lin YP, Wharton SA, Martin J, Skehel JJ, Wiley DC, Steinhauer DA. Adaptation of egg-grown and transfectant influenza viruses for growth in mammalian cells: selection of hemagglutinin mutants with elevated pH of membrane fusion. Virology. 1997 Jul;233(2):402–10.

147. Wormann X, Lesch M, Welke R-W, Okonechnikov K, Abdurishid M, Sieben C, et al. Genetic characterization of an adapted pandemic 2009 H1N1 influenza virus that reveals improved replication rates in human lung epithelial cells. Virology. 2016 May;492:118–29.

148. Nakowitsch S, Wolschek M, Morokutti A, Ruthsatz T, Krenn BM, Ferko B, et al. Mutations affecting the stability of the haemagglutinin molecule impair the immunogenicity of live attenuated H3N2 intranasal influenza vaccine candidates lacking NS1. Vaccine. 2011 Apr 27;29(19):3517–24.

149. Brass AL, Huang IC, Benita Y, John SP, Krishnan MN, Feeley EM, et al. The IFITM Proteins Mediate Cellular Resistance to Influenza A H1N1 Virus, West Nile Virus, and Dengue Virus. Cell. 2009;139(7):1243–54.

150. Shapira SD, Gat-Viks I, Shum BO V, Dricot A, de Grace MM, Wu L, et al. A

physical and regulatory map of host-influenza interactions reveals pathways in H1N1 infection. Cell. 2009 Dec;139(7):1255–67.

151. Everitt AR, Clare S, Pertel T, John SP, Wash RS, Smith SE, et al. IFITM3 restricts the morbidity and mortality associated with influenza. Nature. 2012 Mar;484(7395):519–23.

152. Huang I-C, Bailey CC, Weyer JL, Radoshitzky SR, Becker MM, Chiang JJ, et al. Distinct Patterns of IFITM-Mediated Restriction of Filoviruses, SARS Coronavirus, and Influenza A Virus. Baric RS, editor. PLoS Pathog. 2011 Jan 6;7(1):e1001258.

153. Feeley EM, Sims JS, John SP, Chin CR, Pertel T, Chen L-M, et al. IFITM3 Inhibits Influenza A Virus Infection by Preventing Cytosolic Entry. Diamond MS, editor. PLoS Pathog. 2011 Oct 27;7(10):e1002337.

154. Desai TM, Marin M, Chin CRC, Savidis G, Brass AAL, Melikyan GGB, et al. IFITM3 Restricts Influenza A Virus Entry by Blocking the Formation of Fusion Pores following Virus-Endosome Hemifusion. Basler CF, editor. PLoS Pathog. 2014 Apr 3;10(4):e1004048.

155. Lin TY, Chin CR, Everitt AR, Clare S, Perreira JM, Savidis G, et al. Amphotericin B Increases Influenza A Virus Infection by Preventing IFITM3-Mediated Restriction. Cell Rep. 2013;5(4):895–908.

156. Sun X, Zeng H, Kumar A, Belser JA, Maines TR, Tumpey TM. Constitutively expressed IFITM3 protein in human pulmonary endothelial cells poses an early infection block to human influenza viruses. J Virol. 2016 Dec 15;90(October):JVI.01254-16.

157. Gerlach T, Hensen L, Matrosovich T, Bergmann J, Winkler M, Peteranderl C, et al. pH-optimum of hemagglutinin-mediated membrane fusion determines sensitivity of influenza A viruses to the interferon-induced antiviral state and IFITMs. J Virol. 2017 Mar 29;JVI.00246-17.

158. Matsuoka Y, Lamirande EW, Subbarao K. The mouse model for influenza.

Curr Protoc Microbiol. 2009 May;Chapter 15:Unit 15G.3.

159. Wu NC, Wilson IA. Structural insights into the design of novel anti-influenza therapies. Nat Struct Mol Biol. 2018 Feb;25(2):115–21.

160. Koday MT, Nelson J, Chevalier A, Koday M, Kalinoski H, Stewart L, et al. A Computationally Designed Hemagglutinin Stem-Binding Protein Provides In Vivo Protection from Influenza Independent of a Host Immune Response. PLoS Pathog. 2016 Feb 4;12(2):e1005409.

161. Fleishman SJ, Whitehead TA, Ekiert DC, Dreyfus C, Corn JE, Strauch E-M, et al. Computational design of proteins targeting the conserved stem region of influenza hemagglutinin. Science. 2011 May 13;332(6031):816–21.

162. Lee KK, Pessi A, Gui L, Santoprete A, Talekar A, Moscona A, et al. Capturing a fusion intermediate of influenza hemagglutinin with a cholesterol-conjugated peptide, a new antiviral strategy for influenza virus. J Biol Chem. 2011 Dec 9;286(49):42141–9.

163. Kadam RU, Juraszek J, Brandenburg B, Buyck C, Schepens WBG, Kesteleyn B, et al. Potent peptidic fusion inhibitors of influenza virus. Science (80-). 2017 Sep 28;eaan0516.

164. White KM, De Jesus P, Chen Z, Abreu P, Barile E, Mak PA, et al. A Potent Anti-influenza Compound Blocks Fusion through Stabilization of the Prefusion Conformation of the Hemagglutinin Protein. ACS Infect Dis. 2015 Feb 13;1(2):98–109.

165. Russell RJ, Kerry PS, Stevens DJ, Steinhauer DA, Martin SR, Gamblin SJ, et al. Structure of influenza hemagglutinin in complex with an inhibitor of membrane fusion. Proc Natl Acad Sci U S A. 2008 Nov 18;105(46):17736–41.

166. Basu A, Antanasijevic A, Wang M, Li B, Mills DM, Ames JA, et al. New small molecule entry inhibitors targeting hemagglutinin-mediated influenza a virus fusion. J Virol. 2014 Feb;88(3):1447–60.

167. Vanderlinden E, Göktas F, Cesur Z, Froeyen M, Reed ML, Russell CJ, et al.

Novel inhibitors of influenza virus fusion: structure-activity relationship and interaction with the viral hemagglutinin. J Virol. 2010 May;84(9):4277–88.

168. Corti D, Cameroni E, Guarino B, Kallewaard NL, Zhu Q, Lanzavecchia A. Tackling influenza with broadly neutralizing antibodies. Curr Opin Virol. 2017;24:60–9.

169. Ochiai H, Sakai S, Hirabayashi T, Shimizu Y, Terasawa K. Inhibitory effect of bafilomycin A1, a specific inhibitor of vacuolar-type proton pump, on the growth of influenza A and B viruses in MDCK cells. Antiviral Res. 1995;27(4):425–30.

170. Chen HW, Cheng JX, Liu MT, King K, Peng JY, Zhang XQ, et al. Inhibitory and combinatorial effect of diphyllin, a v-ATPase blocker, on influenza viruses. Antiviral Res. 2013;99(3):371–82.

171. Müller KH, Kainov DE, El Bakkouri K, Saelens X, De Brabander JK, Kittel C, et al. The proton translocation domain of cellular vacuolar ATPase provides a target for the treatment of influenza A virus infections. Br J Pharmacol. 2011;164(2):344–57.

172. Nicholas B, Staples KJ, Moese S, Meldrum E, Ward J, Dennison P, et al. A Novel Lung Explant Model for the Ex Vivo Study of Efficacy and Mechanisms of Anti-Influenza Drugs. J Immunol. 2015;194(12):6144–54.

173. Sato SB. Interference with the endosomal acidification by a monoclonal antibody directed toward the 116 (100)-kD subunit of the vacuolar type proton pump. J Cell Biol. 1994 Oct 1;127(1):39–53.

174. Kadam RU, Wilson IA. Structural basis of influenza virus fusion inhibition by the antiviral drug Arbidol. Proc Natl Acad Sci U S A. 2016 Dec 21;201617020.

175. Corti D, Voss J, Gamblin SJ, Codoni G, Macagno A, Jarrossay D, et al. A neutralizing antibody selected from plasma cells that binds to group 1 and group 2 influenza A hemagglutinins. Science. 2011;333(6044):850–6.

176. Chai N, Swem LR, Reichelt M, Chen-Harris H, Luis E, Park S, et al. Two

Escape Mechanisms of Influenza A Virus to a Broadly Neutralizing Stalk-Binding Antibody. Palese P, editor. PLoS Pathog. 2016 Jun 28;12(6):e1005702.

177. Wang W, Song HS, Keller PW, Alvarado-Facundo E, Vassell R, Weiss CD. Conformational Stability of the Hemagglutinin of H5N1 Influenza A Viruses Influences Susceptibility to Broadly Neutralizing Stem Antibodies. J Virol. 2018;92(12).

178. Murakami S, Horimoto T, Ito M, Takano R, Katsura H, Shimojima M, et al. Enhanced growth of influenza vaccine seed viruses in vero cells mediated by broadening the optimal pH range for virus membrane fusion. J Virol. 2012;86(3):1405–10.

179. Webster RG, Yakhno M, Hinshaw VS, Bean WJ, Murti KG. Intestinal influenza: replication and characterization of influenza viruses in ducks. Virology. 1978 Feb;84(2):268–78.

180. Smeenk CA, Wright KE, Burns BF, Thaker AJ, Brown EG. Mutations in the hemagglutinin and matrix genes of a virulent influenza virus variant, A/FM/1/47-MA, control different stages in pathogenesis. Virus Res. 1996 Oct;44(2):79–95.

181. Keleta L, Ibricevic A, Bovin N V., Brody SL, Brown EG. Experimental Evolution of Human Influenza Virus H3 Hemagglutinin in the Mouse Lung Identifies Adaptive Regions in HA1 and HA2. J Virol. 2008 Dec 1;82(23):11599–608.

182. Ilyushina NA, Khalenkov AM, Seiler JP, Forrest HL, Bovin N V, Marjuki H, et al. Adaptation of pandemic H1N1 influenza viruses in mice. J Virol. 2010 Sep;84(17):8607–16.

183. Rybak SL, Murphy RF. Primary cell cultures from murine kidney and heart differ in endosomal pH. J Cell Physiol. 1998 Jul;176(1):216–22.

184. Marvin SA, Russier M, Huerta CT, Russell CJ, Schultz-Cherry S. Influenza Virus Overcomes Cellular Blocks To Productively Replicate, Impacting

Macrophage Function. J Virol. 2017 Jan 15;91(2):JVI.01417-16.

185. Hashimoto Y, Moki T, Takizawa T, Shiratsuchi A, Nakanishi Y. Evidence for phagocytosis of influenza virus-infected, apoptotic cells by neutrophils and macrophages in mice. J Immunol. 2007 Feb 15;178(4):2448–57.

186. Watanabe Y, Hashimoto Y, Shiratsuchi A, Takizawa T, Nakanishi Y. Augmentation of fatality of influenza in mice by inhibition of phagocytosis. Biochem Biophys Res Commun. 2005 Nov 25;337(3):881–6.

187. Ghoneim HE, Thomas PG, McCullers JA. Depletion of alveolar macrophages during influenza infection facilitates bacterial superinfections. J Immunol. 2013 Aug 1;191(3):1250–9.

188. Wee YS, Roundy KM, Weis JJ, Weis JH. Interferon-inducible transmembrane proteins of the innate immune response act as membrane organizers by influencing clathrin and v-ATPase localization and function. Innate Immun. 2012 Dec;18(6):834–45.

189. Sorrell EM, Wan H, Araya Y, Song H, Perez DR. Minimal molecular constraints for respiratory droplet transmission of an avian-human H9N2 influenza A virus. Proc Natl Acad Sci U S A. 2009 May 5;106(18):7565–70.

190. Varble A, Albrecht RA, Backes S, Crumiller M, Bouvier NM, Sachs D, et al. Influenza A virus transmission bottlenecks are defined by infection route and recipient host. Cell Host Microbe. 2014 Nov 12;16(5):691–700.

191. Wilker PR, Dinis JM, Starrett G, Imai M, Hatta M, Nelson CW, et al. Selection on haemagglutinin imposes a bottleneck during mammalian transmission of reassortant H5N1 influenza viruses. Nat Commun. 2013 Oct 23;4:420–8.

192. McCrone JT, Woods RJ, Martin ET, Malosh RE, Monto AS, Lauring AS. Stochastic processes constrain the within and between host evolution of influenza virus. Elife. 2018 May 3;7.

193. Bischoff WE, Swett K, Leng I, Peters TR. Exposure to Influenza Virus Aerosols During Routine Patient Care. J Infect Dis. 2013 Apr 1;207(7):1037–46.

194. Yan J, Grantham M, Pantelic J, Bueno de Mesquita PJ, Albert B, Liu F, et al. Infectious virus in exhaled breath of symptomatic seasonal influenza cases from a college community. Proc Natl Acad Sci U S A. 2018 Jan 30;115(5):1081–6.

195. Milton DKDDK, Fabian MP, Cowling BJBBJ, Grantham ML, McDevitt JJJJ, Fabian P, et al. Influenza Virus Aerosols in Human Exhaled Breath: Particle Size, Culturability, and Effect of Surgical Masks. Fouchier RAM, editor. PLoS Pathog. 2013 Mar 7;9(3):e1003205.

196. Fabian P, McDevitt JJ, DeHaan WH, Fung ROP, Cowling BJ, Chan KH, et al. Influenza virus in human exhaled breath: an observational study. PLoS One. 2008 Jul 16;3(7):e2691.

197. Haig CW, Mackay WG, Walker JT, Williams C. Bioaerosol sampling: sampling mechanisms, bioefficiency and field studies. J Hosp Infect. 2016 Jul;93(3):242–55.

198. Fabian P, McDevitt JJ, Houseman EA, Milton DK. Airborne influenza virus detection with four aerosol samplers using molecular and infectivity assays: considerations for a new infectious virus aerosol sampler. Indoor Air. 2009 Oct;19(5):433–41.

199. Cao G, Noti JD, Blachere FM, Lindsley WG, Beezhold DH. Development of an improved methodology to detect infectious airborne influenza virus using the NIOSH bioaerosol sampler. J Environ Monit. 2011 Dec;13(12):3321–8.

200. McDevitt JJ, Koutrakis P, Ferguson ST, Wolfson JM, Fabian MP, Martins M, et al. Development and Performance Evaluation of an Exhaled-Breath Bioaerosol Collector for Influenza Virus. Aerosol Sci Technol. 2013 Apr;47(4):444–51.

201. Pan M, Bonny TS, Loeb J, Jiang X, Lednicky JA, Eiguren-Fernandez A, et al. Collection of Viable Aerosolized Influenza Virus and Other Respiratory Viruses in a Student Health Care Center through Water-Based Condensation Growth. Raskin L, editor. mSphere. 2017 Oct 25;2(5).

202. Lindsley WG, Noti JD, Blachere FM, Thewlis RE, Martin SB, Othumpangat S, et al. Viable influenza A virus in airborne particles from human coughs. J Occup Environ Hyg. 2015;12(2):107–13.

203. Lindsley WG, Blachere FM, Beezhold DH, Thewlis RE, Noorbakhsh B, Othumpangat S, et al. Viable influenza A virus in airborne particles expelled during coughs versus exhalations. Influenza Other Respi Viruses. 2016 Sep;10(5):404–13.

204. Roberts KL, Shelton H, Stilwell P, Barclay WS. Transmission of a 2009 H1N1 Pandemic Influenza Virus Occurs before Fever Is Detected, in the Ferret Model. Cowling BJ, editor. PLoS One. 2012 Aug 29;7(8):e43303.

205. Gustin KM, Katz JM, Tumpey TM, Maines TR. Comparison of the Levels of Infectious Virus in Respirable Aerosols Exhaled by Ferrets Infected with Influenza Viruses Exhibiting Diverse Transmissibility Phenotypes Kortney. J Virol. 2013 Jul 15;87(14):7864–73.

206. Russier M, Yang G, Marinova-Petkova A, Vogel P, Kaplan BS, Webby RJ, et al. H1N1 influenza viruses varying widely in hemagglutinin stability transmit efficiently from swine to swine and to ferrets. Lowen AC, editor. PLoS Pathog. 2017 Mar 10;13(3):e1006276.

207. Maurer-Stroh S, Lee RTC, Eisenhaber F, Cui L, Phuah SP, Lin RT. A new common mutation in the hemagglutinin of the 2009 (H1N1) influenza A virus. PLoS Curr. 2010 Jun 1;2:RRN1162.

208. Zanin M, Wong S-S, Barman S, Kaewborisuth C, Vogel P, Rubrum A, et al. Molecular basis of mammalian transmissibility of avian H1N1 influenza viruses and their pandemic potential. Proc Natl Acad Sci U S A. 2017 Oct 17;114(42):11217–22.

209. Marr LC, Tang JW, Van Mullekom J, Lakdawala SS. Mechanistic insights into the effect of humidity on airborne influenza virus survival, transmission and incidence. J R Soc Interface. 2019 Jan 31;16(150):20180298.

210. Yang W, Marr LC. Mechanisms by which ambient humidity may affect viruses in aerosols. Appl Environ Microbiol. 2012 Oct;78(19):6781–8.

211. Wei H, Vejerano EP, Leng W, Huang Q, Willner MR, Marr LC, et al. Aerosol microdroplets exhibit a stable pH gradient. Proc Natl Acad Sci U S A. 2018;115(28):7272–7.

212. Pulit-Penaloza JA, Belser JA, Tumpey TM, Maines TR. Swine-Origin H1 Influenza Viruses Isolated from Humans Exhibit Sustained Infectivity in an Aerosol State. Appl Environ Microbiol. 2019 May 15;85(10):e00210-19.

213. Prussin AJ, Schwake DO, Lin K, Gallagher DL, Buttling L, Marr LC. Survival of the Enveloped Virus Phi6 in Droplets as a Function of Relative Humidity, Absolute Humidity, and Temperature. Appl Environ Microbiol. 2018 Jun 15;84(12).

214. Minhaz Ud-Dean SM. Structural explanation for the effect of humidity on persistence of airborne virus: seasonality of influenza. J Theor Biol. 2010 Jun 7;264(3):822–9.

215. Lindsley WG, Blachere FM, Thewlis RE, Vishnu A, Davis KA, Cao G, et al. Measurements of airborne influenza virus in aerosol particles from human coughs. Pekosz A, editor. PLoS One. 2010 Nov 30;5(11):e15100.

216. Hatagishi E, Okamoto M, Ohmiya S, Yano H, Hori T, Saito W, et al. Establishment and clinical applications of a portable system for capturing influenza viruses released through coughing. Yen H-L, editor. PLoS One. 2014 Aug 1;9(8):e103560.

217. Little JW, Douglas RG, Hall WJ, Roth FK. Attenuated influenza produced by experimental intranasal inoculation. J Med Virol. 1979;3(3):177–88.

218. Killingley B, Enstone J, Booy R, Hayward A, Oxford J, Ferguson N, et al. Potential role of human challenge studies for investigation of influenza transmission. The Lancet Infectious Diseases Nov, 2011 p. 879–86.

219. Watson JM, Francis JN, Mesens S, Faiman GA, Makin J, Patriarca P, et al.

Characterisation of a wild-type influenza (A/H1N1) virus strain as an experimental challenge agent in humans. Virol J. 2015;12(1):13.

220. Tellier R. Aerosol transmission of influenza A virus: a review of new studies. J R Soc Interface. 2009 Dec 6;6 Suppl 6(Suppl 6):S783-90.

221. Alford RH, Kasel JA, Gerone PJ, Knight V. Human influenza resulting from aerosol inhalation. Proc Soc Exp Biol Med. 1966 Jul;122(3):800–4.

222. Carrat F, Vergu E, Ferguson NM, Lemaitre M, Cauchemez S, Leach S, et al. Time lines of infection and disease in human influenza: a review of volunteer challenge studies. Am J Epidemiol. 2008 Apr 1;167(7):775–85.

223. Klein EY, Serohijos AWR, Choi J-M, Shakhnovich EI, Pekosz A. Influenza A H1N1 pandemic strain evolution--divergence and the potential for antigenic drift variants. PLoS One. 2014;9(4):e93632.

224. Yang L, Cheng Y, Zhao X, Wei H, Tan M, Li X, et al. Mutations associated with egg adaptation of influenza A(H1N1)pdm09 virus in laboratory based surveillance in China, 2009–2016. Biosaf Heal. 2019 Mar 12;1(1):41–5.

225. Zhang Y, Zhang Q, Gao Y, He X, Kong H, Jiang Y, et al. Key Molecular Factors in Hemagglutinin and PB2 Contribute to Efficient Transmission of the 2009 H1N1 Pandemic Influenza Virus. J Virol. 2012 Sep 15;86(18):9666–74.

226. Belser JA, Jayaraman A, Raman R, Pappas C, Zeng H, Cox NJ, et al. Effect of D222G Mutation in the Hemagglutinin Protein on Receptor Binding, Pathogenesis and Transmissibility of the 2009 Pandemic H1N1 Influenza Virus. Park M-S, editor. PLoS One. 2011 Sep 22;6(9):e25091.

227. Tse H, To KKW, Wen X, Chen H, Chan K-H, Tsoi H-W, et al. Clinical and Virological Factors Associated with Viremia in Pandemic Influenza A/H1N1/2009 Virus Infection. Norris PJ, editor. PLoS One. 2011 Sep 27;6(9):e22534.

228. Kilander A, Rykkvin R, Dudman SG, Hungnes O. Observed association between the HA1 mutation D222G in the 2009 pandemic influenza A(H1N1)

virus and severe clinical outcome, Norway 2009-2010. Euro Surveill. 2010 Mar 4;15(9).

229. Chen H, Wen X, To KKW, Wang P, Tse H, Chan JFW, et al. Quasispecies of the D225G substitution in the hemagglutinin of pandemic influenza A(H1N1) 2009 virus from patients with severe disease in Hong Kong, China. J Infect Dis. 2010 May;201(10):1517–21.

230. Piralla A, Pariani E, Rovida F, Campanini G, Muzzi A, Emmi V, et al. Segregation of Virulent Influenza A(H1N1) Variants in the Lower Respiratory Tract of Critically Ill Patients during the 2010–2011 Seasonal Epidemic. Costa C, editor. PLoS One. 2011 Dec 14;6(12):e28332.

231. Lakdawala SS, Jayaraman A, Halpin RA, Lamirande EW, Shih AR, Stockwell TB, et al. The soft palate is an important site of adaptation for transmissible influenza viruses. Nature. 2015 Oct 23;526(7571):122–5.

232. Broberg E, Melidou A, Prosenc K, Bragstad K, Hungnes O, countries on behalf of the WER and the EISN members of the reporting. Predominance of influenza A(H1N1)pdm09 virus genetic subclade 6B.1 and influenza B/Victoria lineage viruses at the start of the 2015/16 influenza season in Europe. Eurosurveillance. 2016 Mar 31;21(13):30184.

233. Mänz B, Dornfeld D, Götz V, Zell R, Zimmermann P, Haller O, et al. Pandemic influenza A viruses escape from restriction by human MxA through adaptive mutations in the nucleoprotein. PLoS Pathog. 2013 Mar;9(3):e1003279.

234. Gabriel G, Klingel K, Otte A, Thiele S, Hudjetz B, Arman-Kalcek G, et al. Differential use of importin-α isoforms governs cell tropism and host adaptation of influenza virus. Nat Commun. 2011 Jan 18;2(1):1–7.

235. Benfield CTO, Lyall JW, Kochs G, Tiley LS. Asparagine 631 Variants of the Chicken Mx Protein Do Not Inhibit Influenza Virus Replication in Primary Chicken Embryo Fibroblasts or In Vitro Surrogate Assays. J Virol. 2008 Aug 1;82(15):7533–9.

236. Resa-Infante P, Bonet J, Thiele S, Alawi M, Stanelle-Bertram S, Tuku B, et al. Alternative interaction sites in the influenza A virus nucleoprotein mediate viral escape from the importin-α7 mediated nuclear import pathway. FEBS J. 2019 Sep 25;286(17):3374–88.

237. Ashenberg O, Padmakumar J, Doud MB, Bloom JD. Deep mutational scanning identifies sites in influenza nucleoprotein that affect viral inhibition by MxA. PLoS Pathog. 2017 Mar;13(3):e1006288.

238. Friede M, Palkonyay L, Alfonso C, Pervikov Y, Torelli G, Wood D, et al. WHO initiative to increase global and equitable access to influenza vaccine in the event of a pandemic: Supporting developing country production capacity through technology transfer. Vaccine. 2011;29:A2–7.

239. Rhorer J, Ambrose CS, Dickinson S, Hamilton H, Oleka NA, Malinoski FJ, et al. Efficacy of live attenuated influenza vaccine in children: A meta-analysis of nine randomized clinical trials. Vaccine. 2009 Feb 11;27(7):1101–10.

240. Singanayagam A, Zambon M, Lalvani A, Barclay W. Urgent challenges in implementing live attenuated influenza vaccine. Lancet Infect Dis. 2018;18(1).

241. Elderfield R a., Watson SJ, Godlee a., Adamson WE, Thompson CI, Dunning J, et al. Accumulation of Human-Adapting Mutations during Circulation of A(H1N1)pdm09 Influenza Virus in Humans in the United Kingdom. J Virol. 2014;88(22):13269–83.

242. Gould P, Easton A, Dimmock N. Live Attenuated Influenza Vaccine contains Substantial and Unexpected Amounts of Defective Viral Genomic RNA. Viruses. 2017 Sep 21;9(10):269.

243. Lindsey BB, Jagne YJ, Armitage EP, Singanayagam A, Sallah HJ, Drammeh S, et al. Effect of a Russian-backbone live-attenuated influenza vaccine with an updated pandemic H1N1 strain on shedding and immunogenicity among children in The Gambia: an open-label, observational, phase 4 study. Lancet Respir Med. 2019 Aug;7(8):665–76.

244. Shcherbik S, Pearce N, Carney P, Bazhenova E, Larionova N, Kiseleva I, et al. Evaluation of A(H1N1)pdm09 LAIV vaccine candidates stability and replication efficiency in primary human nasal epithelial cells. Vaccine X. 2019 Aug 9;2:100031.

245. Grohskopf LA, Sokolow LZ, Fry AM, Walter EB, Jernigan DB. Update: ACIP Recommendations for the Use of Quadrivalent Live Attenuated Influenza Vaccine (LAIV4) — United States, 2018–19 Influenza Season. MMWR Morb Mortal Wkly Rep. 2018 Jun 8;67(22):643–5.

246. Singanayagam A, Zambon M, Lalvani A, Barclay W. Can defective interfering RNAs affect the live attenuated influenza vaccine? – Authors' reply. Lancet Infect Dis. 2017;17(12).

247. Yeolekar LR, Dhere RM. Development and validation of an egg-based potency assay for a trivalent live attenuated influenza vaccine. Biologicals. 2012 Mar;40(2):146–50.

248. Fischer WA, King LS, Lane AP, Pekosz A, Pekosz A. Restricted replication of the live attenuated influenza A virus vaccine during infection of primary differentiated human nasal epithelial cells. Vaccine. 2015 Aug 26;33(36):4495–504.

249. Forero A, Fenstermacher K, Wohlgemuth N, Nishida A, Carter V, Smith EA, et al. Evaluation of the innate immune responses to influenza and live-attenuated influenza vaccine infection in primary differentiated human nasal epithelial cells. Vaccine. 2017;35(45):6112–21.

250. Cao P, Yan AWC, Heffernan JM, Petrie S, Moss RG, Carolan LA, et al. Innate Immunity and the Inter-exposure Interval Determine the Dynamics of Secondary Influenza Virus Infection and Explain Observed Viral Hierarchies. PLoS Comput Biol. 2015 Aug;11(8):e1004334.

251. Laurie KL, Guarnaccia TA, Carolan LA, Yan AWC, Aban M, Petrie S, et al. Interval Between Infections and Viral Hierarchy Are Determinants of Viral

Interference Following Influenza Virus Infection in a Ferret Model. J Infect Dis. 2015 Dec 1;212(11):1701–10.

252. Laurie KL, Horman W, Carolan LA, Chan KF, Layton D, Bean A, et al. Evidence for Viral Interference and Cross-reactive Protective Immunity Between Influenza B Virus Lineages. J Infect Dis. 2018 Jan 30;217(4):548–59.

253. Karron RA, Talaat K, Luke C, Callahan K, Thumar B, DiLorenzo S, et al. Evaluation of two live attenuated cold-adapted H5N1 influenza virus vaccines in healthy adults. Vaccine. 2009 Aug 6;27(36):4953–60.

254. Rudraraju R, Mordant F, Subbarao K. How Live Attenuated Vaccines Can Inform the Development of Broadly Cross-Protective Influenza Vaccines. J Infect Dis. 2019 Apr 8;219(Supplement_1):S81–7.

255. Matrosovich M, Matrosovich T, Carr J, Roberts NA, Klenk H-D. Overexpression of the alpha-2,6-sialyltransferase in MDCK cells increases influenza virus sensitivity to neuraminidase inhibitors. J Virol. 2003 Aug;77(15):8418–25.

256. World Health Organisation (WHO). WHO information for molecular diagnosis of influenza virus - update. [Internet]. 2014. Available from: http://www.who.int/influenza/gisrs_laboratory/molecular_diagnosis/en/

257. Zhou B, Donnelly ME, Scholes DT, St George K, Hatta M, Kawaoka Y, et al. Single-reaction genomic amplification accelerates sequencing and vaccine production for classical and Swine origin human influenza a viruses. J Virol. 2009 Oct;83(19):10309–13.

258. Li H, Handsaker B, Wysoker A, Fennell T, Ruan J, Homer N, et al. The Sequence Alignment/Map format and SAMtools. Bioinformatics. 2009 Aug 15;25(16):2078–9.